



UNIFORMED SERVICES UNIVERSITY OF THE HEALTH SCIENCES
F. EDWARD HÉBERT SCHOOL OF MEDICINE
4301 JONES BRIDGE ROAD
BETHESDA, MARYLAND 20814-4799



June 16, 2008

GRADUATE PROGRAMS IN THE
BIOMEDICAL SCIENCES AND
PUBLIC HEALTH

APPROVAL SHEET

Ph.D. Degrees

Interdisciplinary
-Emerging Infectious Diseases
-Molecular & Cell Biology
-Neuroscience

Departmental
-Clinical Psychology
-Environmental Health Sciences
-Medical Psychology
-Medical Zoology

Doctor of Public Health (Dr.P.H.)

Physician Scientist (MD/Ph.D.)

Master of Science Degrees

-Public Health

Masters Degrees

-Military Medical History
-Public Health
-Tropical Medicine & Hygiene

Graduate Education Office

Eleanor S. Metcalf, Ph.D., Associate Dean
Janet Anastasi, Program Coordinator
Tanice Acevedo, Education Technician

Web Site

www.usuhs.mil/geo/gradpgm_index.html

E-mail Address

graduateprogram@usuhs.mil


Phone Numbers

Commercial: 301-295-9474
Toll Free: 800-772-1747
DSN: 295-9474
FAX: 301-295-6772


Title of Dissertation: "Study of EPR/ESR Dosimetry in Fingernails as a Method for Assessing Dose of Victims of Radiological Accidents/Incidents"

Name of Candidate: Ricardo Reyes
Doctor of Philosophy
17 June 2008


Dissertation and Abstract Approved:


Donald Lundy, Ph.D.
Department of Preventive Medicine & Biometrics
Committee Chairperson

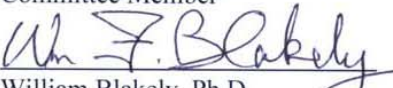
17 June 2008
Date


Alex Romanyukha, Ph.D.
Department of Radiology
Committee Member

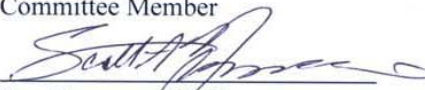
17 June 2008
Date


Luis Benevides, Ph.D.
Department of Radiology
Committee Member

17 June 2008
Date


William Blakely, Ph.D.
Department of Preventive Medicine & Biometrics
Committee Member

17 June 2008
Date

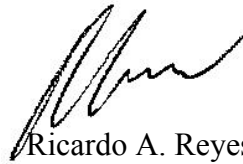

Scot Nemmers, Ph.D.
Department of Preventive Medicine & Biometrics
Committee Member

17 June 2008
Date

The author hereby certifies that the use of any copyrighted material in the dissertation manuscript entitled:

**“STUDY OF ELECTRON PARAMAGNETIC RESONANCE (EPR) / ELECTRON
SPIN RESONANCE (ESR) DOSIMETRY IN FINGERNAILS AS A METHOD
FOR ASSESSING DOSE OF VICTIMS OF RADIOLOGICAL
ACCIDENTS/INCIDENTS”**

beyond brief excerpts, is with the permission of the copyright owner and will save and hold harmless the Uniformed Services University of the Health Sciences from any damage which may arise from such copyright violations.

A handwritten signature in black ink, appearing to read 'Ricardo A. Reyes'.

Ricardo A. Reyes,
MAJ, MSC, U.S. Army
Department of Preventive Medicine and
Biometrics
Uniformed Services University of the
Health Sciences

ABSTRACT

“STUDY OF ELECTRON PARAMAGNETIC RESONANCE (EPR) / ELECTRON SPIN RESONANCE (ESR) DOSIMETRY IN FINGERNAILS AS A METHOD FOR ASSESSING DOSE OF VICTIMS OF RADIOLOGICAL ACCIDENTS/INCIDENTS”

by

MAJ Ricardo A. Reyes, Doctor of Philosophy, 2008

Dissertation Directed by: Dr. Alex Romanyukha
Assistant Professor
Department of Radiology and Radiological Sciences

The threat of nuclear terrorism and the potential for the use of radiation as a weapon make having an efficient and accurate radiation dosimetry methodology paramount. Finger and toenails can efficiently be used as biomarkers in EPR dosimetry during a radiological emergency. EPR signals in these samples show a distinctively measurable radiation induced signal (RIS) but also show two other affecting signals, background (BKS) and mechanically induced (MIS). This study addresses their effect, dose response improvements using chemical treatment, and the variability in dose-response.

During the first stage of this study, a model that would explain the mechanical and dosimetric properties of human fingernails and an effective rapid sample water treatment were developed. This stage addressed the isolation of the MIS, BKS, and RIS, their origin, their evaluation under proposed treatment conditions, and treatment effect on dose dependence. The second stage evaluated these dosimetric properties in treated and

untreated samples and assessed the variability in radiation response.

This study gives a physical/mechanical explanation to the behavior of EPR signals in fingernail dosimetry by modeling fingernails as sponges. Since previous work was performed using stressed (untreated) samples, they do not represent the realistic behavior of unstressed (treated) fingernails. The developed treatment eliminates the combined effect of the mechanical EPR signals, MIS1 (former MIS), and MIS2 (former BKS). As nail samples are physically restored with treatments, are not stressed, and display a response closer to that of *in vivo* specimens. The RIS is proportional to the radiation dose and shows a curvilinear dose response in unstressed samples using the additive dose method that can be modeled with a saturating exponential model (Grun model) for predicting residual or accidental radiological dose.

Water content and mechanical stress were identified as the major factors affecting radiation sensitivity and its shape in fingernail EPR measurements respectively. It is proposed that treated samples be used in fingernail EPR dosimetry because they show more stable signals than untreated ones and have lower interpersonal and intrapersonal variability. Practical conditions of sample collection, preparation, and measurements at an accident site can be met with techniques illustrated in this study.

**“STUDY OF ELECTRON PARAMAGNETIC RESONANCE (EPR) / ELECTRON
SPIN RESONANCE (ESR) DOSIMETRY IN FINGERNAILS AS A METHOD
FOR ASSESSING DOSE OF VICTIMS OF RADIOLOGICAL
ACCIDENTS/INCIDENTS”**

by

Ricardo A. Reyes
Nuclear Medical Science Officer
U.S. Army

A dissertation submitted to the Faculty of the
Department of Preventive Medicine and Biometrics,
Uniformed Services University of the Health Sciences
in partial fulfillment of the requirements for the degree
of

DOCTOR OF PHILOSOPHY
IN ENVIRONMENTAL HEALTH SCIENCES
(MEDICAL HEALTH PHYSICS)

DEDICATION

I dedicate this doctoral dissertation to my wife, Mercy, and daughters, Zoe and Chloe. They truly understand how much this goal means to me. They are my inspiration and the backbone of everything I do in life, every goal I set, and every goal I meet. This is for their unconditional love and support, which will always be reciprocated by me. I would not have been able to complete this dissertation without their support and that of my parents, and Obbatala.

ACKNOWLEDGEMENTS

I am extremely grateful to the support and mentorship of my committee members. Every member of my committee had an impact on my research and my personal life. I am thankful to LTC Lundy and CDR Benevides for their encouragement and continuous reinforcement, Maj Nemmers for his selfless assistance during a period when lectures seemed endless, and Dr. Blakely for his every opportune advice and mentorship throughout the entire time of my research. A special thank goes to LTC Darrell Criswell for his assistance during my defense and to Dr. Alex Romanyukha, my thesis advisor. Dr. Romanyukha's persistence during the experimental phase of my research and guidance made the completion of the manuscripts possible. It was with their continuous support that I have been able to complete this dissertation.

I must thank the U.S. Army Long Term Education and Training program for this opportunity. I also would like to give special thanks to COL Mark Melanson, my military and professional career mentor. His uninterrupted mentoring guided me through this endeavor.

TABLE OF CONTENTS

ABSTRACT	iii
TITLE PAGE	v
DEDICATION	vi
ACKNOWLEDGEMENTS	vii
LIST OF TABLES	x
LIST OF FIGURES	xi
CHAPTER 1. INTRODUCTION	1
1.1. PRELIMINARY STUDIES REVIEW	1
1.2. BACKGROUND AND SIGNIFICANCE OF RESEARCH	3
1.3. HISTORY OF EPR	5
1.4. EPR SPECTROSCOPY	6
1.5. EPR PARAMETERS AND FACTORS AFFECTING SPECTRA	10
1.6. THE ENDOR EXPERIMENT	11
1.7. EPR SPECTROMETERS	12
1.8. EPR DOSIMETRY	15
1.9. EPR DOSIMETRY IN FINGERNAILS	18
CHAPTER 2. RESEARCH OBJECTIVES AND METHODOLOGY	28
2.1. SPECIFIC AIMS	31
2.2. EXPERIMENTAL DESIGN	31
2.3. MANUSCRIPTS	44
CHAPTER 3. “Electron paramagnetic resonance in human fingernails: the sponge model implication”	46

CHAPTER 4. “EPR dose dependence in fingernails: Variability and possibilities of initial dose assessment”	84
CHAPTER 5. CONCLUSION	134
5.1. DISCUSSION OF RESEARCH FINDINGS	134
5.2. PUBLIC HEALTH RELEVANCE.....	138
5.3. RECOMMENDATIONS FOR FUTURE RESEARCH.....	139
5.4 CONCLUSION.....	140
APPENDIX A. Effect of “sample number of cuts” on radiation dose dependence in fingernails dosimetry.	144
APPENDIX B. Development of saturation curve lines for finger nails in support of proposed treatment of nails for EPR measurements and the sponge behavior theory....	151
APPENDIX C. Evaluation of dose buildup during irradiation of samples.	160
APPENDIX D. Study of the fading of the EPR signals after irradiation.....	168
BIBLIOGRAPHY	176

LIST OF TABLES

Table 1-1. Tabulation of waveband with corresponding wavelength, frequency and magnetic field.....	15
Table 2-1. Average EPR response for fingernail clippings measuring 10 samples and normalizing to weight.	40
Table 2-2A. Preliminary data for samples 1 – 10.	42
Table 2-2B. Preliminary data for samples 11 – 20.....	42
Table 3-1. EPR parameters of three spectral components in fingernails at room temperature.	73
Table 4-1. Practical sample requirements for fingernail EPR dosimetry.....	113
Table 4-2. EPR recording conditions – Spectrometer settings.....	113
Table 4-3A. Peak to peak amplitude of EPR signals in stressed fresh fingernail samples at 0, 2, 5, 10, and 15 Gy added radiation dose, slope for each sample, and R^2	114
Table 4-3B. Peak to peak amplitude of EPR signals in stressed old fingernail samples at 0, 2, 5, 10, and 15 Gy added radiation dose, slope for each sample, and R^2	114
Table 4-4. Weight difference after treatment of samples and time after cut for first set of treated samples.....	115
Table 4-5. Dose response in treated (unstressed) samples (each value is the average obtained from split samples, two samples per donor, n=40).	116
Table 4-6. Dose offset, D_E , and saturation dose, D_0 , determined from the fit of experimental data of three samples made of powder, large and small pieces using the Grun formula.....	116

LIST OF FIGURES

Figure 1-1. Illustration of the dipolar moment of electrons and the resonance magnetic field at which ΔE is defined.....	8
Figure 1-2. Illustration of the absorbance and first derivative EPR spectra at resonance magnetic field B_0	9
Figure 1-3. Diagram of a typical spectrometer [46].....	12
Figure 1-4. Illustration of the additive dose method for EPR dose assessment.....	17
Figure 1-5. Chemical illustration of alpha keratin in finger and toe nails.	19
Figure 1-6. Diagram of two possible species of MIS [27].....	22
Figure 1-7. MIS spectra after cut and 3 hours later (MIS spectrum: $g = 2.015$ $\Delta H=10$ G).	22
Figure 1-8. Fingernail MIS spectra from different sample size.....	23
Figure 1-9. MIS spectra after cut and after a 3 hour delay.	24
Figure 1-10. BKS spectrum from un-irradiated sample (BKS parameters: $g=2.0075$, $\Delta H=9$ G).....	25
Figure 1-11. Radiation induced radical [27].	26
Figure 1-12. Spectra of the RIS at 1, 5, and 8 Gy (RIS parameters: $g=2.0088$ $\Delta H=9$ G).	27
Figure 2-1. Effect of water treatment on freshly and previously cut fingernail samples.	35
Figure 2-2. Effect of water treatment on the MIS and BKS signals in freshly cut fingernail samples.	36
Figure 2-3. Effect of continuous water treatment on the EPR signals amplitude in freshly cut fingernails (20 mg).....	36

Figure 2-4. Effect of water treatment on the MIS, BKS, and RIS signals in freshly cut fingernail samples (40 mg).	37
Figure 2-5. Plot of the average EPR signal of 10 untreated fingernail samples.	41
Figure 3-1. Time evolution of the EPR spectrum in an unirradiated fingernail sample (15mg) after fingernail trimming.	73
Figure 3-2. Dependence of the BKS and MIS signals on microwave power.	74
Figure 3-3. Subtraction of the EPR spectrum acquired at 1 mW (dashed line) from that acquired from the same un-irradiated fingernail sample at 16 mW (solid line), for identification of the MIS component (bold line).	74
Figure 3-4. Subtraction of the EPR spectrum acquired at 16 mW and multiplied by a correction factor of 0.25 (dashed line), from that acquired from the same un-irradiated fingernail sample at 1 mW (solid line), for isolation of the BKS component (bold line).	75
Figure 3-5. Time dependence of normalized MIS and BKS intensity in unirradiated fingernail sample after trimming	75
Figure 3-6 a). MIS recorded in the same unirradiated sample after making additional cuts.	76
Figure 3-6 b). BKS recorded in the same sample after making additional cuts.	76
Figure 3-7 a). Dependence of MIS intensity on time-after-cut using the same unirradiated sample before and after additional cuts.	77
Figure 3-7 b). Dependence of BKS intensity on time-after-cut using the same unirradiated sample before and after additional cuts.	77
Figure 3-8. Changes of the peak-to-peak amplitude of the EPR signal in an unirradiated fingernail sample, shortly after cut and after five consequent 5 min water treatments	78

Figure 3-9. Growth of BKS in water-treated fingernails with time after treatment.....	78
Figure 3-10. Weight change of fingernail samples after periodical soaking in water and weighting after a short drying period.....	79
Figure 3-11. EPR spectra in water-treated fingernails exposed to different radiation doses.....	80
Figure 3-12. Dose dependence of the EPR signal in a water-treated fingernail sample.	80
Figure 3-13. Dose dependence of the RIS component in untreated fingernails.	81
Figure 3-14. Scanning electron micrographs of the fracture surfaces of torn nail clippings.....	82
Figure 3-15. Schematic model of the deformation of fingernails at the edge of a cut and subsequent restoration of its shape while soaking in water	82
Figure 3-16. Schematic picture of two possible types of fingernail deformation.....	83
Figure 4-1. Experimental steps for the assessment of radiological doses using fingernails as biophysical dosimeters.	117
Figure 4-2. Flow chart illustrating experimental steps for the assessment of radiological doses using fingernails as biodosimeters.	118
Figure 4-3. EPR Signal dose response in stressed (untreated) fingernails (30 mg / 8 clippings).....	119
Figure 4-4. Average EPR dose response in freshly (“fresh”) and previously cut (“old”) fingernail samples at 0, 2, 5, 10, and 15 Gy added radiation dose (30 mg / 8 clippings).	120
Figure 4-5. Slope variation in EPR added radiation dose response in freshly-cut (a) and old (b) fingernails (values are the average for each donor’ split sample).....	121

Figure 4-6. SPSS output showing the correlation between the slope of the dose curve and the time-since-cut for all stressed (untreated) samples.	122
Figure 4-7. Interpersonal and intrapersonal variability of EPR radiation response (peak-to-peak amplitude) for added dose values of 0, 2, 5, 10, and 15 Gy for freshly-cut, older samples, and for all stressed samples.....	123
Figure 4-8. Weight increase after treatment versus time since cut plot for fresh (a) and old (b) fingernail samples (values are from the first sample of each donor' split set). ..	124
Figure 4-9. SPSS output showing the correlation between the weight increase in unstressed (treated) fingernails and the time-since-cut.....	125
Figure 4-10. Dose dependence in unstressed (treated) fingernail samples; (a) shows the data for 20 donors and (b) show the average for freshly-cut and older samples (pilot data fitted to plot).	126
Figure 4-11. Signal reduction for 20 old unstressed samples after last irradiation of 20 Gy (cumulative).	127
Figure 4-12. Interpersonal and intrapersonal variability of EPR radiation dose measurements for added dose values of 0, 2, 5, 10, 15, and 20 Gy for freshly-cut, older samples, and for all unstressed samples.....	128
Figure 4-13. Dose dependences for treated fingernail samples with different number of clippings and size.....	129
Figure 4-14. Dose dependences for samples from fresh fingernails, collected from the same person, at the same time, but prepared differently.....	130
Figure 4-15. Saturation dose versus dose offset for three samples with different size and number of clippings in the sample.	131

Figure 4-16. EPR fingernail dosimetry protocol for use in radiation incidents and accidents.....	132
Figure 4-17. Correlation between D_0 and D_E in stressed and unstressed fingernails samples.....	133
Figure A-1. MIS and BKS size dependence.	146
Figure A-2. EPR spectra after cut and treatment.	147
Figure A-3. Spectra progression with radiation (normalization to 20 mg).....	148
Figure A-4. Dose dependences for samples from fresh fingernails, collected from the same person, at the same time, but prepared differently.....	149
Figure B-1. Plot of water absorption curves for fingernail samples 1-8.....	155
Figure B-2. Plot of water absorption curves for fingernail samples 9-10.....	156
Figure C-1. Illustration of geometric location of the irradiated samples in irradiation cavity.....	161
Figure C-2. Plot of NDC dose versus delivered dose.....	163
Figure C-3. Plot of NDC reported dose for all 4 chips, P1, P2, P3, and P4 versus the plexiglass thickness.....	165
Figure C-4. Plot of NDC reported dose (averaged from all 4 chips, P1, P2, P3, and P4) versus the plexiglass thickness.....	166
Figure D-1. EPR signal changes with time in stressed samples after 15 Gy irradiation.	170
Figure D-2. EPR signal changes with time in unstressed samples after irradiation (20 Gy).	171
Figure D-3. EPR signal change with time in stressed (after 15 Gy irradiation) and	

unstressed (after 20 Gy irradiation) fingernail samples.	172
Figure D-4. EPR signal fading after high acute irradiations of 100 and 200 Gy for samples kept at freezing temperatures and ATP conditions.	173
Figure D-5. EPR signal fading after irradiation of 8 samples that were followed for two years.	174

CHAPTER 1

INTRODUCTION

Many radiation/nuclear accidents/incidents and radiation overexposures resulting from ionizing radiation that are reported worldwide involve activities related to nuclear power plants, weapons, industrial, medical, and research radiation sources, or most recently, terrorism [1, 2]. Today, the threat of global terrorism that may involve the intentional contamination with radioisotopes, radiation dispersal devices (RDD), “dirty bombs”, radiation emitting devices (RED), or the detonation of improvised nuclear devices, has made the need for rapid and accurate ionizing radiation dosimetry paramount. Electron Paramagnetic Resonance (EPR), also called Electron Spin Resonance (ESR), is an effective and accurate method for quantifying the exposure to ionizing radiation that can be used with other complementary dosimetric methods during the triage of affected individuals.

1.1. PRELIMINARY STUDIES REVIEW

Researchers have supported the use of EPR/ESR as the dosimetric standard for victims of radiological accidents [1, 3, 4]. The use of EPR dosimetry for detecting free radicals produced from exposure to ionizing radiation has employed biological samples (teeth, hair, bones, etc.) and other biological samples and pieces of clothing from potentially exposed individuals. The inherent difficulties in collecting and processing biological samples have been addressed by previous authors [5-14]. Preliminary studies

have used calcified tissues, alanine, various sugars, quartz in rocks and sulfates, as EPR dosimeters [15]. Alternatively, radiation-induced EPR signals have been detected using other biological substances, such as amino acids, proteins, fatty acids, and hydroxyl acids, as indicators of radiation damage to tissues [16, 17]. The fast decay and variability of the signals in soft tissues have not been useful for EPR dosimetry; however, other hard tissues, such as bones, teeth and nails, are more desirable [5].

In the nineteen sixties, Becker [18] studied the radiation-independent signal in hydroxyapatite $[\text{Ca}_{10}(\text{PO}_4)_6(\text{OH})_2]$, which is the main mineral component of tooth enamel, dentin, and bones. Carbonate impurities in these tissues are incorporated into or are attached to the surface of hydroxyapatite and are converted into CO_2^- radicals during ionizing radiation exposures. The measurement of these radiation-induced radicals in hydroxyapatite has been the basis for many retrospective EPR studies [19]. Ikeya et al. [20] identified this signal in dental enamel and Pass and Aldrich [21] quantified the magnitude dependence on microwave power. Several researchers have also studied the changes of both the radiation induced signal and background signals with microwave power with the intent of improving accuracy in tooth EPR dosimetry [22-26].

The use of EPR for radiation dosimetry studies has been successfully used in bone, teeth enamel and dentine. However, it has also shown challenges involving the collection of and processing of these kinds of samples, especially during a radiological emergency, a time when not only an accurate dosimetry method is crucial for the proper assessment of dose but also the rapid collection and processing of samples. Current research is not only focusing on ways to improve sample collection and preparation of teeth and bones but also the use of fingernails, toenails, and hair samples. The latter, has shown to have

problems inferred by a high background signal. Fingernails and toenails EPR signals have shown a distinctively measurable radiation induced signal but have also shown the presence of two other affecting signals, background and mechanically induced. Symons et al. identified problems with the time decay of signals from the radicals in fingernails [27]. Aside from the background signal, Romanyukha et al. identified a mechanically induced signal from the collection and preparation of fingernail samples as a confounding factor [28].

The literature shows ongoing research efforts but no standardized technology protocol for the characterization of gamma exposure using human nails as biosamples for dosimetric analysis *in vivo* or retrospectively. Moreover, these research endeavors have not addressed the improvements in sensitivity using chemical treatment of human nail samples or the interpersonal effects on dose-response curves. These are addressed in the study described in this dissertation.

1.2. BACKGROUND AND SIGNIFICANCE OF RESEARCH

Radiation dose assessment using EPR is recognized by the IAEA Safety Report Series No. 4, *Planning the medical response to radiological accidents*, as a method for estimating radiation dose without the use of physical dosimeters and using exposed clothes, teeth and other solid materials [29]. This research stems from previous studies to further justify the use of ESR as a dosimetric standard, much in the same fashion as Swartz et al. proposed in their publications about the use of *in vivo* teeth EPR dosimetry during a terrorist event, accident or war involving ionizing radiation sources [30, 31]. It

offers specific recommendations for the evaluation parameters that would be most effective in producing the data needed for the development of an EPR dosimetry response protocol, in a similar fashion as that reported in Trompier et al. and Alexander et al. [32, 33]. A protocol of this type can be used to evaluate radiation exposures right after a radiological/nuclear accident/incident and in retrospective dose studies, and can set the stage for the development of *in vivo* fingernail EPR dosimetry.

The development of dose-response curves that would match EPR data to dose is difficult and has many limitations, including limited sensitivity [12, 34]. This research builds on previous studies of exposed nail biological samples [27, 28] and involves exposing samples to gamma radiation fields in a similar fashion to that done by Trompier in 2004 with tooth enamel [35]. This study is aimed to overcome some of the documented obstacles in using fingernail EPR dosimetry for dose assessment of exposed individuals during a radiological emergency. The recommendations derived in this study can be used to evaluate acute exposures to gamma radiation¹. Results from this research can be used in a protocol that would assess dose to individuals from whom samples were collected right after an event or sometime thereafter (retrospectively). These can also be used in support of epidemiological studies and to estimate the dose for others who were, or may be, exposed to the same source, at the same location, under the same circumstances, and for the same period of time. Therefore; this adds a preventive aspect to the scenario by being able to address measures to avoid further detrimental biological effects and recommend proper treatment and evaluation of risk to potentially exposed populations.

¹ This approach can also be applicable to assess chronic exposure, which is beyond the scope of the present protocol.

1.3. HISTORY OF EPR

EPR was discovered by Yevgeniy Konstantinovich Zavoyskiy in 1944 and developed independently at the same time by Brebis Bleaney at Oxford University [36, 37]. Prior to this discovery and as early as 1897, Pieter Zeeman reported the energy line splitting in an external magnetic field, Otto Stern and Walter Gerlach showed that it was possible to quantify this kind of fields in 1922, and Goldsmith and Uhlenbeck reported on the spin of the electron in 1925 [14, 38]. However, it was Zavoyskiy who would then detect a radiofrequency absorption line from a $\text{CuCl}_2 \cdot 2\text{H}_2\text{O}$ sample in 1944 [39].

Nuclear Magnetic Resonance (NMR) and EPR are very similar in nature. Both techniques of magnetic resonance look at the “flip-flop” in a magnetic field of the spins of the atomic nuclei and the electron respectively. In 1946 Block, Purcell, and Pond performed the first NMR experiment and in 1958, twelve years later, Bill Mims performed the first pulse EPR experiment [38, 40]. Wrachtrup, Köhler, Groenen, and Borczyskowski performed the first single molecule EPR experiment in 1993 [41, 42], almost fifty years after Zavoyskiy’s discovery.

Traditional magnets had many limitations and could not produce fields above 1.5 T. The first multifunctional millimeter EPR spectrometer with a superconducting solenoid was developed by several Russian research groups in the early to mid 1970s [43]. The German Bruker Company produced W-band EPR techniques in the 1990s, two decades later. Today, EPR/ESR dosimetry in biological samples remains an uncommon technique, internationally recognized to derive sensitive detection of free radicals in

paramagnetic molecules but with very few scientific centers with the capability to perform these measurements [44]. The many applications of EPR/ESR dosimetry have been described elsewhere [4, 7-10, 13, 14, 19, 45].

1.4. EPR SPECTROSCOPY

EPR spectroscopy studies free radicals in paramagnetic materials based on their magnetic properties. It quantifies the differences between the energy states of electrons in atoms that have one or more unpaired electrons, such as organic and inorganic free radicals or inorganic complexes possessing a transition-metal ion. Paramagnetic materials have positive magnetic moments in the presence of magnetic fields. EPR uses these strong applied magnetic fields to split Zeeman levels (atomic energy levels under the influence of a magnetic field). Electromagnetic waves in the gigahertz region induce magnetic dipole transitions to cause resonances in a range of microwave frequencies. This would show absorption spectra that are studied in EPR spectroscopy. We obtain the EPR spectra by measuring the attenuation versus the frequency or wavelength of electromagnetic radiation as it passes through matter [37].

If we define the difference in energy, $\Delta E = h \cdot \nu$, the product of h , Planck's constant, and ν , the radiation frequency, we can show the relationship between ΔE and the absorption of electromagnetic field. This absorption causes a transition from lower to higher energy states. When we look at these transitions that vary with frequencies, we obtain a spectrum.

The Zeeman Effect is the splitting of an electron energy state into several components depending on its spin quantum number (own magnetic momentum) in the presence of a static magnetic field. EPR experiments use electromagnetic waves in the gigahertz microwave region based on this effect. The electronic Zeeman splitting for a system with electron spin $s=1/2$ is illustrated in Figure 1-1. The unpaired electrons have a spin quantum number $s=1/2$, and magnetic dipole moment, m_s , which aligns with an external magnetic field at a state of lower energy ($m_s=-1/2$) and opposes the direction of this field at a state of higher energy ($m_s=+1/2$) (see Fig. 1-1 below). The energy E can be described as $E = \pm \frac{1}{2} g_e \cdot \mu_B \cdot B_0$, where g_e is the g-factor (2.00232 for free electron), also called the Landé g-factor, μ_B is the Bohr magneton, equal to $9.2740 \text{ E-}24 \text{ J T}^{-1}$, and B_0 is the magnetic field strength [37]. The separation between the two energy states, ΔE , would then be: $\Delta E = g_e \cdot \mu_B \cdot B_0$, which is equal to the product of h and ν ($h \cdot \nu$), described above. Then, $h \cdot \nu = g_e \cdot \mu_B \cdot B_0$, the equation often described as the fundamental equation of EPR spectroscopy.

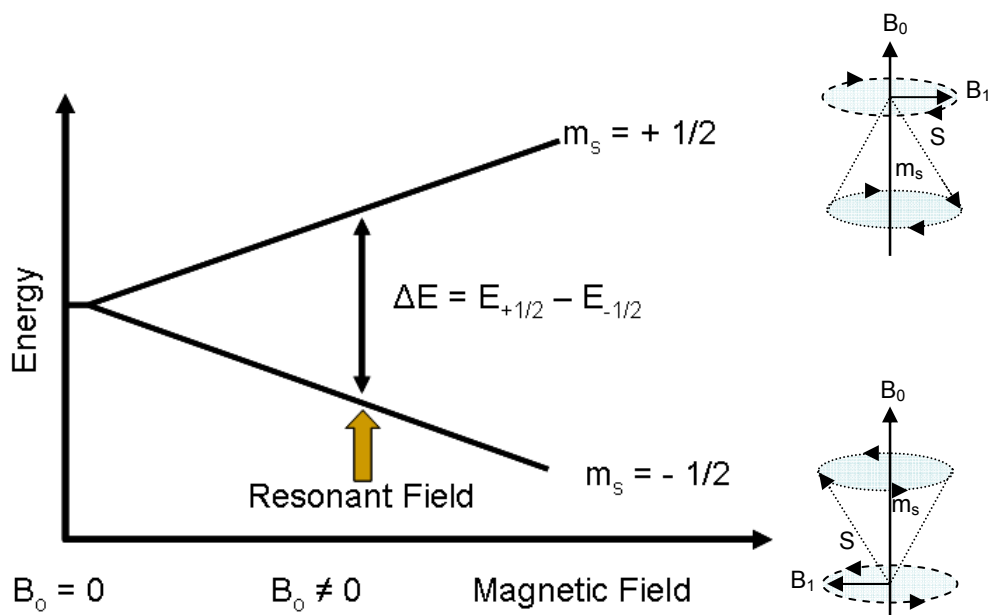


Figure 1-1. Illustration of the dipolar moment of electrons and the resonance magnetic field at which ΔE is defined. To the right is an illustration of the torque exerted on the angular momentum S in the presence of magnetic field B_0 at the angular frequency (Larmor frequency), with an additional rotary moment arisen from the action of field B_1 [38].

The difference of the two electron spin states with different energies in the presence of a magnetic field varies linearly with the increase of the magnetic field strength. This allows us to obtain spectra by scanning the frequency under an applied magnetic field, or by keeping the frequency constant and scanning the magnetic field. In practice, the latter is used to identify the resonance when a peak in the absorption region occurs, as the magnetic field tunes the two spin states, matching the energy difference to that of the radiation [46].

The g-factor gives us information about the magnetic symmetry of paramagnetic centers, as the unpaired electrons respond to both the spectrometer's applied magnetic field and the local magnetic fields of atoms and molecules. Because of this, a more

applicable equation for ΔE would be $\Delta E = g \cdot \mu_B \cdot B_e$, which is equal to $h \cdot \nu$. In this case, g and B_e are the g -factor and effective magnetic strength that also take into account the contribution of the local fields, σ . They are derived as follows: $B_e = B_0 + B_{\text{local}} = B_0 (1 - \sigma)$, and $g = g_e (1 - \sigma)_e$ or $B_e = (g/g_e) B_0$ [37]; therefore, $g = (h \cdot \nu) / (\mu_B \cdot B_e)$. At lower magnetic fields, we see higher values of g and vice versa.

Given a specific microwave frequency ν , and a g -factor, we can calculate the value of B_0 at the predicted resonance site. At this site, the direction of magnetic moment of unpaired electrons and their spin state change, having more electrons at the lower energy state. The net absorption energy from the electrons, which follows the Maxwell-Boltzmann distribution, is monitored and converted into an EPR spectrum. Figure 1-2 shows two different forms of a simulated spectrum at a resonance location; most spectra are commonly shown as first derivatives.

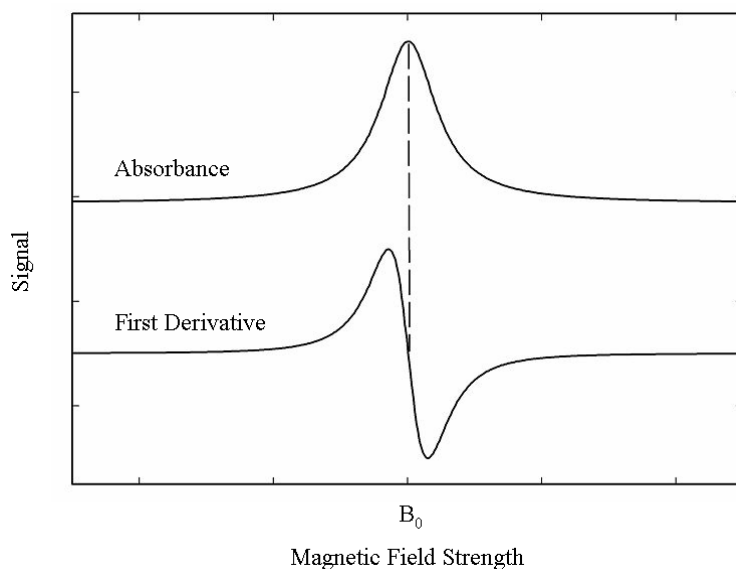


Figure 1-2. Illustration of the absorbance and first derivative EPR spectra at resonance magnetic field B_0 .

1.5. EPR PARAMETERS AND FACTORS AFFECTING SPECTRA

EPR spectral parameters, peak-to-peak amplitude, g-factor, and linewidths have been extensively described in the literature [37, 38]. The maximum height of the EPR spectrum curve (amplitude) depends on experimental factors such as power, sensitivity, amplifier settings, sample composition, and temperature [37]. The g-factor, described above, is independent of the microwave frequency. EPR linewidths are defined in terms of the magnetic induction and are measured along the x axis of the spectrum from the center of the resonance line to the point where the absorption value is half the maximum.

EPR line shapes can often be described by Lorentzian or Gaussian functions. Even though line profiles are never perfectly Lorentzian or Gaussian, they occur in case of homogeneous (due to “micro” impurities / paramagnetic-defects in material that have local magnetic fields) and inhomogeneous (EPR line encompasses many other homogeneously broadened lines) line broadening respectively. Homogeneous broadening occurs when spins see the same magnetic field, have the same parameters, and the lineshape is the same for each dipole. Linewidths take a Lorentzian shape if there is no hyperfine broadening, the concentration of paramagnetic centers is low, and there is dynamic averaging. The latter affects the lineshape when there are dynamic processes in and around the paramagnetic center, and leads to homogeneous line broadening. Inhomogeneous broadening occurs when resonance frequencies are distributed over an unresolved band without broadening the lines from the individual spins. The magnitude of the magnetic field observed by unpaired electrons is not exactly the same and therefore, only a small fraction of the spins is in resonance at any time. This causes a

superposition of many individual line components and the observed line takes a Gaussian shape [37, 38, 47].

Since electrons are not isolated in nature and associate with other electrons and atoms, they can gain or loose angular momentum. Hyperfine interaction is the interaction between the magnetic moment of an unpaired electron and that of a nearby nucleus or nuclei. Additional multi-lined spectra from the interactions of the unpaired electrons with nearby nuclear spins occur as a result of hyperfine coupling. The spacing between these spectral lines is an indication of the degree of these interactions.

1.6. THE ENDOR EXPERIMENT

In 1956, the use of the electron nuclear double resonance (ENDOR) technique showed that a better resolution of EPR spectrum could be attained [48]. Double resonance experiments are based on the effect of enhancement. These experiments are useful when we have two or more paramagnetic defects and indistinctness in the identification and assignment of the different superimposed component spectra. We may also use them when we are not be able to detect the spacing of hyperfine lines (split) if it does not exceed the line width in EPR. In ENDOR experiments a magnetic field, strong enough to resonate an EPR transition, is used; a second alternating field is applied with frequencies sweeping across the range of resonance frequencies. A partially saturated EPR signal is then evaluated as a function of the second set of frequencies [37].

1.7. EPR SPECTROMETERS

The development of EPR spectrometers that became commercially available took place within 10 years after the experimental exercises done by theoretical physicists Zavoyskiy and Bleaney. They essentially had three main components, a magnet, a source of electromagnetic field, and a detector. Figure 1-3 shows a block diagram of a typical spectrometer. As depicted in this figure, the main components of a typical EPR spectrometer are the bridge, sample cavity, magnet, signal channel, field controller, and the console/computer generated spectrum.

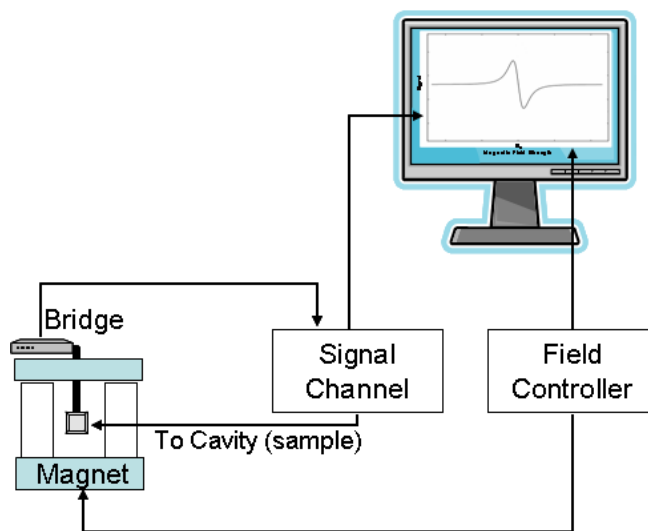


Figure 1-3. Diagram of a typical spectrometer [46].

The microwave bridge houses the electromagnetic field source and detector. The microwave source has a system, internal to the bridge that controls the microwave field and therefore, the microwave power seen by the sample. There are EPR transmission and reflection spectrometers, called as such because they respectively measure the amount of

microwave field transmitted through or reflected back from the sample cavity. The latter type is most common and is what we used in our research. The bridge has a circulator, a barrier diode, a reference arm, a phase shifter, and a protection circuitry. The circulator facilitates the reflection of the microwave field and does not allow it to go back to the cavity. The barrier diode is used to detect the reflected microwaves. This diode converts the microwave power to electrical current and controls a gradual transition between the operations at low and high power. Square law detectors run at low powers ($< 1\mu\text{W}$) and the electrical power is proportional to the square of the voltage or current. Linear detectors run at higher power ($> 1\text{mW}$) and the diode current is proportional to the square root of the microwave power. This is the region of choice for operating the diode for quantity and signal intensity measurements. The reference arm supplies the detector with bias microwave power in order to guarantee the operation at higher levels. The phase shifter ensures that the microwaves in the reference arm are in phase with the reflected signals microwaves when they combine at the detector diode. The protection circuitry monitors the current from the diode and protects the bridge from exceeding $400\ \mu\text{A}$.

The EPR sample cavity is a metal box, which has dimensions to provide conditions for standing microwaves. The Q value is an indicator of how efficiently microwave energy is stored in the cavity, and is directly proportional to the sensitivity of the cavity at the moment of measurement. The iris, controlled by the “iris screw”, is a hole used to couple the microwaves into the cavity and waveguide. Its size controls how much enters or is reflected from the cavity by matching the transforming impedance (wave resistance) of the cavity and the waveguide (pipe used to transmit microwaves). The Q value is lowered when samples absorb microwave energy because of the increase losses. The

impedance of the samples changes and therefore, the coupling also changes. When this happens, the cavity is not critically coupled and there are microwaves reflecting back to the bridge, which result in an EPR signal.

The signal channel is in the spectrometer console and is responsible for doing phase sensitive detection, which is used in spectroscopy to enhance sensitivity. This allow us to have less noise from the detection diode, eliminate baseline instabilities due to the drift in DC electronics, and distinguish the EPR signals are from background noise. In this channel, the magnetic field strength at the sample site is modulated sinusoidally at modulation frequency. The field modulation modulates the reflected microwave signals at the same frequency as the EPR signal, when there is one. The signal is transformed into a sine wave proportional in amplitude to the slope of the original signal. Signals that do not have the same frequency and phase as the field modulated signals are suppressed. Noise is high-frequency filtered out by a time constant. Modulation amplitude, frequency, and time constant can distort the EPR signals.

The magnetic field controller uses a Hall sensor, which measures and stabilizes the magnetic field and allows us to have a controlled sweep of the magnetic field. One part of the magnetic field controller sets the field values and the timing of the field sweep and is controlled by a microprocessor. The other regulates the current in the magnet to reach the requested magnetic field.

The voltage of the signal channel is plotted versus the controlled voltage of the Hall sensor as a measure of magnetic field and ultimately produces an EPR spectrum. The console has the signal processing, control electronics, and computer. This computer is used for the analysis of the data and the setting of the units for the spectrum.

The evolution of EPR spectrometers has allowed us to work with several wavebands, predetermined by the frequency or wavelength of the microwave source. An example of several wavebands available today is shown in table 1-1. We obtain better resolution with increasing frequency. Even though most EPR experiments are currently done in the X band and some in the Q band, the increasing in waveband means a compromise in energy, cost, sample size, and most importantly, resolution and accuracy of measurements.

Table 1-1. Tabulation of waveband with corresponding wavelength, frequency and magnetic field.

Waveband	L	S	X	K	Q	W	F
$\lambda(\text{mm})$	300	100	30	12.5	8.5	3.2	2.7
ν (GHz)	1	3	10	24	35	95	111
B_0 (T)	0.03	0.11	0.33	0.86	1.25	3.5	3.9

1.8. EPR DOSIMETRY

A little over ten years after the Zavoyskiy and Bleaney's discovery, radiation induced EPR signals in proteins and a persistent signal in irradiated skull bone were reported by Gordis et al. [17]. EPR dosimetry is a physical method of assessing radiation dose that bases its measurements on this persistency and the stability of the radiation induced radicals. After radiation exposure of calcified tissues, rich in the hydroxyapatite ($\text{Ca}_{10}(\text{PO}_4)_6(\text{OH})_2$), stable radiation induced radicals are formed, which are measured

using EPR in radiation dosimetry. In 2002, the IAEA recognized the use of EPR biodosimetry in calcified tissues (teeth and bones) as an accurate method for retrospective radio-epidemiological studies. It recommended the use of EPR dosimetry as a complement and validation method to other biological and physical dosimetric methods, such as cytogenetic biodosimetry, fluorescence *in situ* hybridization (FISH), thermoluminescence (TL), and optically stimulated luminescence (OSL) [1].

EPR retrospective studies in calcified tissues are based on the measurements of radiation induced radicals in hydroxyapatite. This is a naturally occurring form of calcium apatite with the formula $\text{Ca}_5(\text{PO}_4)_3(\text{OH})$, usually written as $\text{Ca}_{10}(\text{PO}_4)_6(\text{OH})_2$ to denote its two molecular crystal unit. It has an average $Z = 16.24$ and makes up 95 – 97 % of tooth enamel, 70 – 75 % of dentin, and 60 -70 % of bones [19].

There is a need in EPR dosimetry to have sensitive enough measurements throughout a desired radiation dose range with a linear response, if possible. Of concern, is the stability of the signals and variation due to ambient conditions, light, temperature, and humidity [17]. Fading of the signal was reported to be from the combination with other paramagnetic species (resulting in diamagnetic products), or transformation into other paramagnetic molecules [49, 50].

EPR dosimetry in teeth and bones is founded on the linear dose dependence used to assign a dose from the magnitude of the peak-to-peak amplitude of the EPR signal. Several dose assessment methods have been proposed in the past, an additive dose method, a partial calibration method, and the use of a universal calibration curve (standard dose response curve) [51]. The additive dose method is based on sample response to an additional dose. The sample serves as its own standard and is individually

calibrated and incrementally irradiated. As shown in Figure 1-4, linear regression analysis is used on the EPR measurements to obtain the original administered or suspected accidental dose, which is derived from the negative intercept of the regression line with the dose axis [1, 52]. A partial calibration method has been described for tooth enamel and deals with the irradiation of a small fraction of the sample to a large dose. The EPR signal is then evaluated for both fractions of the sample [53, 54]. The universal calibration curve method uses already established calibration curves, developed using linear regression for a set of doses. It assumes that there is not significant change between samples [1, 3].

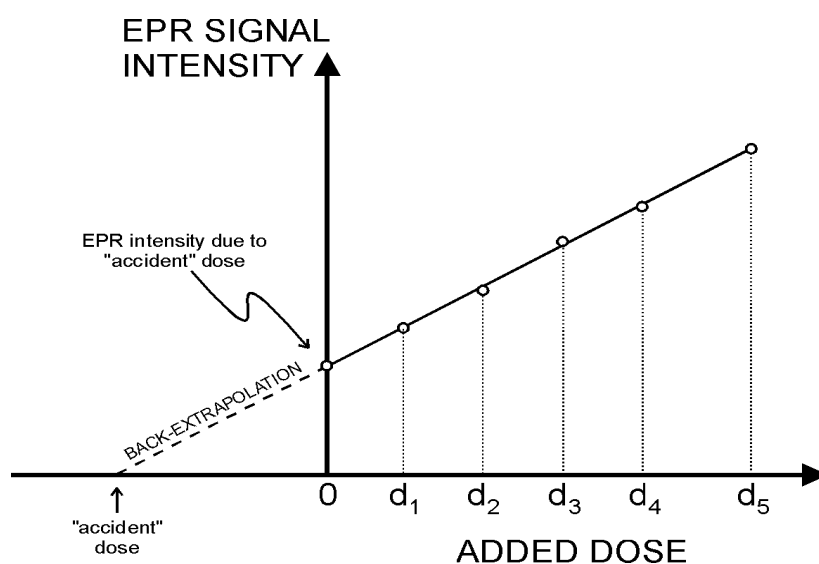


Figure 1-4. Illustration of the additive dose method for EPR dose assessment

The EPR response to radiation has to be assessed prior to any dose assessment. Several methods have been documented for accurately isolating this response in calcified tissues. These include deconvolution, spectrum subtraction, selective saturation, and second derivative methods [51, 55]. The deconvolution method uses mathematical

approximation of EPR signals using the first least-square technique or the second approximation routine, which is based on the multivariate statistical decomposition method [1, 56]. The spectrum subtraction method involves several ways of subtracting the spectrum obtained from a non-irradiated reference sample, as done with tooth enamel samples [1, 51]. The selective saturation method banks on the fact that with increase power, a background (native) signal saturates and therefore, it can be eliminated by its subtraction from the dose response signal [24]. The second derivative method employs the second derivative spectrum, without any subtraction [57].

The presence of other non-radiation-induced signals in the EPR spectra makes it difficult to use EPR dosimetry at low doses, below 5 Gy. The reproducibility of EPR dosimetry measurements has been associated with random errors, such as instrumental fluctuations and environmental conditions. These and other sources of uncertainties in EPR tooth and bone dosimetry have been well documented [7, 19, 51, 55, 58-61]. However, EPR dosimetry remains a very sensitive technique for retrospective dosimetry and epidemiological studies [11, 62-68] with recent advancements that allows in vivo measurements [69].

1.9. EPR DOSIMETRY IN FINGERNAILS

Radiation-dose dependence of EPR signals were extensively studied in the fifties using several biological dosimeters, such as proteins, amino acids, fatty acids, and hydroxyl acids [16]. Later on, hard tissues, such as teeth enamel and dentine, bone, hair and nails were considered [5]. The use of fingernails EPR dosimetry has attracted the

research community because of its potential as a good technique with reported high sensitivity and easier sample collection techniques and handling methods [27, 33, 70, 71]. It is obviously easier to collect people's fingernails or toenails than teeth and bones after a radiological accident or incident. Finger and toenails are mostly composed of alpha keratin (Figure 1-5), a protein that has three long alpha helical peptide chains twisted in a left-handed coil and strengthened by sulfur bridges formed from cystine groups. The alpha keratin in fingernails has a greater amount of sulfur crosslinks than other tissues, such as hair tissue, giving nails a more rigid structure. Fingernails grow at an average rate of 1 mm per week [72] with faster rates being common. It takes about 3 to 6 months to completely regrow fingernails, whereas toenails take 12 to 18 months. Age, season, exercise levels, and other factors, including some hereditary factors, affect the actual growth of human nails.

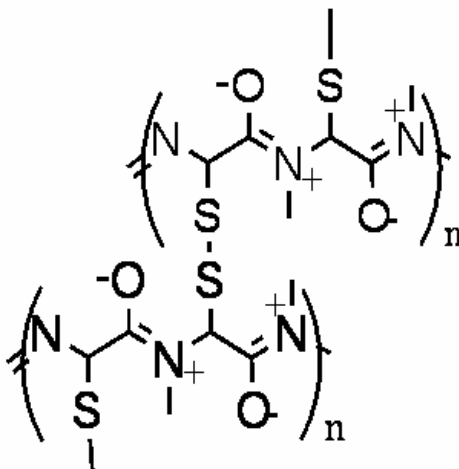


Figure 1-5. Chemical illustration of alpha keratin in finger and toe nails.

The exact chemical composition of fingernails has been mainly studied in forensic medicine and dermatology [73, 74]. Many metal and other traces have been documented

in human nails using several techniques, such as photon-induced x-ray emission (PIXE) technology, atomic absorption spectrophotometry, neutron activation analysis, and isotope ratio mass spectroscopy [75-80]. Olabanji reported high levels of Sulfur (5,778 - 47,460 $\mu\text{g/g}$) in human fingernails and compared the mean values of the its elemental composition in ppm ($\mu\text{g/g}$) with other authors using the same (PIXE) and other techniques [79]. Vellar studied the composition of human fingernail and reported that nitrogen was the major component, and that the levels were compatible with that of dry hair [81]. This makes sense because keratin is the major component of fingernails and hair. Vellar also found that the annual loss of the reported components was negligible [81] after cut. This means that changes in the weight of fingernail samples after cut are due to the drying process with no significant loss of its chemical constituents (except water content). Furthermore, it may help explain some of the behavior of fingernails EPR signals.

The idea of studying freshly cut fingernails is guided towards simulating the cutting immediately or soon after a radiological accident. However, retrospective studies of past exposures using fingernails as biological dosimeters have shown to be just as useful for this technique of biodosimetry. EPR fingernail dosimetry studies are done in normal fingernails and do not address illness that may cause physical deformation, thinning, thickening, brittleness, or other changes. It is not known if any of these changes have an impact on the EPR signal of finger or toenails.

The most challenging factor to consider when using fingernail EPR dosimetry is the presence of other-than radiation induced signals that will mask the RIS. These signals have been characterized as the background signal (BKS) and the mechanically induced

signals (MIS) [27, 82]. The BKS has similar spectral parameters, linewidth, shape, and g-factor to the RIS. When the combined effect of the MIS, BKS and RIS is not carefully considered, an overestimation of the dose is inevitable.

After correction for the combined effect of the MIS and the BKS, fingernail samples do give a unique RIS that is proportional to the radiation dose. In order to make fingernails a practical biosample for EPR dosimetry a method for isolating the MIS and BKS needs to be developed. The MIS has been documented as the signal produced from the formation of radicals in fingernails after cutting, which is most intense on freshly-cut samples [82]. The cutting of fingernails generates these radicals because of the small probability of having the scissors' blades slipping between the strongly held strands [27]. Figure 1-6 shows an illustration of two possible species of MIS. The C-C, C-S and peptide C=N-R bonds are stronger than the S-S bonds, which are assumed to break, creating sulfide free radicals as a result of the mechanical stress at cutting. The dominant MIS species are sulfur centered radicals with a characteristic spectrum [27]. The doublet splitting of about 8.5 G has been assigned to a proton in the unique cystine (cross-linked dimer) or cystiene (monomer) residue side chain. Figure 1-7 shows the spectra obtained by subtraction of the residual BKS spectrum after complete MIS fading of an un-irradiated fingernail sample. Sample size affects the EPR spectra from the MIS and therefore, it is important to consider it in fingernail dosimetry. Figure 1-8 shows the MIS increase in amplitude with sample size. Figure 1-9 illustrates how fading of the MIS is stabilized after 24 hours. This fading can be fit well with 2 exponential decays, with $t_1=0.28$ hr, and $t_2=2.5$ hr.

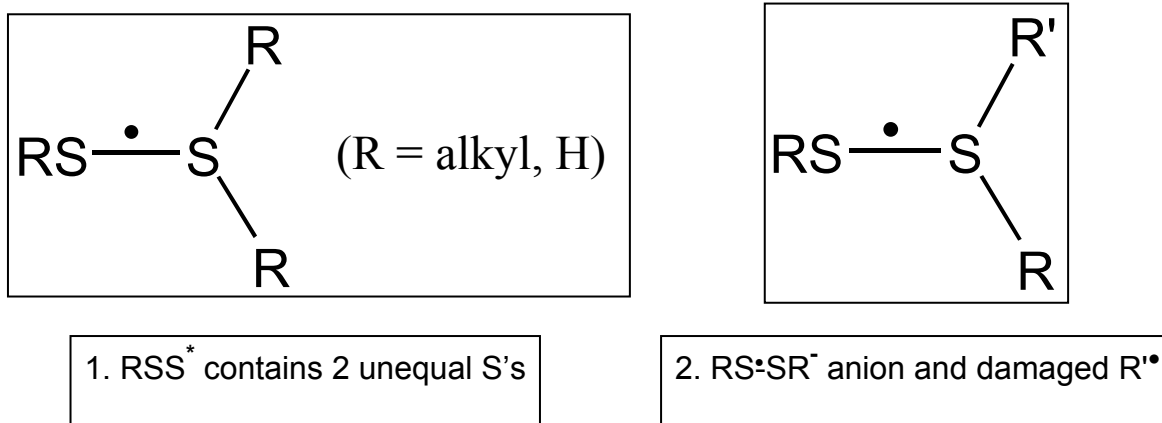


Figure 1-6. Diagram of two possible species of MIS [27].

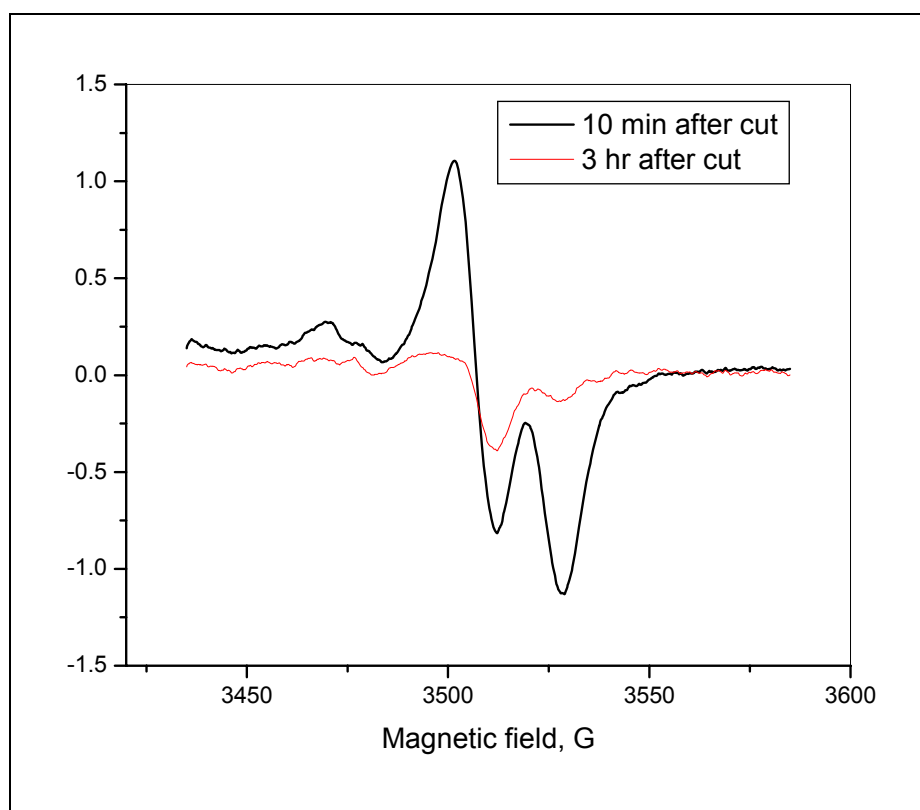


Figure 1-7. MIS spectra after cut and 3 hours later (MIS spectrum: $g = 2.015$ $DH=10$ G).

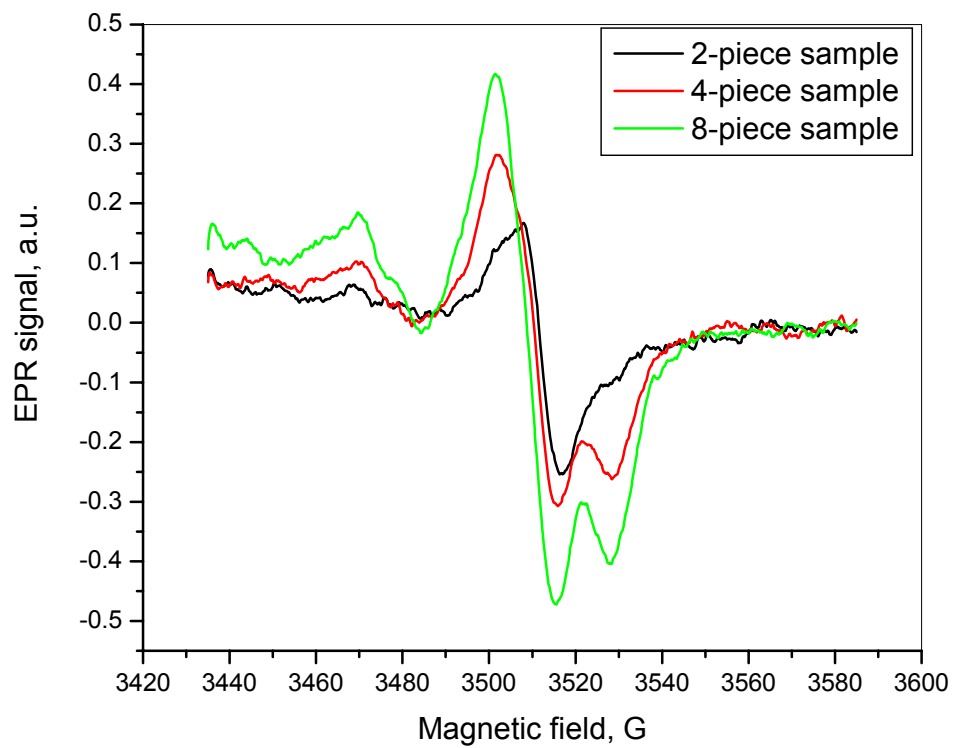


Figure 1-8. Fingernail MIS spectra from different sample size.

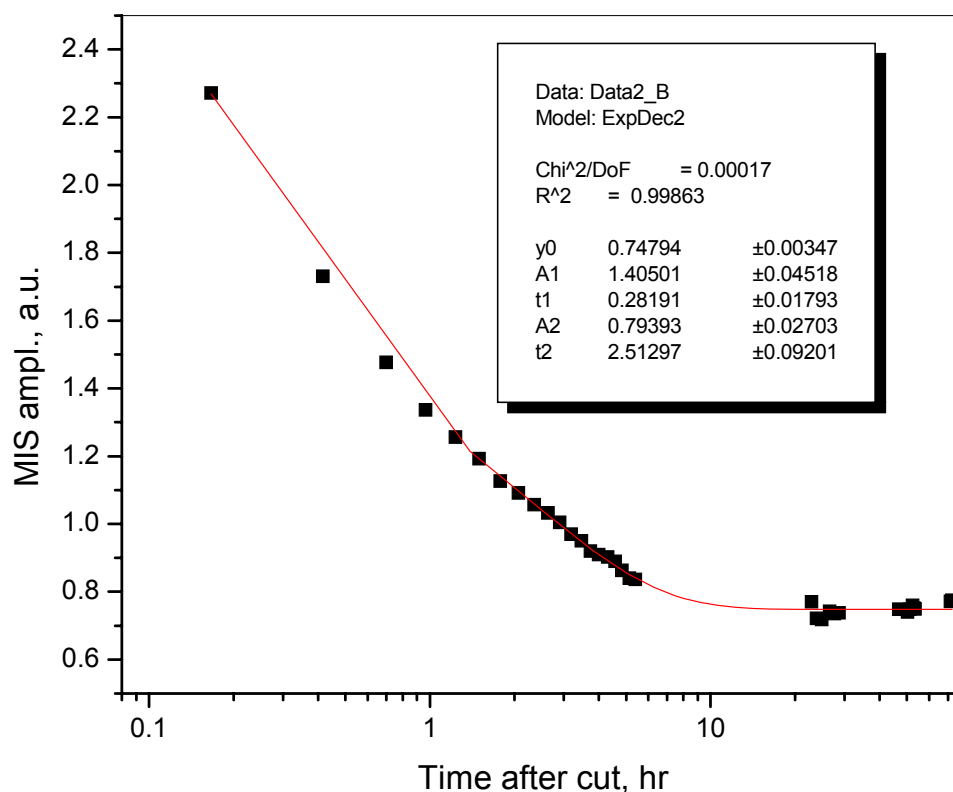


Figure 1-9. MIS spectra after cut and after a 3 hour delay.

It has been reported that treatment with sodium thioglycollate drastically reduces the MIS, which would naturally fade out in approximately 24 hours, and that it is nearly impossible to distinguish the MIS from the BKS. The origin of this BKS has not been identified yet. However, current research has focused on the mechanical behavior of the BKS as it increases with time, with the possibility that this signal may be directly proportional to the degree of elastic deformation of the fingernail sample as it dries out. Figure 1-10 shows the spectrum of the BKS, obtained from an un-irradiated sample after the complete fading of the MIS, 24 hours after the trimming of the fingernail.

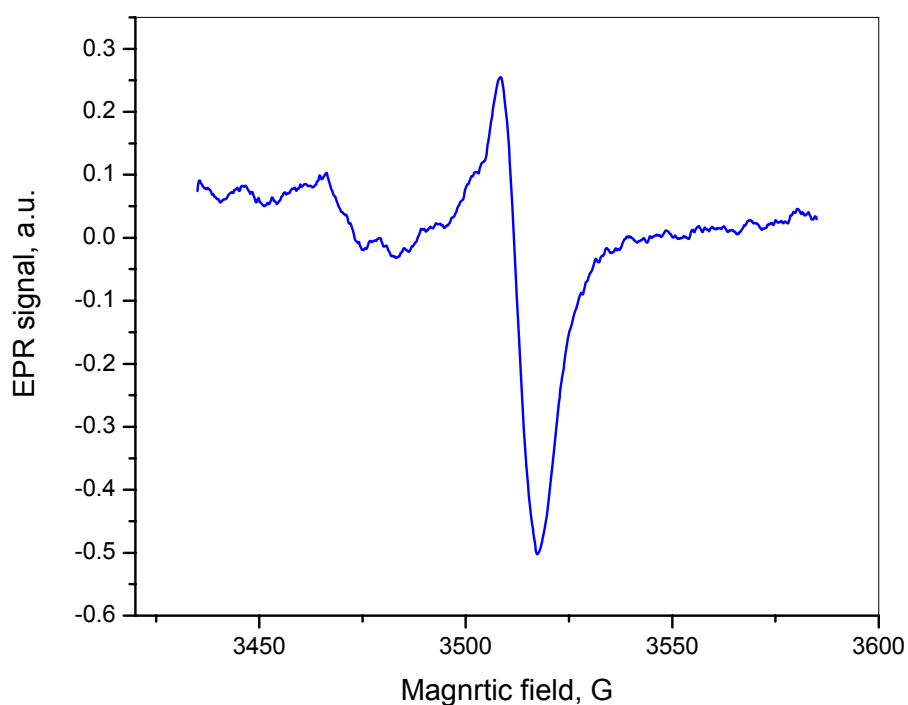


Figure 1-10. BKS spectrum from un-irradiated sample (BKS parameters: $g=2.0075$, $\Delta H=9$ G).

The origin of the RIS has been documented by Symons et al. [27, 83, 84]. The range of back-bone amide radicals, formed by the proton loss from the amide radical cations, located randomly in the amide back-bone, were identified as the initial “*hole centre*”, illustrated in Figure 1-11. These “*centres*” are rapidly trapped due to the higher rate of proton transfer than hole transfer. Aside from this, Symons et al. suggested the probability of having more than one type of radical involved, as secondary radicals formed from the secondary reactions with MIS radicals [27]. Figure 1-12 shows RIS spectra obtained by subtraction of BKS spectrum recorded prior to irradiation. The RIS has about the same linewidth as the BKS, but more symmetric lineshape and slightly

higher g-factor (+0.001). Although there is fading of the RIS with time, irradiated samples that are kept at low temperatures have shown no significant fading, which is a positive characteristic for fingernail dosimetry.

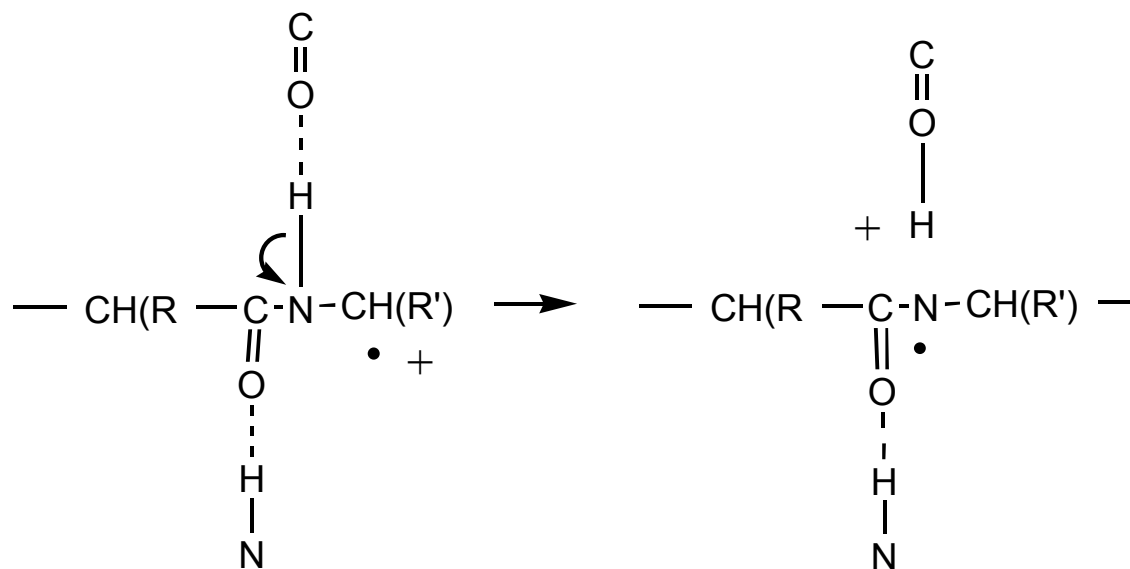


Figure 1-11. Radiation induced radical [27].

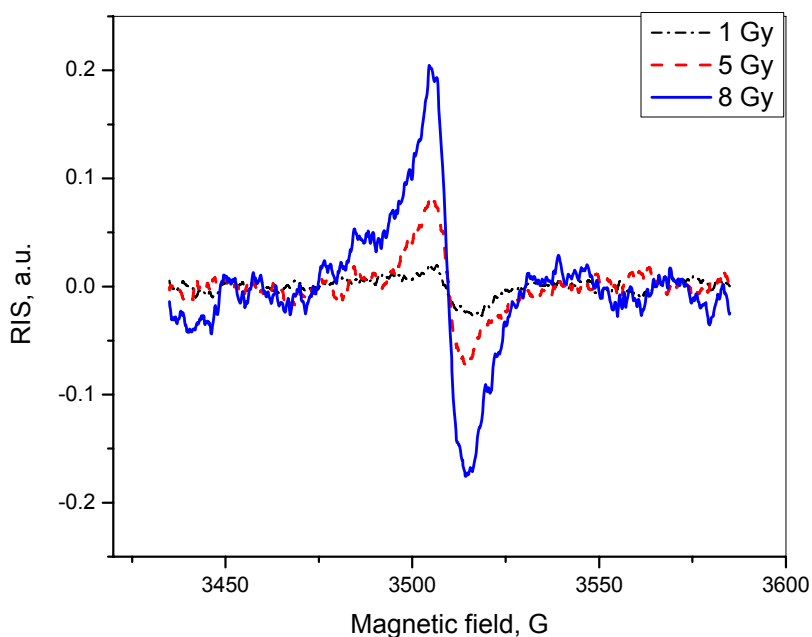


Figure 1-12. Spectra of the RIS at 1, 5, and 8 Gy (RIS parameters: $g=2.0088$ $\Delta H=9$ G).

The development of a viable method for using fingernails as biodosimeters is made possible by determining all the modifying factors that do affect the assigned dose, which is based on this measured RIS. Some of these factors are being addressed by scientific groups looking to reduce or eliminate the effect of non-desirable EPR signals, reporting on innovative chemical treatments to address the effect of these signals that perturb the RIS [70] and its potential use in radiological emergency protocols [33]. However, sources of error in fingernail EPR dosimetry may still emerge from: radiation source homogeneity characteristics or lack thereof, mixed radiation fields, partial-body exposures, and interpersonal variability among people with skin conditions that affect fingernails.

CHAPTER 2

RESEARCH OBJECTIVES AND METHODOLOGY

The use of EPR dosimetry technology on teeth and bones involves invasive procedures, as compared to using cut fingernails as biophysical samples. Fingernails exposed to gamma radiation, simulating exposure to individuals, can serve as biological dosimeters (biodosimeters) in the event of radiological accidents/incidents. These nails can be collected for measurements at the site of treatment during the triage phase or later on for a retrospective dose assessment.

This study is part of a larger investigational project in EPR dosimetry: Center for Biophysical Assessment and Risk Management Following Irradiation – EPR Dosimetry. Approval for this research study design and recruitment of donors was obtained from the Institutional Review Board of the Uniformed Services University of the Health Sciences. The following are summarized steps addressed in this research for the development of fingernail EPR dosimetry as a practical technique:

- (1) study of fingernail clippings - effects of sample collection and preparation techniques on EPR signals;
- (2) evaluation of EPR properties of irradiated and unirradiated, treated and untreated, fingernail samples and the physical properties of its spongy-like tissue that affect EPR signals;
- (3) evaluation of the interpersonal and intrapersonal variability of fingernail samples in EPR dosimetry measurements;

- (4) investigation of the EPR signal stability and evaluation of its dose dependence variable, which is non-linear in nature, in order to determine if it could be used for dose assessment when appropriate sample collection, storage, and preparation procedures are developed; and
- (5) further detailed study of the effect of cutting at sample collection after *in vivo* treating of irradiated fingernails, sample storage, and further preparation prior to EPR measurements.

This research hypothesizes that fingernail clippings can be used as rapid and effective biodosimeters for suspected radiological casualties using EPR/ESR dosimetry technology.

Null Hypothesis, H_0 : Fingernail clippings cannot be used as biodosimeters of suspected radiological casualties using EPR/ESR dosimetry technology.

In order to evaluate the fingernail EPR signals, one needs to identify and evaluate all of the contributing factors: weight, number of clippings, spectrometer settings, sample collection and preparation, temperature, and the presence of other signals. The EPR signals increase with sample weight, as seen in preliminary studies, and therefore, measurements are normalized to weight. The same effect is observed with increased number of untreated nail parings (clippings), as shown in the introductory chapter. The Bruker ELEXSYS 500 (Bruker BioSpin) spectrometer, equipped with a super-high-Q resonator ER 4123SHQE in X-band (9-10 GHz) was used for measurements at room temperature. The spectrometer settings, derived as most efficient for fingernail dosimetry during preliminary studies, were set as follows: HF modulation: 100 kHz; amplitude of

HF modulation: 5 G; microwave power: variable; receiver gain: 60 db; time constant: 81.92 ms; number of points: 1024; sweep time: 41.96 s; number of scans: 10; total recording time: 7 min; central field: 3510 G; and sweep width: 150 G. During sample collection, fingernails were cut using a sharp scissor, having the majority of the sample trimmings used in the study sized to 1-2 mm by 4-7 mm clippings, with weights between 15 and 30 mg. Samples were prepared by chemical treatment with an aqueous solution² (water) using methodology described in and protected by US patent (provisional # 60/924,034) [71]. Changes in RIS signals with time after exposure have shown that at low storage temperatures ($\approx -20^{\circ}\text{C}$), these signals persist with no noticeable fading. Therefore, irradiated samples that were used for studying dose dependency were stored at freezing temperatures. The presence of other signals, MIS and BKS, has been documented to obscure the RIS at low doses and are difficult to separate. This is addressed by proposing three methods for isolating these signals, as shown in the first manuscript [85], which also includes descriptions of several experiments used to isolate the MIS and BKS. After evaluation of these factors, the null hypothesis, H_0 , will be rejected if we can show that there is a direct strong correlation between radiation exposure and fingernail EPR signals and that the interpersonal variability does not significantly affect the behavior of these signals.

² The process of chemical treatment is the subject of a patent disclosure (provision patent 60/924,034 was filed on 04/27/07).

2.1. SPECIFIC AIMS

The following specific aims are drawn to support our hypothesis:

- (1) Characterization and independent evaluation of the fingernail EPR signals: MIS, BKS and the RIS, development of ways to reduce or eliminate the confounding effect of the non-radiation signals (MIS and BKS), and isolation of the RIS.
- (2) Study the behavior of these signals with time and the dose dependency of the RIS using untreated and treated samples, as a rapid method for sample processing (including treatment) during a radiological emergency is investigated.
- (3) Evaluation of the statistical correlation between EPR signals of irradiated fingernails and radiation dose and documentation of the interpersonal and intrapersonal differences of this correlation.

2.2. EXPERIMENTAL DESIGN

We used the Bruker Elexsys E 500 spectrometer for our measurements. The EPR radiation induced signal intensity is proportional to the radiation dose at constant linewidth and signal shape and is quantified using the value of the peak-to-peak amplitude of the EPR signals. The specific method used in this study is based on methods published by Dalgarno et al. in 1989 [6] and Romanyukha et al. in 1996 [59] and follows USUHS protocols G18983 and T087M3 [86, 87]. This study was designed in three stages in order to be able to perform the desired measurements and characterize the EPR response to radiation dose in fingernails. Stage 1 includes the collection and

preparation of samples. During stage 2 samples are irradiated using a gamma irradiator (Gammacell 40, ^{137}Cs : 44Gy/hr). Stage 3 encompasses the data interpretation and statistical analysis for the study of the interpersonal and intrapersonal variability of the EPR radiation induced signals in treated and untreated fingernails samples with increasing absorbed dose.

STAGE 1. Sample collection and preparation.

Sample collection and preparation were done in accordance with already established USUHS protocols G18983 and T087M3 [86, 87]. During this stage, many experiments were designed to evaluate several sample collection and storage techniques and the effect of treatments on the EPR signals before and after irradiations. The sample treatment of choice with water was evaluated during this stage to see if there was a general improvement of signal response (sensitivity) in a similar fashion to that performed in the study done by Toyoda [88].

The method for sample collection using sharp scissors and preparation was developed after several experiments during the preliminary data gathering stages of this research. Some of these experiments included the measurements of fingernail trimmings with no treatment and for various mass weights, the *in vivo* treatment of fingernails prior to cutting, and the treatment of fingernails after trimming.

Measuring of fingernails without treatment showed EPR signals that were obstructed by an increasing BKS and simultaneously fading MIS, as shown in the first manuscript [85]. After correction for these two obstructing signals, the use of untreated

samples for fingernail EPR dosimetry using the additive dose method showed a linear response. However, this technique may be hindered by the instability of these signals in untreated fingernail samples. Various weights were used during preliminary studies, finding most convenient to use samples that are at least 15 mg and 1-2 mm by 4-7 mm for a loose fitting inside EPR spectrometer sample tubes. Normalization to weight allows EPR measurements of samples below 15 mg but with limited compromising on the magnitude of the EPR signals.

Appendix A shows a preliminary study in which we evaluated the effect on the number of cuts and size of fingernail clippings on EPR radiation dose measurements. A significant finding of this study was that the number of cuts in treated fingernail samples did not significantly affect the radiation sensitivity. Samples with small pieces showed a higher BKS and powdered samples proved to be best for dose measurements. However, the goal of using a simple method for sample preparation of this study would not be met if we have to crush every collected sample after freezing it with liquid nitrogen, as it was done in the preliminary study.

The *in vivo* treatment of fingernails for several minutes prior to cutting still showed a MIS, induced at the time of cutting. Only treatment of the fingernail clippings after cutting showed a significant reduction of the induced MIS, as shown in manuscript 1 [85]. Romanyukha et al. reported on the chemical treatment of fingernails for EPR dosimetry [70]. Chemical treatments using aqueous solutions had a physical/mechanical effect on the samples. As explained by the sponge model described in manuscript 1, these treatments restored the shape of the spongy tissue of the fingernail samples, which had been mechanically deformed by the forces exerted on the samples at time of cutting.

This physical restoration of the samples by water absorption was the basis for the development of the water treatment that would eliminate the combined effect of the MIS and BKS.

A set of experiments, designed to measure the amount of water fingernails can absorb and the effect of this absorption on the EPR signals, followed. Appendix B shows an experiment designed to develop saturation curve lines for finger nails in order to evaluate the proposed treatment of nails with water for EPR measurements and the sponge behavior theory, explained in manuscript 1. This manuscript also showed a quick method of determining the porosity of the spongy tissue in fingernails, as the fraction of void space, by using the ratio of maximum volume absorbed in water and the original volume of the sample obtained in this experiment.

The proposed treatment is a water bath for 10 minutes with at least 5 minutes of drying time before measurements. The combined effect of the MIS and the BKS was reduced by a factor of 3 in average with the same treatment for nails that had been collected for longer than 24 hours and by up to a factor of 10 for recently cut fingernails. This is shown in Figure 2-1. The data was collected for ten samples that were made of freshly cut fingernails and ten samples made from previously collected nails. The clear difference in the amplitude of the signals from the recently cut versus those previously collected fingernail samples may be explained by the magnitude of the mechanical stress, which samples are subjected to at both time of clipping *in vivo* and during further cutting at time of sample preparation. Sample thickness and the number of cuts might have also affected the amplitude of these signals and therefore it is also possible that one treatment did not completely reduce the MIS and BKS signals in some of the previously collected

samples. For freshly cut fingernail samples, the treatment of 10 minutes with water and 5 minutes dry time was sufficient to eliminate the MIS and reduce its combined effect with the BKS by close to 90 percent, as shown in Figure 2-2. Figure 2-3 shows the effect of water treatment on the MIS and BKS signals in freshly cut fingernails. For this experiment 4 samples were used and the average signal intensity were recorded and plotted. The signal was reduced by close to 90 percent and continuous water treatment of samples did not further reduce the signal.

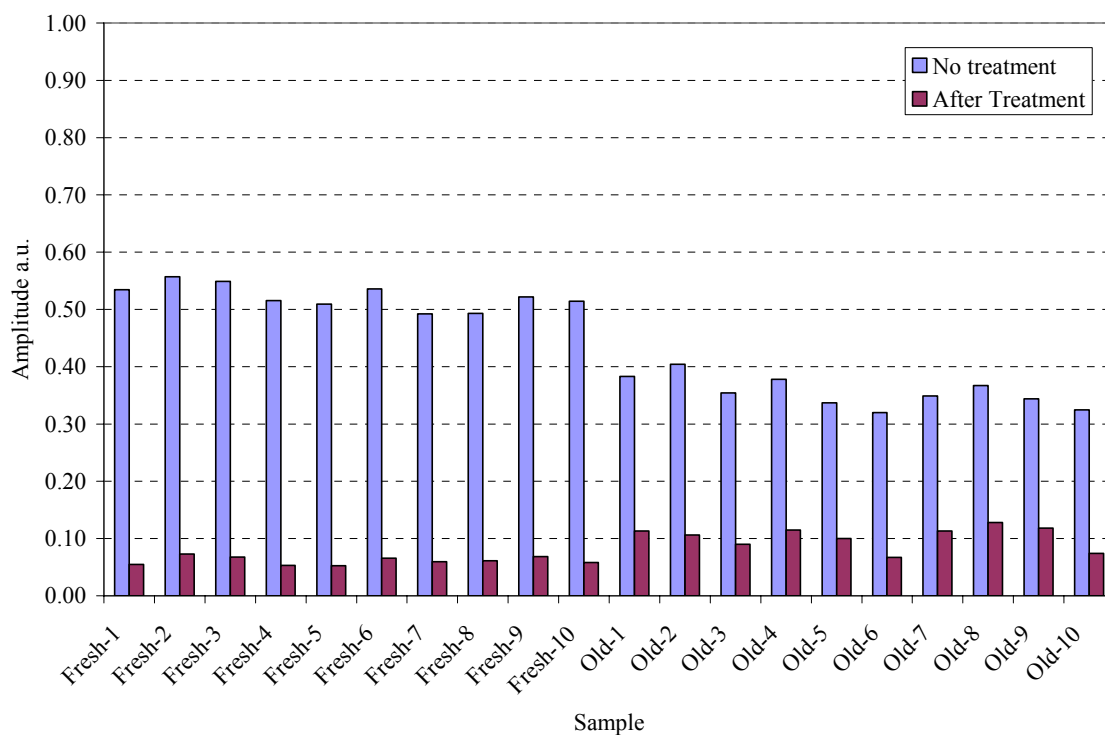


Figure 2-1. Effect of water treatment on freshly and previously cut fingernail samples (15 mg).

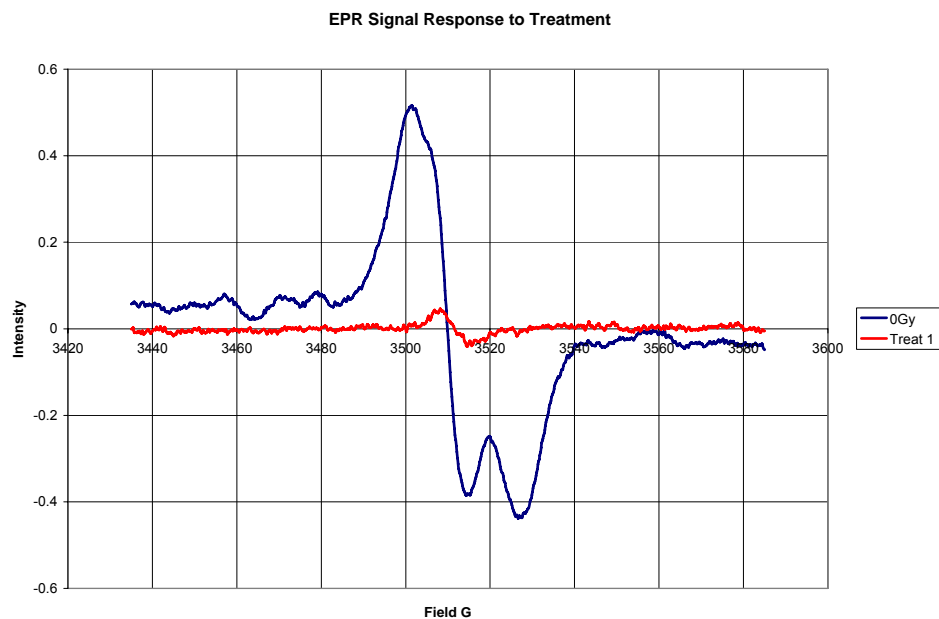


Figure 2-2. Effect of water treatment on the MIS and BKS signals in freshly cut fingernail samples.

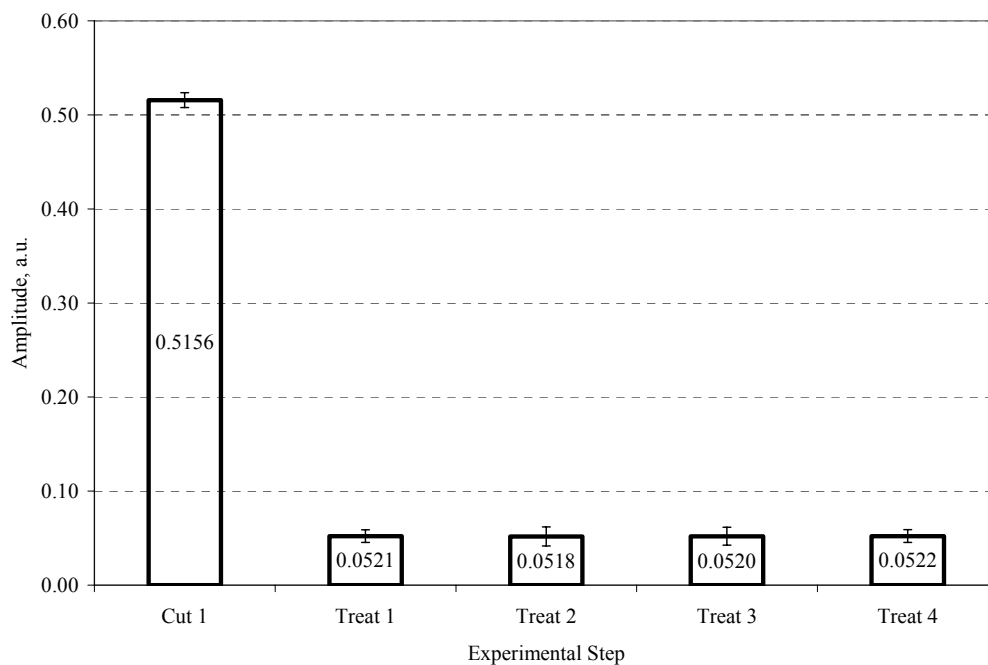


Figure 2-3. Effect of continuous water treatment on the EPR signals amplitude in freshly cut fingernails (20 mg).

Figure 2-4 shows the results of a prototype experiment that included two freshly cut samples from the same donor. The values in this chart are the mean values of their EPR signals amplitude. Treatment of the samples reduced the signal to close to a factor of 10. Irradiations of treated samples caused a definite increase of the signals. Measurements after the second cuts indicated an increase in the signal due to the mechanical stress from the cutting during sample preparation. The second treatment reduced the signal that had increased from the second cutting to a value close to the first irradiation. Consecutive treatments after irradiation did not significantly change the RIS showing that the water treatment of 10 minutes with a drying time of 5 minutes was sufficient to eliminate the MIS and significantly reduce the BKS without affecting the RIS.

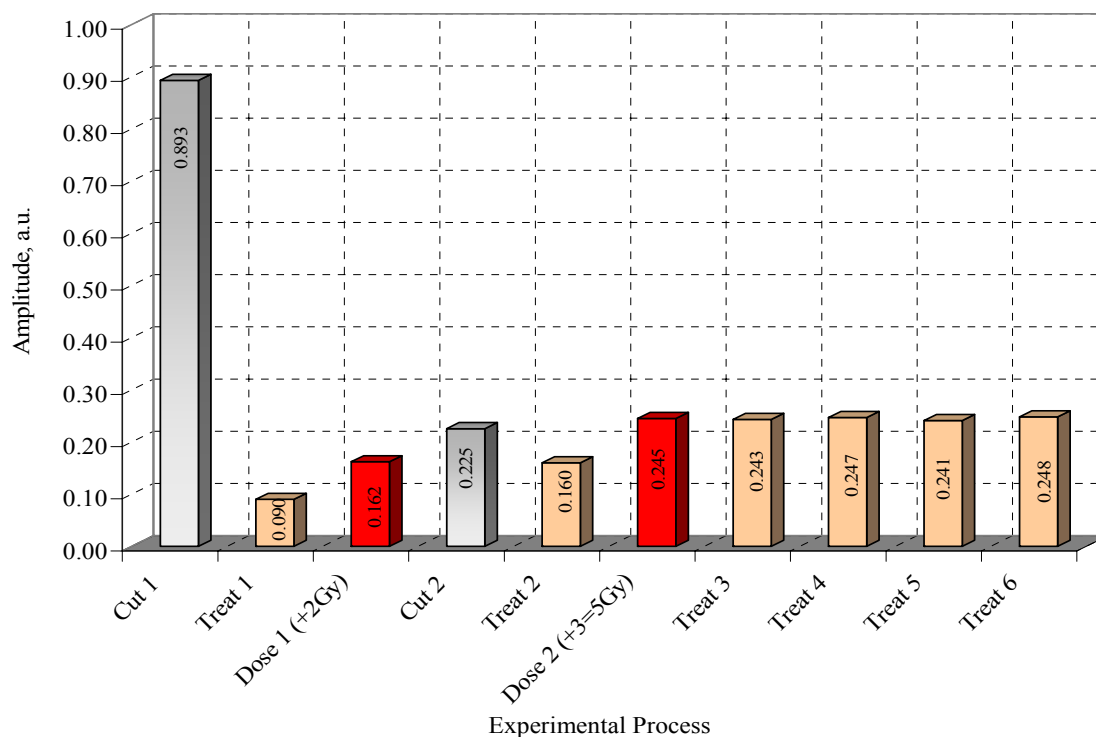


Figure 2-4. Effect of water treatment on the MIS, BKS, and RIS signals in freshly cut fingernail samples (40 mg).

STAGE 2. Irradiation.

In order to simulate radiation exposure, collected biosamples were irradiated with a gamma source (Gammacell 40, ^{137}Cs : 44 Gy/hr) and analyzed using the Bruker Elexsys E 500 EPR spectrometer in the X band (9 GHz). This stage included the measurement of background samples using both, freshly cut and previously collected fingernail samples. During this stage, fingernail samples were irradiated in steps of increase dose without the use of any chemical treatment and weighted (to use data in normalization). Treated samples were irradiated and measured in the same fashion. The step increase in dose is designed to derive the data for linear regression and prediction of lower dose points (additive dose method), as described in Desrosiers and Schauer for tooth enamel [19].

The Gammacell 40 is a Cs 137 irradiation unit manufactured by Atomic Energy of Canada Limited. It is designed for use in an unshielded room and provides means for uniform gamma irradiation of small biological samples. The Cs 137 encapsulated capsules are mounted in brass encased lead filled horizontal cylinders, 2.5 in (6.35 cm) diameter and 16 in (4.64 cm) long, held together by Truarc retaining rings (one to each capsule). The Cs 137 double encapsulated sources are housed in each of two cylindrical sliding drawers, one above and one below the sample cavity. The drawers are moved from the shielded position to the irradiate position by pneumatic cylinders. The sample cavity itself is made of an aluminum ring 13.0 in (33.02 cm) inside diameter by 4.875 in (12.38 cm) deep. The cavity is open at the top and bottom and has hanger slots in the top rim from which to suspend the sample tray. The ring is secured to a hinged door such that when opened, the sample tray swings out with the door and is accessible without reaching

into the irradiation cavity.

Even though buildup (ratio of detector's response to collided photons over its response to uncollided photons) was not expected due to the plexiglass containers used during irradiations with the Cs 137 irradiators, we performed a simple experiment, which is delineated in Appendix C. Buildup can be explained as the ratio of the intensity of the radiation (including primary and scattered radiations) to that of the primary radiation only at the sample site. Based on the results shown in appendix C, we can set our buildup factor to 1.

STAGE 3. Data interpretation - EPR signal correlation and interpersonal variation.

The collected data is used for investigating what type of EPR dose signal (peak to peak) dependence on the delivered dose is there (using statistical regression). We can then use the results for characterizing and quantifying radiation exposure in human nails, as attempted in manuscript 2. Furthermore, these results are used to reevaluate and optimize sample preparation procedures used in stage 1 and support recommendations for further research.

Although the data to be produced would give accurate dose estimations within the range of exposures, linear regression may offer the estimation of other points at lower levels of radiation, which would otherwise be very difficult to assess. This study supports the analysis of dose-response and variations in sensitivity between nail samples, as shown in manuscript 2 and in a similar fashion to what has been done for tooth enamel and reported by Romanyukha et al. [89].

The variability of continuous measurements was tested during preliminary measurements and the development of pilot data. Table 2-1 shows the average response for 10 nail clippings, and Figure 2-5 its corresponding plots. Each sample was consecutively measured 10 times and the reported values were normalized to weight. The average weight of the samples was 20.5 mg. The average reading was 0.3771 with a standard deviation of 0.0431 for all measured samples and the highest standard deviation, found in sample 8, was 0.0059. Measurements showed a slight change possibly due to the combined effect of the fading MIS and the increasing BKS during the measurement period. None of the samples used were treated and may have had different number of clippings that could have affected the minimal statistical fluctuations observed. By having the same number of clippings and all samples treated the same way, these statistical fluctuations are expected to be minimized or disappeared.

Table 2-1. Average EPR response for fingernail clippings measuring 10 samples and normalizing to weight.

Measurement	No. 1	No. 2	No. 3	No. 4	No. 5	No. 6	No. 7	No. 8	No. 9	No. 10
1	0.4160	0.3219	0.3270	0.3336	0.3631	0.4104	0.4618	0.3618	0.3443	0.3795
2	0.4178	0.3241	0.3301	0.3372	0.3700	0.4130	0.4641	0.3664	0.3493	0.3811
3	0.4189	0.3244	0.3310	0.3375	0.3700	0.4107	0.4639	0.3670	0.3484	0.3814
4	0.4188	0.3238	0.3316	0.3377	0.3680	0.4107	0.4672	0.3680	0.3459	0.3787
5	0.4230	0.3281	0.3319	0.3393	0.3713	0.4148	0.4684	0.3684	0.3508	0.3795
6	0.4200	0.3287	0.3336	0.3395	0.3730	0.4123	0.4656	0.3680	0.3475	0.3800
7	0.4205	0.3254	0.3311	0.3393	0.3766	0.4180	0.4689	0.3754	0.3492	0.3852
8	0.4295	0.3295	0.3372	0.3399	0.3771	0.4189	0.4700	0.3746	0.3492	0.3820
9	0.4235	0.3299	0.3378	0.3418	0.3754	0.4205	0.4709	0.3784	0.3484	0.3800
10	0.4164	0.3287	0.3344	0.3443	0.3770	0.4205	0.4672	0.3798	0.3434	0.3787
Average	0.4204	0.3265	0.3326	0.3390	0.3722	0.4150	0.4668	0.3708	0.3476	0.3806
SD	0.0040	0.0028	0.0033	0.0029	0.0046	0.0041	0.0029	0.0059	0.0024	0.0020

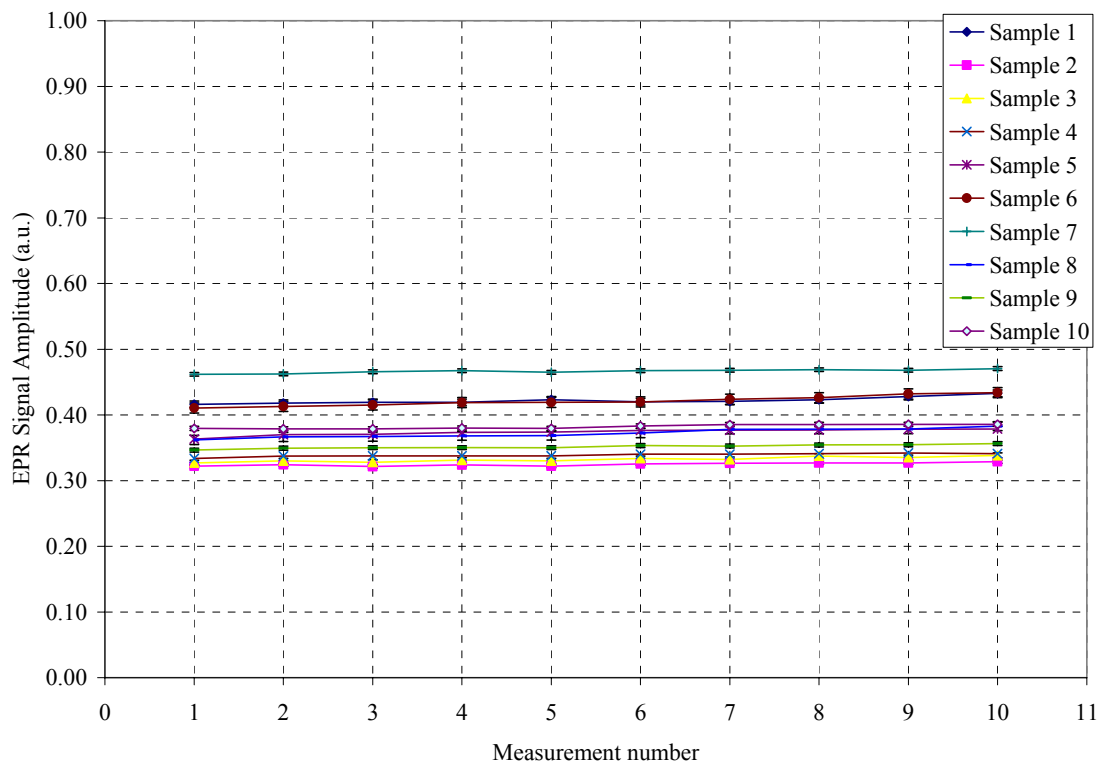


Figure 2-5. Plot of the mean EPR signal peak-to-peak amplitude for 10 untreated fingernail samples. Symbols represent the mean value of three measurements (10 scans each).

To estimate the sample size is difficult based on the limited number of studies of fingernail EPR dosimetry and the small sample sizes used in preliminary studies. Twenty samples, including those from the set above, were used during the preliminary studies in order to determine the number of samples necessary to have a sample set representative of normal fingernail EPR response. These were irradiated to in steps to 2, 3, and 5 Gy and measurements were made at their cumulative dose of 2, 5, and 10 Gy respectively. The slope was then computed for each data set, as shown in tables 2-2-a and -b.

We evaluated the pilot data in a similar fashion as that done by Dupont and Plummer for linear regressions [90]. We used the nQuery Advisor computer program by

Elastoff³ to calculate the necessary number of fingernail samples for comparing variations (slopes) in the dose response curves. The resulting values of n , using the preliminary data, are found in tables 2-2 A and 2-2 B. The mean slope for all samples was 0.0234 with a standard deviation of 0.0054. The highest estimated value of n , necessary for our experiments, was 16, based on the individual sets of data points from this pilot data for a minimum power of 80% with a 95% confidence interval (two sided significant level of 0.05).

Table 2-2 A. Preliminary data for samples 1 – 10.

Dose	No 1	No 2	No 3	No 4	No 5	No 6	No 7	No 8	No 9	No 10
0	0.4325	0.3285	0.3632	0.3440	0.3771	0.4380	0.466	0.3791	0.3552	0.3800
2	0.4700	0.3725	0.4230	0.3953	0.4014	0.4880	0.5158	0.4194	0.3976	0.4086
5	0.5395	0.4345	0.4900	0.4687	0.4680	0.5500	0.6042	0.4880	0.4621	0.4530
10	0.6282	0.5376	0.6500	0.5540	0.5760	0.6200	0.7338	0.5784	0.5579	0.5800
Slope	0.0198	0.0208	0.0284	0.0209	0.0204	0.0179	0.0270	0.0200	0.0203	0.0201
N	4	3	5	13	7	5	3	4	3	14

Table 2-2 B. Preliminary data for samples 11 – 20.

Dose	No 11	No 12	No 13	No 14	No 15	No 16	No 17	No 18	No 19	No 20
0	0.3218	0.3280	0.3401	0.4387	0.4284	0.3781	0.3570	0.3581	0.3733	0.3682
2	0.3730	0.3598	0.3995	0.4963	0.4559	0.4310	0.3890	0.4380	0.4337	0.4430
5	0.4510	0.4070	0.4887	0.5920	0.5110	0.5070	0.4730	0.5080	0.5243	0.5420
10	0.6180	0.4960	0.6800	0.7180	0.5980	0.5843	0.5250	0.6640	0.6500	0.6802
Slope	0.0297	0.0168	0.0340	0.0280	0.0172	0.0205	0.0173	0.0298	0.0276	0.0309
N	4	3	4	4	3	16	8	4	4	4

As shown in manuscript 2, for each collected sample, the slope is obtained by regressing the amplitude of the first derivative spectrum as a function of the ionizing radiation dose. The predicted dose is obtained from the interception of the regression

³ Copyright © 1995-2008 by Janet D. Elastoff.

line with the x axis. The mean and standard deviation were calculated for the slopes for $i=1...20$. This mean and standard deviation can be used to characterize the population of victims in a specific radiological accident/incident. The computer program SPSS 12.0.1 for windows was used for the statistical analysis of the data for both untreated and treated sets of samples ($n=40$), so that we could evaluate the correlation of the EPR radiation induced signals with the delivered dose and the interpersonal/intrapersonal variability. At the end of this stage, we offer recommendations, reported in manuscript 2, in support of the development of a method for fast retrospective radiation dosimetry using EPR and human nails as biological dosimeters.

Preliminary studies showed that the RIS magnitude is preserved at low temperatures with no noticeable fading. Appendix D shows a set of experiments that illustrate the study of the fading of the RIS in stressed and unstressed samples using two temperature conditions: low/freezing temperature ($\approx -20^{\circ}\text{C}$), and ambient temperature ($20-24^{\circ}\text{C}$ in laboratory). The RIS is stable at low temperatures and changes at ambient temperatures.

2.3. MANUSCRIPTS

“Electron paramagnetic resonance in human fingernails: the sponge model implication”

This manuscript is based on a study of the characteristics of the EPR signals in fingernail dosimetry with and without treatment and shows how during this study the sponge behavior of fingernail clippings was discovered. It offers details about the signals of non-radiation-origin (the MIS and BKS), which obstruct the RIS, and it shows three methods for isolating and eliminating their effect. The obvious spongy characteristics of fingernail clippings helped understand the behavior of EPR signals, which were related to the physical stress exerted on the samples at cutting and during their drying process with time. This manuscript describes the elastic and plastic deformations that affect the MIS and BKS respectively and suggests the use of 10 minutes water soaking of samples for its physical restoration. A proposed method for measuring porosity of the spongy tissue in fingernails and description of the EPR signals are offered. It was found that EPR signals of treated fingernails were less intensive and had a non-linear dependence. The findings in this study set the state for understanding fingernail EPR dosimetry and doing *in vivo* measurements in the future.

“EPR dose dependence in fingernails: Variability and possibilities of initial dose assessment”

This manuscript reports on the evaluation of the EPR dose dependence on fingernails and its variability. Five groups of samples were studied based on the time of fingernails collections, the level of mechanical stress in them, and their number and size of clippings: 1) stressed-fresh, controlled; 2) unstressed-fresh, controlled; 3) stressed-old, controlled; 4) unstressed-old, controlled; and 5) unstressed-fresh, uncontrolled. Except for the fifth selected group, variability of the dose dependence inside all groups were found to be statistically insignificant although the variability between the different groups was significant. Comparison of the mean dose dependences, obtained for each group, allowed selecting of key factors responsible for radiation sensitivity (dose response per unit of mass and dose) and the shape of dose dependence in fingernails. The major factor responsible for radiation sensitivity of fingernails was identified as their water content, which can affect radiation sensitivity up to 35%. The major factor responsible for shape of the radiation sensitivity was identified as the mechanical stress. At a significant level of mechanical stress, the shape of dose dependence is linear in the studied dose range (<20 Gy), and in lesser-stressed samples, it is of an exponential growth with saturation type which depends on the degree of mechanical stress. This manuscript showed the possibility for developing universal dose response curves in samples in which strict controls for weight, number of clippings, and time-since-cut are taken and offered recommendations on the appropriate ways of doing dose measurements in fingernails.

CHAPTER 3

“Electron paramagnetic resonance in human fingernails: the sponge model implication”

R.A. Reyes¹, A. Romanyukha^{1,2}, F. Trompier³, C.A. Mitchell¹, I. Clairand³, T. De⁴, L.A. Benevides², H.M. Swartz⁵

¹Uniformed Services University of the Health Sciences, Bethesda, MD, USA

²United States Naval Dosimetry Center, Bethesda, MD, USA

³Institut de Radioprotection et de Sûreté Nucléaire, Fontenay-aux-roses, France

⁴Howard University, Washington, DC, USA

⁵Dartmouth Medical School, Hanover, NH, USA

ABSTRACT

The most significant problem of electron paramagnetic resonance fingernail dosimetry is the presence of two signals of non-radiation origin that overlap the radiation-induced signal (RIS), making it almost impossible to perform dose measurements below 5 Gy. Historically, these two non-radiation components were named mechanically-induced signal (MIS) and background signal (BKS). In order to investigate them in detail, three different methods of MIS and BKS mutual isolation have been developed and implemented. Having applied these methods, it is shown here that fingernail tissue, after cut, can be modeled as a deformed sponge, where the MIS and BKS are associated with the stress from elastic and plastic deformations, respectively. A sponge has a unique mechanism of mechanical stress absorption, which is necessary for fingernails in order to perform its everyday function of protecting the fingertips from hits and trauma. Like a sponge, fingernails are also known to be an effective water absorber. When a sponge is

saturated with water, it tends to restore to its original shape, and when it loses water, it becomes deformed again. The same happens to fingernail tissue. It is proposed that the MIS and BKS signals of mechanical origin be named MIS1 and MIS2 for mechanically induced signals 1 and 2, respectively. Our suggested interpretation of the mechanical deformation in fingernails gives also a way to distinguish between the MIS and RIS. The obtained results show that the MIS in irradiated fingernails can be almost completely eliminated without a significant change to the RIS by soaking the sample for 10 minutes in water. The proposed method to measure porosity of the fingernails gave values of 0.46 – 0.48 (% void space) for three of the studied samples. Existing results of fingernail dosimetry have been obtained on mechanically stressed samples and are not related to the “real” *in vivo* dosimetric properties of fingernails. A preliminary study of these properties of pre-soaked (unstressed) fingernails has demonstrated their significant difference from fingernails stressed by cut. They show a higher stability signal, a less intensive non-radiation component, and a non-linear dose dependence. The findings in this study set the stage for understanding fingernail EPR dosimetry and doing *in vivo* measurements in the future.

Key words: accidental dosimetry, EPR, ESR, fingernails, external exposure, radiation dose reconstruction

INTRODUCTION

Fingernails have been proposed as a means to determine radiation dose to humans by measuring the density of radiation-induced radicals using electron paramagnetic resonance (EPR) [1-4]. An important advantage of such a technique is that fingernails can be quickly and painlessly obtained from an individual who has potentially been exposed to radiation doses in the range that may cause acute biological effects in humans (approximately, > 2 Gy). Previous studies however, have indicated that the radiation-induced EPR signal (RIS) is difficult to isolate from the native signal present in un-irradiated fingernails and the signal induced by the cutting process to obtain the fingernail sample. Furthermore, the EPR spectrum in fingernails is strongly dependent on the time and the manner the nail was cut. The purpose of this work was to determine if fingernails could be used as an accurate and ubiquitous dosimeter by overcoming these limitations.

The role of human fingernails is to provide protection to the fingertips from impact and contact with different media. Therefore, it is important to know the mechanical and chemical properties of fingernails and factors which can affect these properties. Generally, the mechanical properties of a material are determined by its chemical composition and structure. The major component of fingernails is α -keratin. This protein is based on three long α -helical peptide chains that are twisted together in a left-handed coil, strengthened by S–S bridges formed from adjacent cystine groups. The S–S bridges provide rigidity to human fingernails. Typical consequences of mechanical damage in any material are its deformation (elastic or plastic) and the creation of mechanically-induced

radicals, which are precursors of destruction. This is important because EPR is a specific and sensitive technique for measuring radicals.

In a previous study [5], an intensive EPR signal was found in freshly-cut fingernails. The authors named the observed signal mechanically-induced signal (MIS) and associated this signal with the sulfur-centered radical induced by mechanical stress during the cutting of fingernails. This study also reported that treatment with sodium thioglycollate eliminated the MIS. Other publications [1-4] discussed the development of ways to reduce or eliminate the MIS because this is an important issue for the use of fingernails as a personal dosimeter of radiation exposure. It has been reported that fingernails have a linear dose dependence on the EPR radiation-induced signal in a broad dose range (up to 100 Gy) with an estimated lower limit of detection of about 1 - 2 Gy [1, 2, 4]. This makes it attractive to consider the use of EPR in fingernails for rapid assessment of dose. However, there are a number of potential limitations for this application. First, the MIS and another signal called the background signal (BKS) severely obscure the radiation-induced signal (RIS) at low doses, and there is no easy way to separate the RIS from the total spectrum at doses below 5 Gy. To complicate things further, according to [1, 3, 4], it is nearly impossible to distinguish between the BKS and RIS when X-band microwaves (about 9 GHz) are used for EPR measurements in fingernails. Second, attempts to use the proposed treatment with sodium thioglycollate prior to dose measurements were not successful; in [1] the authors stated that they discontinued the use of this treatment because it “significantly modified the radiation response in fingernails”. In a recent study [3] seven chemical treatments were evaluated

and they were found to have an effect on the RIS. Third, the linear dose dependence in untreated fingernails became non-linear with RIS dose saturation at about 5-10 Gy in this study [3]. To date, the change of dose dependence has yet to be explained. Finally, and to make things even more complex, the authors of [4] reported a significant reduction of all EPR signals, e.g. MIS, BKS and RIS, after treatment of fingernails with just water. This fact could also significantly affect the applicability of EPR fingernail dosimetry because of the frequent contact between fingernails and water in the normal course of human behavior and especially after exposure to radioactive particulates.

Summarizing the known facts of fingernail dosimetry, we can conclude that in spite of the existence of some high-potential and attractive features, there is currently no model that can provide a general understanding of the mechanical and dosimetric properties of fingernails. The main goal of this study is to develop a model that explains the mechanical and dosimetric properties of human fingernails. In a detailed study, we will focus on the main components of the fingernails EPR spectra paying special attention on the following issues:

- isolation of the MIS and BKS in the total EPR spectrum of fingernails;
- determination of the origin of the MIS and BKS components of the EPR spectrum in fingernails;
- explanation of the reduction of the MIS and BKS with the treatment of fingernails with water; and
- identification of the effect of water treatment on the dose dependence of the RIS.

MATERIALS AND METHODS

Fingernail samples were collected from 10 different donors at different times (over 50 samples altogether) using a pair of sharp scissors to cut the fingernails. All fingernail samples were approximately 1-2 mm wide and about 4 -7 mm long. Each sample mass consisted of several pieces totaling 15-25 mg. Distilled and tap water were used in the experiments to evaluate the effects of water treatment on fingernails. A ^{137}Cs irradiator (Atomic Energy of Canada Limited Gammacell 40) with a dose rate of 0.7 Gy/min was used for irradiations. The EPR measurements were performed using a Bruker ELEXSYS 500 (Bruker BioSpin) spectrometer, equipped with a super-high-Q resonator ER 4123SHQE in X-band (9-10 GHz) at room temperature, and with the following recording conditions: high frequency (HF) modulation: 100 kHz; amplitude of HF modulation: 5 G; microwave power: variable; receiver gain: 60 db; time constant: 81.92 ms; number of points: 1,024; sweep time: 41.96 s; number of scans: 10; total recording time: 7 min; central field: 3,510 G (0.351 T); and sweep width: 150 G (0.015 T).

Several experiments were designed to investigate the separation of the MIS and BKS, their origin, the effect of water treatment on these signals, and the effect and modification of radiation dose dependences in treated and untreated fingernails. Two different types of experiments were designed to investigate the effect of fingernail cuts on the intensity of the MIS and BKS.

The first type of experiment was based on the time dependence of the MIS and BKS in the fingernail spectrum and was conducted on six different samples collected from three different volunteers at different times of the year. A single fingernail-clip was cut in two approximately equal pieces and measured with the EPR spectrometer at 1 mW of mw power. After 24 hours, when the MIS component of the signal had almost completely faded away, the EPR spectrum of this sample was recorded again in order to measure the BKS. After that, each of the two pieces was cut again into two approximately equal pieces, so that the original sample became a four-piece sample. The same measurements were performed on the four-piece sample as those done with the two-piece sample.

The second type of the experiment was based on the isolation of the MIS and BKS components by recording EPR spectra at two different powers (1 and 16 mW) and subtracting the spectrum collected at 16 mW (algebraically modified by using a multiplication factor, $(1/16)^{1/2}$) from that collected at 1 mW. Similar to the first type of experiments, a comparison was made between the intensity of the MIS and BKS before and after additional sample cuts.

In order to study effect of the treatment of fingernails with water in more detail, the following experiment was conducted on ten different fingernail samples:

- EPR spectra at our standard recording conditions and two mw powers (1 and 16 mW) were recorded on freshly-cut fingernail samples shortly after trimming;

- each sample was treated by soaking it in water (both distilled and tap water have the same effect on EPR signals) for 5 min, placing it on a paper towel, and letting it dry in open air for 5 minutes;
- EPR spectra were recorded on treated samples with the same conditions used for freshly-cut samples; and
- the above-described treatment, followed by EPR spectra recording, was repeated 5 times to determine an optimum time of the treatment.

In order to understand the effect of water treatment on the EPR spectrum of fingernails, the water absorption in fingernails was studied by repeatedly weighing the samples between periodic soakings and five-min drying intervals. The goals of this experiment were:

- to determine if there was any difference in water absorption at the first soaking of the fingernail between the time when a large reduction of the MIS component was observed and when only an insignificant change of the BKS component was observed;
- to determine if the absorbed water was chemically bound to fingernail matter; and
- to measure the maximum amount of water which can be absorbed by fingernails.

Eight different samples of clipped fingernails from six different persons and from the same persons at different times were collected either immediately before the experiment or up to one year before. These samples were repeatedly put into water for five minutes, wiped with a paper towel, and then air dried for five minutes. There were

more than ten cycles of soaking and drying the fingernails. After ten cycles of soaking and drying, the samples were split into two groups:

1. Samples 2, 3, 6, and 7 were left to dry and three or four additional measurements of their weights were performed at later times.
2. Samples 1, 4, 5, and 8 were left in the water bath and three or four additional measurements of their weights were performed at later times.

It has already been documented that water treatment of irradiated fingernails causes a strong reduction of the RIS [4]. However, the EPR radiation response in water-treated fingernails has not been studied yet. In an attempt to fill this gap, freshly-cut fingernails were first soaked for five minutes in water, dried and then during the same day, the EPR spectra were recorded after the sample was exposed to different doses of radiation starting from 0 to 4 Gy in 1 Gy steps.

The effect of water treatment on the MIS and BKS components has been found above to be similar to the effect of long-time (~200 hr) storage of untreated fingernails at room temperature. Unfortunately, at room temperature the RIS component in untreated fingernails fades away [1,2]. This makes it difficult to study the effect of time storage on the dose dependence in untreated fingernails at room temperature. Therefore, the dose dependence was first measured on a set of five untreated fingernail samples collected from the same person at the same time and irradiated with added doses of 0, 1, 3, 8 and 21.5 Gy, respectively. Then, these samples were stored in a freezer at -20° C for 82 days and re-measured with the EPR spectrometer because it has been noted in [1,2] that

storage of irradiated fingernails at low temperatures can drastically reduce dose fading.

RESULTS

Isolation of the MIS and BKS components

The main components of the fingernail spectrum (i.e., the MIS, BKS and RIS signals) have been previously identified [1-5] and were defined in the Introduction. Because of the lack of detail in published data, we have re-measured these main components and summarize their EPR parameters in Table 1. Similar to [1, 3, 4], our experiments demonstrated a significant change in the appearance of the EPR spectrum with time after trimming the fingernails (Fig. 1). Initially the spectrum includes a doublet, but after approximately 20 hours, it becomes a singlet, identified in [1] as the MIS and BKS, respectively. The initial MIS doublet shape is better seen if a higher microwave power (>10 mW) is used for its measurements than if that which was applied to record the spectra depicted in Fig. 1 is used. Consequently, the MIS and BKS could be isolated from each other based on their different behavior over time: shortly after the fingernail is cut, the MIS doublet dominates the total spectrum; however, after about 20 hours, the BKS singlet becomes dominant. Therefore, in order to compare the MIS appearance and behavior in different samples, one needs to measure their EPR spectra shortly after cutting. Accordingly, to compare the BKS components in the samples, one needs to wait about 20 hours after the samples have been cut. Based on this approach, we were able to obtain the MIS and BKS dependencies on microwave (mw) power (Fig. 2). As seen from

this figure, the MIS does not show power saturation, whereas the BKS saturates at an incident microwave power of about 2 mW in this spectrometer.

The difference in power dependence of the MIS and BKS components allowed us to develop an alternative way to isolate the two signals without waiting for the MIS to decay. Similar to the EPR method in tooth enamel described in [6], the non-saturated MIS component of the fingernails spectrum can be isolated by subtraction of the spectrum acquired at low mw power (< 2 mW) from the spectrum of the same sample acquired at high mw power (> 2 mW). As seen in Fig. 2, a pair of measurements at 1 and 16 mW represents the perfect combination for such manipulation because the BKS intensity is approximately the same at these two microwave powers; whereas, the MIS is approximately a factor of 2 more intensive at 16 mW than at 1 mW. As a result of such subtraction, a pure MIS spectrum is obtained (Fig. 3). In order to isolate the saturating BKS component, the spectrum recorded at the higher mw power should be reduced by a calculated factor, and then subtracted from the low-power spectrum. Based on the basic theory of magnetic resonance, the spectral amplitude of the non-saturated signal depends linearly on the square root of the mw power (as seen in Fig. 2). Therefore, in the case of the spectra recorded at 1 and 16 mW, in order to isolate the BKS (saturated signal) one simply needs to multiply the high-power spectrum by $(1/16)^{1/2}$ (calculated factor) and subtract it from the low-power spectrum (Fig. 4).

With this second method for isolating the MIS and BKS, we were able to obtain the time dependences of the peak-to-peak amplitude for the BKS and MIS components

separately (Fig. 5). The time interval is the same for the largest decrease in the MIS and the largest increase in the BKS. This suggests that there may be a connection between these two signals.

Origin of the MIS and BKS components

Chandra and Symons [5] noticed that there is a direct correlation between the number of cuts in a fingernail sample and the MIS intensity. However, there have been no published reports on such a correlation for the BKS intensity. The number of cuts in the sample can be directly related to the degree of mechanical stress on the sample or, as it was suggested in [5], with the concentration of mechanically-induced radicals. The design of the experiments to investigate the effect of fingernail cuts on the intensity of the MIS and BKS was based on the two previously described approaches to isolate the these signals' components.

Fig. 6, obtained from the first type of experiment, shows the evolution of the MIS (panel (a)) and the BKS (panel (b)) and their appearance with the increased number of clipping in the sample. Figure 6 shows a significant increase in both MIS and BKS intensity with increased numbers of cuts in the sample. This type of experiments was conducted on six different samples collected from three different volunteers at different times of the year. When a fingernail sample consisted of cuts having approximately equal dimensions, the correlation between inverse number of cuts and both the MIS and BKS intensities seemed to be linear.

As seen from Fig. 7, obtained from the second type of experiment, cutting the sample into two approximately equal parts caused an increase of both MIS and BKS intensities by almost a factor of 2. This result is consistent with the result of the first type of experiments, where a linear correlation between the inverse number of pieces in the sample and the MIS and BKS intensities was found. The time constants of MIS decay and BKS growth are very close in Fig. 7, i.e., approximately 1 hr, which again is consistent with the results shown in Fig. 5. Figure 7 demonstrates that the time constants of MIS decay and BKS growth do not change with additional cuts, which suggests that these values may reflect the individual mechanical properties of the fingernails on a microscopic scale. It is interesting to note that a similar exponential behavior was seen in fingernails from other individuals, but the time constants varied significantly from about 1 hour up to 4 hours.

Both types of experiments for the investigation of cuts on the MIS and BKS clearly demonstrated a direct and very similar correlation between the intensities of these signals and the degree of mechanical stress in the sample. Our results could be summarized as follows:

- Both the MIS and BKS components are caused by a mechanical stress on the fingernails from cutting.
- The timing of the MIS decrease is very similar to that of the growth of the BKS. It seems reasonable to conclude that the MIS somehow evolves into the BKS.

- MIS fading and BKS growth times seem to be unique for each fingernail sample. If so, they may be used to characterize (describe) the mechanical properties of a sample.

Effect of water treatment on MIS and BKS

Similar to [4], our results showed that treatment of fingernails with distilled and tap water from different geographic locations (Maryland, France and New Hampshire) produced the same effect on the EPR signals. Fig. 8 shows the effect of consecutive five-minute water treatments on the EPR peak-to-peak amplitude in an unirradiated fingernail sample after cut. Immediately after cut (2-3 min), a strong MIS signal is observed. The appearance of this signal is the same as that depicted on Fig. 1 at 0 hr or on panel a) of Fig. 6. After a first five-minute water treatment, the signal shape and peak-to-peak amplitude is changed significantly, the peak-to-peak amplitude is reduced by factor of 9, and the signal shape looks like the one from the untreated sample, almost 200 hr later after cut (Fig.1). In other words, the water treatment drastically accelerated the natural transformation of the spectrum, changing from an MIS to a BKS dominated spectrum, as it had been observed after the storage of fingernail clippings in open air. The only significant difference was that the BKS intensity, after treatment, was significantly less than that observed after 200 hours in open air. Typically, the residual BKS, after a five-minute water treatment, had peak-to-peak amplitude that was a factor of 8-9 less than the original MIS; whereas, after 176 hours in freshly-cut fingernails at room temperature (Fig. 1), this residual BKS was reduced by a factor of only 3. Repeated water treatments

(Fig. 8) resulted in insignificant further reduction of the BKS peak-to-peak amplitude, making it a factor of almost 10 less than the original signal after cutting. The optimal time of water treatment was found to be 10-15 minutes, which is very close to the optimal time of chemical treatment found in [3].

Another interesting result is the substantial growth of the BKS component during a delay between water treatment and acquisition of the EPR spectra (Fig. 9). The BKS increased to almost twice its original peak-to-peak amplitude 220 hours after water treatment. An exponential fit of the experimental data gives 0.7 as the saturation value for the BKS, and a BKS time growth factor (signal growth rate) of 2.33, which is not very different from that observed in untreated fingernails, 176 hours after cut (Fig. 1). Simple repetition of water treatment after this delay allowed reduction of the BKS to its original value, as occurred promptly after a single treatment. After repeated 5 minute water treatment the BKS again demonstrates growth (similar to Fig. 9) with time, which can be again reduced by water treatment to its original value as it was after the first treatment. This procedure can be repeated many times.

Figure 10 shows the results obtained from the eight different samples that were repeatedly put into water for five minutes, wiped with a paper towel, and then air dried for five minutes in more than ten cycles of soaking and drying. Similar to the results obtained by Finlay et al. in [7], we found that with the exception of the first soaking cycle, the change of the fingernails weight after soaking is quite stable and equal to 5-7%. For samples that had been collected between many months and one year ago, the weight

change after the first soaking was found to be larger (3 ± 1 %) than that for recently-cut ones. Subsequent cycles for all samples showed continuous weight increase.

For samples 2, 3, 6, and 7, it was found that the absorbed water is not chemically bound to fingernail matter because after drying for 20 hours, each sample weight was found to be exactly the same as it was at the beginning of the experiment. For samples 1, 4, 5, and 8, a direct comparison of the sample weights at the beginning (28-30 mg) and at the end (40-41 mg) showed that fingernails can absorb up to 30% of their mass of water after having been soaked in water for 20 hours.

RIS in water-treated fingernails

Because water treatment produces a strong effect on the MIS and BKS components in fingernails, it is also important to investigate if there is an effect on the dose dependence of the RIS after water treatment. It is known from previously published work [1, 2, 4] that the dose dependence of the RIS component in untreated fingernails is linear up to about 100 Gy; whereas, for chemically-treated fingernails, this dependence was found to be non-linear, with saturation at about 8 Gy [3].

Figure 11 shows the EPR spectra obtained from the freshly cut samples used in the evaluation of the radiation response in water-treated fingernails. One can see a significant difference between the 0 and 1 Gy spectra, which suggests that the lower limit of detection of dose may be below 1 Gy. The dose dependence of the peak-to-peak

amplitude in the water-treated fingernails (Fig. 12) was non-linear with saturation at about 8-10 Gy, similar to that observed after chemical treatment [3].

As seen in Fig. 13, the linear dose dependence obtained on freshly-cut untreated fingernails after 24 hours, was transformed after an 82-day storage period at -20°C to an exponential dose dependence with saturation at about 10-12 Gy. This dependence is very similar to the dose dependence obtained on the water-treated sample shown in Figure 12.

DISCUSSION

The results obtained in the present study may be summarized as follows:

- 1) Both the MIS and the BKS component are caused by mechanical stress of the fingernails from cutting. The rate of MIS fading in time is very similar to or may even coincide with the rate of BKS growth, and it appears that the MIS somehow evolves into the BKS. The MIS fading time and BKS growth time do not depend on the size and number of pieces in the particular sample; in other words, they are unique to each fingernail sample and may be used to characterize (describe) the mechanical properties (mostly elasticity) of a particular fingernail sample.
- 2) Soaking fingernail samples in water completely eliminates the MIS and significantly reduces the BKS, even though this BKS has demonstrated a significant growth with time after treatment. This effect can be eliminated by repeated water treatments. To some degree, the effect of water treatment can be described as an

acceleration of the processes that occur in fingernails after cutting and storage in air at room temperature, e.g., MIS fading and BKS growth.

3) The amount of water absorbed by fingernails when they are soaked for the first time after cutting is larger than in all following cycles of water absorption. The water does not chemically react with fingernail matter because the weight of the samples after drying, each of which had gone through more than 20 cycles of water absorption, was the same as it was at the beginning and before the soaking experiment.

4) The dosimetric properties of water-treated fingernails are very different from those of freshly-cut samples. Particularly, the dose dependence of water-treated fingernails is non-linear with saturation at about 8-10 Gy, and the intensity of the radiation-induced signals in these water-treated samples is considerably lower than in freshly-cut ones. The experiments with the long-time storage period of the untreated fingernail samples irradiated to different doses have shown that the dosimetric properties of water-treated fingernails are much more similar to the properties of unstressed *in vivo* fingernails.

Result 1) suggests the BKS to be a product of the MIS component, better termed MIS2. This conclusion is important by itself because it means that if one is to develop an *in vivo* EPR dosimetry in fingernails, as it has been done for EPR tooth dosimetry [8] and finger bone [9], there will not be a problem of overlapping signals, which currently obscure the radiation response. Thus, one will be able to directly measure radiation-

induced signals in fingernails *in vivo*. Similar to [8, 9] lower microwave frequencies (L and S bands) may be more suitable for *in vivo* EPR measurements of fingernails than the X-band used in this paper.

As seen in Fig. 14 (based on part B of Fig. 4 from Farren et al. [10]), the microscopic structure of fingernails consists of many pores, strongly resembling a sponge. Similarly, the observed cyclic behavior of water absorption in fingernails may also resemble water absorption in a sponge. In order to restore the original shape of a sponge, one needs to only soak it in water (Fig. 15). According to results of *in vivo* measurements [11] the normal water content in fingernails is 10-20%. As soon as fingernails are cut off they start to lose water. The water in fingernails is trapped in the pores' walls or inside the pores themselves. Because water in the walls of pores is strongly bound, one would expect that it will require longer time to be lost. During first soaking water is absorbed by both the pores' walls and the pores, while at all following 5 minute drying-soaking cycles mostly the water inside pores is being lost and filled back again. This could explain why there is a large first increase of water absorption especially for fingernails cut long time ago. In recently-cut fingernails the largest increase during first soaking is observed because there was a strong loss of both types of water at the cutting edges, while the other parts of the fingernails lost water only from the pores. Of course, one needs more water to compensate the water loss in the whole sample (old fingernails) than in part (recently-cut fingernails).

The amount of water required for restoration of the original fingernail shape is the difference between the amount of water absorbed by the fingernail at the first soaking and that absorbed after each subsequent soaking stages (*e.g.* in our case it was 3-5 %). Certainly, this amount depends on the surface area of the edges of the fingernail pieces. This may be due to the fact is that samples with smaller pieces lose relatively more water at cutting than samples with larger pieces, where the majority of the sample is not stressed. Consequently, more water will be necessary for restoration of the original shape of a fingernail sample that is composed of many small pieces than of a sample that is just one large piece.

The maximum amount of water absorbed by a fingernail sample should be proportional to the total volume of pores in the sample. This provides an option to determine the porosity of fingernails. According to Fig. 10, samples 1, 4, and 5 had masses of 28-30 mg before extended soaking, while at the end of the experiment, after having been in water for 20 hours, there masses were 40-41 mg. The initial volume of the samples can be calculated by dividing the sample mass by its density. With a density of α -keratin of about 1.3 g/cm^3 [12], the volumes of samples 1, 4, 5 can be calculated to be in the range of $21\text{-}23 \text{ mm}^3$, while – with a water density of 1 g/cm^3 - the volume of the absorbed water is about $11\text{-}12 \text{ mm}^3$ for these samples. By definition, porosity is the fraction of void space in the sponge material. In the present case it is the ratio of the maximum volume of absorbed water to the original volume of the fingernail sample, i.e., $0.46 - 0.48$. This ratio can be used in the future for the individual characterization (identification) of fingernails samples obtained from different donors during the analysis

of their radiation sensitivity correlation.

The effect of water treatment on the MIS1 and MIS2 components becomes understandable in view of the proposed sponge-like behavior of fingernails: water (and all other aqueous chemical solutions used in [3, 4]) simply fills the pores of stressed fingernail parings and restores their original state (before cutting). Thus, one may speculate on the sources of the MIS1 and MIS2 components and their time behavior. The MIS1 doublet may be associated with the stress of the S – S bridges between the three left-twisted backbone peptide chains (Fig. 16, right panel), whereas the MIS2 component (formerly called BKS) may originate from stress of the keratin helix as a whole (Fig. 16, left panel). Di-sulphur (S-S) bonds are the strongest bonds in the keratin structure, and make fingernails hard. Therefore, stressing them causes so-called elastic deformations, which probably last for less than several hours. These elastic deformations do not need additional energy to restore the original fingernail shape. The peptide helix, however, is much more stable because stress does not cause any large shift of electron spin density on the chain. This kind of deformation requires some energy (in our case from the water surface tension) to restore the sample's original shape; it can therefore be associated with a plastic deformation of fingernails. Thus, Fig. 5 simply means that the fast reduction of elastic deformation in fingernails (MIS1, called MIS in the figure) naturally coincides with the growth of plastic deformation (MIS2, called BKS in the figure). In other words, a strong stress on the S – S bonds (intensive MIS1) that connect the twisted peptide chains elastically transforms into a relatively small plastic deformation of the helix (weak MIS2). Based on this, the time constant of the MIS1 and MIS2 components can be used

for characterization of the mechanical properties of fingernails, because it simply represents the time required for shape restoration after cut of a particular fingernail sample. In principle, based on the time evolution of the EPR signal in freshly-cut fingernails, one may try to develop a kind of “stress test” (Fig. 7) to characterize their elasticity.

Just as with a sponge, an effective way to restore the plastic and elastic deformations in fingernails is to put them into water (Fig.15), as this has been shown to be an effective way to reduce both the MIS1 and MIS2 components. This also explains why no differences were seen among the variety of aqueous chemical treatments previously tested on fingernails [3]. The observed growth of the MIS2 (formerly called BKS) component with time after water treatment (Fig. 9), can be explained by an increase in the plastic deformation of the sponge-like structure of the fingernails as they are drying.

It should also be noted that because all previously published results on fingernail EPR dosimetry were obtained on stressed samples, they may not be directly related to the actual properties of fingernails that would be used for *in vivo* dosimetry measurements. *In vivo* samples would not have had the stress caused by cutting prior to irradiation. A detailed study of dosimetric properties of unstressed fingernails is clearly needed and currently underway.

The sponge model also allows explaining the strong reduction of the RIS component after water treatment of irradiated fingernail parings. Water treatment provides a fast restoration of the stressed structure of cut fingernails and represents a process that naturally eliminates most of the radiation-induced radicals. However, it also appears that during *in vivo* irradiation, fingernails are not stressed and therefore water treatment would not cause a reduction of the RIS component.

As pointed out in [1], radiation-induced radicals in fingernails produce a signal that is visually indistinguishable in X-band EPR from the MIS2 signal, which makes measurement of radiation dose in the biologically important dose range below 5 Gy (below the LD50/60). The method proposed here for treating the MIS1 and MIS2 components could allow isolation of the RIS, and therefore enhance the feasibility of performing retrospective dosimetry in fingernails. Thus, the proposed model will serve as a basis for the development of EPR dosimetry in fingernails [13].

By interpreting the structure of fingernails as sponge-like, we have been able to describe the EPR spectra in terms of deformation of α -keratin. The MIS and BKS components (which we propose to call MIS1 and MIS2, respectively) can be isolated by using the difference in their dependences on mw power. Furthermore, these signals can be removed (MIS1) or significantly reduced (MIS2) by water treatment. While this insight was discussed in the context of retrospective radiation dosimetry, many other applications may benefit from the proposed sponge model for the description of the mechanical properties of fingernails and their water content (see for example, [10, 11,

14]). As it follows from our model, the actual water content (and other properties as well) in fingernail parings is different from its *in vivo* state. Therefore, it may be necessary to rethink experimental designs of numerous studies where the effect of different treatments on fingernail properties was measured using trimmed pieces of fingernails.

CONCLUSIONS

Based on the proposed sponge model of fingernails, several important conclusions can be drawn:

- Most of the published results on fingernail dosimetry (except those obtained on chemically treated nails) have been obtained on mechanically stressed samples, which are not related to the “real” *in vivo* dosimetric properties of fingernails.
- Radiation-induced radicals in stressed samples are different from those in unstressed fingernail samples.
- Dosimetric properties of unstressed fingernails need to be studied on pre-soaked samples, shortly after water treatment.
- The reduction of the RIS component after water treatment can be explained by mechanical stress-reduction and sample-shape restoration.
- The elimination of the MIS and BKS components after “chemical” treatment of fingernails is most likely not caused by any chemical reaction of the mechanically-induced radicals with the reagents. Rather, it has the same explanation as the effect of water treatment.

The results presented here suggest the mechanism of radical formation in fingernails under mechanical stress to be fully understood in terms of the sponge-like behavior and deformation of fingernails. In a sponge a unique mechanism of mechanical stress absorption takes place, which is also used by fingernails to protect the fingertips from trauma. Like a sponge, fingernails are also known to be an effective water absorber. When a sponge is saturated with water it tends to restore to its original shape, and when it loses water, it again becomes deformed. The same behavior is observed in fingernail tissue. The suggested interpretation of mechanical fingernail deformation offers a way to distinguish between mechanically-induced and radiation-induced EPR signals. Our results demonstrate that the MIS in irradiated fingernails can be almost completely eliminated without significant change in the RIS by soaking the sample for several minutes in water. The proposed method to measure the porosity of the fingernails gave values of 0.46–0.48 for 3 of the studied samples. The finding that fingernails behave similarly to a sponge may also lead to a better understanding of various fingernail diseases and their treatment, of the mechanisms of water supply and, most importantly for us, it gives a clue as to how to develop effective radiation dosimetry in fingernails.

REFERENCES

1. Symons MC, Chandra H, Wyatt JL (1995) Electron paramagnetic resonance spectra of irradiated finger-nails: A possible measure of accidental exposure. *Radiat Prot Dosim* 58:11-15.
2. Dalgarno BG, McClymont JD (1989) Evaluation of ESR as a radiation accident dosimetry technique. *Appl Radiat Isot* 40:1013-1020.
3. Romanyukha A, Trompier F, LeBlanc B, Calas C, Clairand I, Mitchell CA, Smirniotopoulos JG, Swartz HM (2007) EPR dosimetry in chemically treated fingernails. *Radiat Meas* 42:1110 – 1113.
4. Trompier F, Kornak L, Calas C, Romanyukha A, LeBlanc B, Clairand I, Mitchell CA, Swartz HM (2007) Protocol for emergency EPR dosimetry in fingernails. *Radiat Meas* 42:1085-1088.
5. Chandra H, Symons MC (1987) Sulphur radicals formed by cutting alpha-keratin. *Nature* 328, 833-834.
6. Ignatiev EA, Romanyukha AA, Koshta AA, Wieser A (1996) Selective saturation method for EPR dosimetry with tooth enamel. *Appl Radiat Isot* 47:333-337.
7. Finlay AY, Frost P, Keith AD, Snipes W (1980) An assessment of factors influencing flexibility of human fingernails. *Br J Dermatol* 103:357-365.
8. Swartz HM, Iwasaki A, Walczak T, Demidenko E, Salikhov I, Khan N, Lesniewski P, Thomas JA, Romanyukha A, Schauer DA, Starewicz P (2006) In vivo EPR dosimetry to quantify exposures to clinically significant doses of ionising radiation. *Radiat Prot Dosim* 120:163-170.

9. Zdravkova M, Crockart N, Trompier F, Beghein N, Gallez B, Debuyst R. (2004) Non-invasive determination of the irradiation dose in fingers using low-frequency EPR. *Phys Med Biol* 49:2891-2898.
10. Farren L, Shayler S, Ennos AR (2004) The fracture properties and mechanical design of human fingernails. *J Exp Biol* 207:735-741.
11. Egawa M, Ozaki Y, Takahashi M (2006) In vivo measurement of water content of the fingernail and its seasonal change. *Skin Res Technol* 12:126-132.
12. Mason P (1963) Density and Structure of Alpha-Keratin. *Nature* 197:179-180.
13. Romanyukha A, Trompier F, Swartz HM EPR dosimetry with fingernails, in US Patent Provisional No. 60/924,034. 2007: USA.
14. Stern DK, Diamantis S, Smith E, Wei H, Gordon M, Muigai W, Moshier E, Lebwohl M, Spuls P (2007) Water content and other aspects of brittle versus normal fingernails. *J Am Acad Dermatol* 57: 31-36.

Table 1. EPR parameters of three spectral components in fingernails at room temperature.

Full name of the component	Acronym	Type of signal	g factor	Linewidth (mT)	Appearance
Mechanically-induced signal	MIS	Doublet $A(^1\text{H}) \approx 0.85$ mT [5]	2.025, 2.010	1.8 mT (central peak)	Fig. 3 (bold line)
Background signal	BKS	Singlet	2.0068	0.6 mT	Fig. 4 (bold line)
Radiation-induced signal	RIS	Singlet	2.0078	0.8 mT	Fig. 11 (4 Gy)

Figures and legends

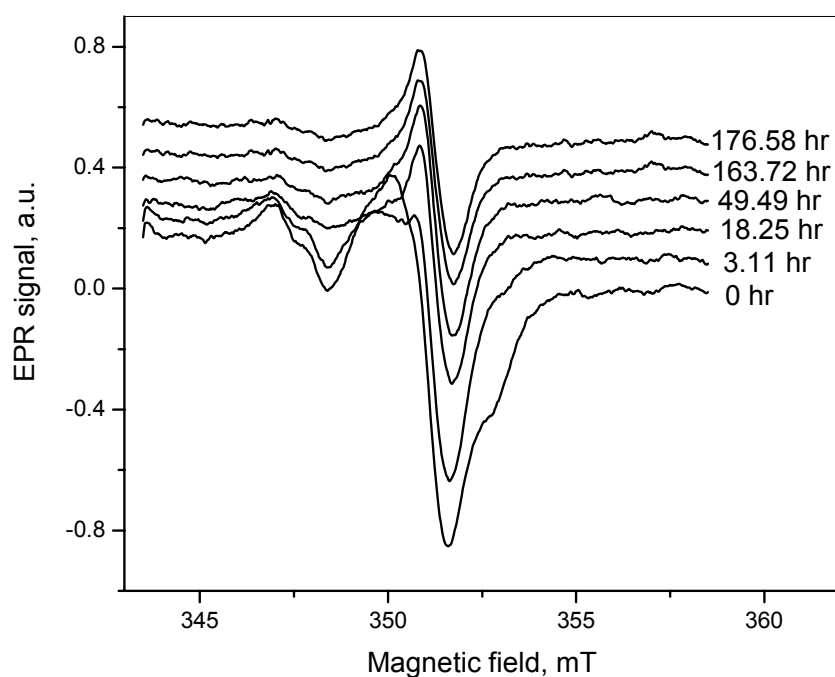


Fig. 1 Time evolution of the EPR spectrum in an unirradiated fingernail sample (15mg) after fingernail trimming. Spectra were recorded at room temperature and 2 mW of microwave (mw) power.

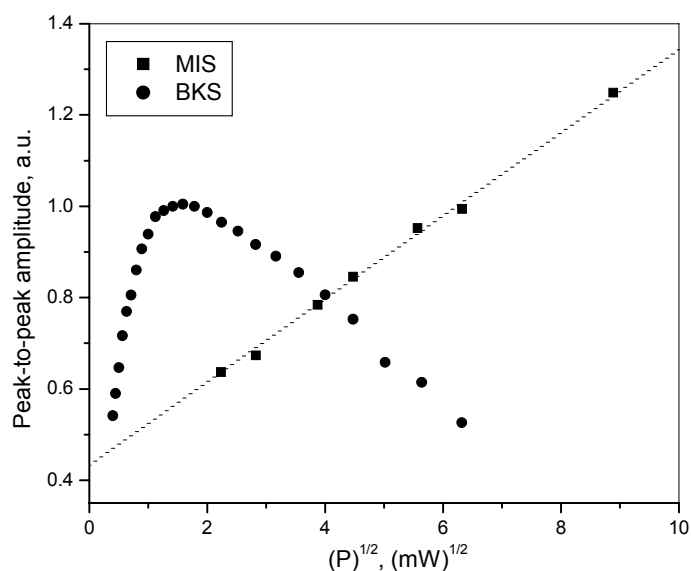


Fig.2 Dependence of BKS and MIS signals on microwave power. The BKS is saturated at 1.8 mW, whereas the MIS does not show saturation in the studied range of microwave power of 0 – 100 mW.

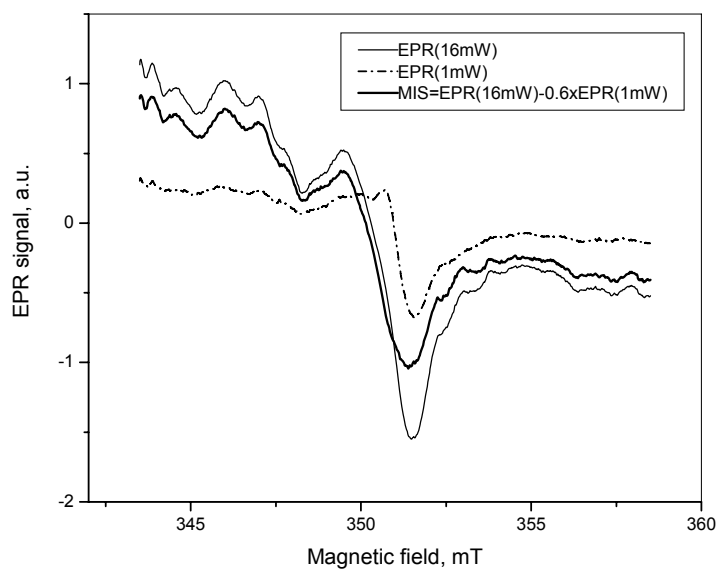


Fig. 3 Subtraction of the EPR spectrum acquired at 1 mW (dashed line) from that acquired from the same un-irradiated fingernail sample at 16 mW (solid line), for identification of the MIS component (bold line).

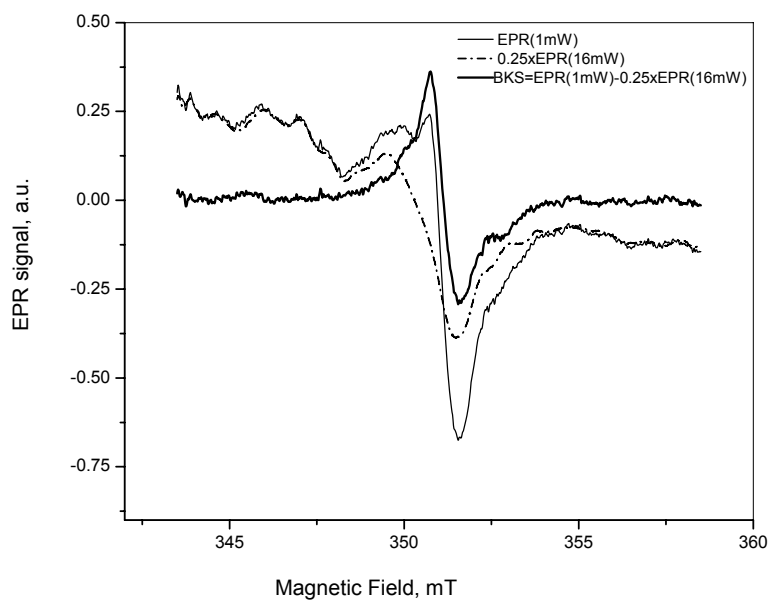


Fig. 4 Subtraction of the EPR spectrum acquired at 16 mW and multiplied by a correction factor of 0.25 (dashed line), from that acquired from the same un-irradiated fingernail sample at 1 mW (solid line), for isolation of the BKS component (bold line).

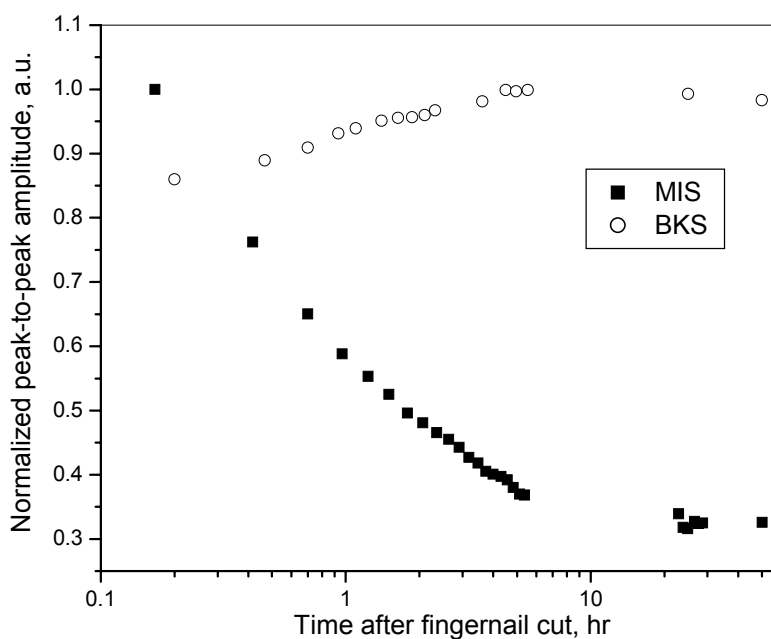
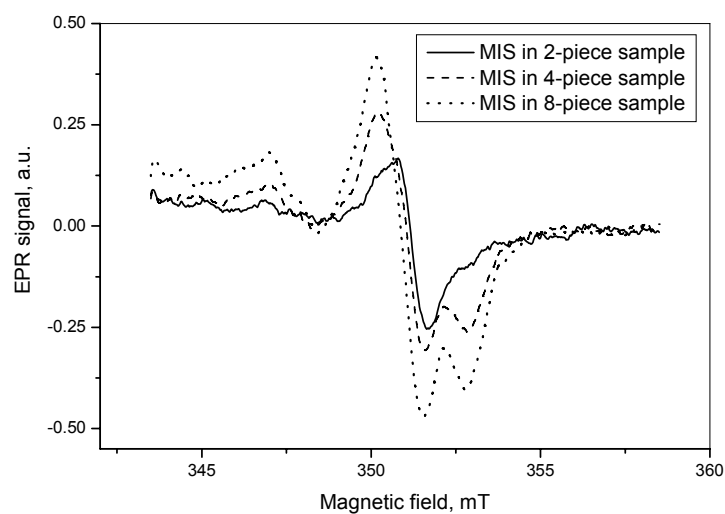
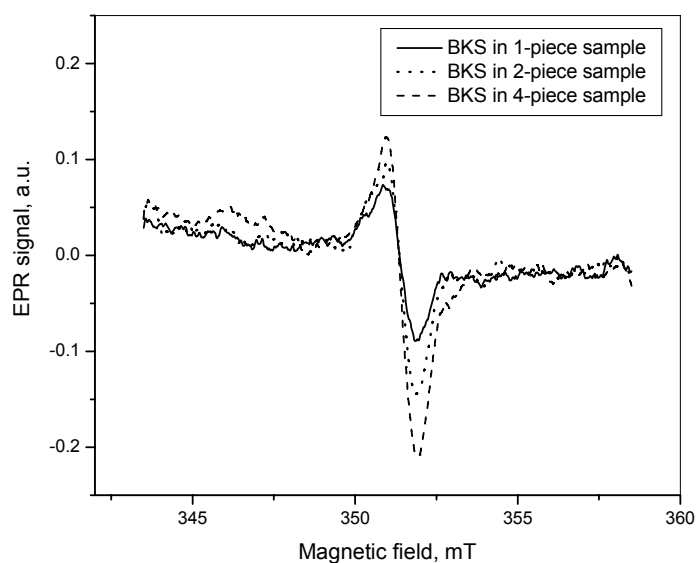


Fig. 5 Time dependence of normalized MIS and BKS intensity in unirradiated fingernail sample after trimming. The BKS and MIS components were separated by their different mw power dependence.

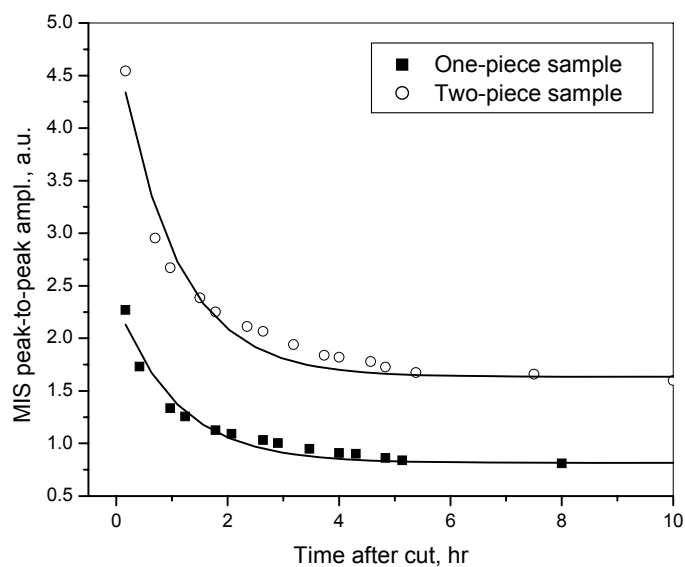


(a)

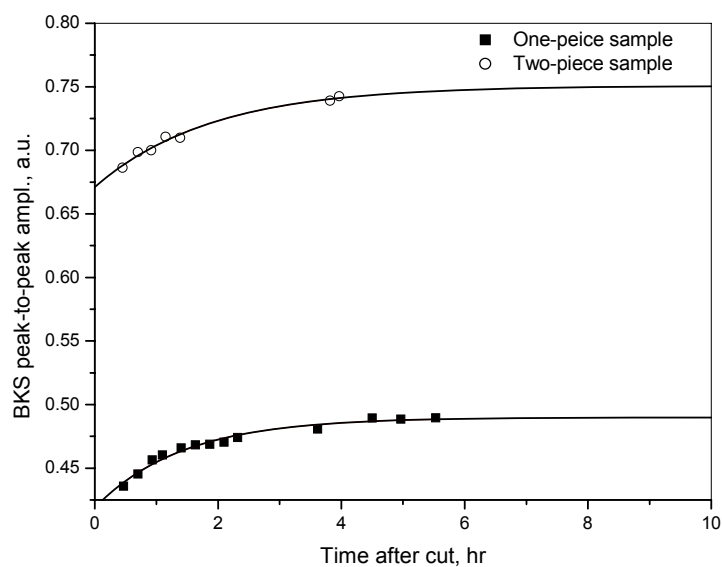


(b)

Fig. 6 a) MIS recorded in the same unirradiated sample after making additional cuts. The same sample demonstrates a more intensive MIS after each additional cut; b) BKS recorded in the same sample after making additional cuts. The BKS was obtained by waiting 24 hours after each cut to fade out the MIS. Similar to the MIS (panel (a)), the same sample demonstrates a significant increase in BKS after each additional cut.



(a)



(b)

Fig. 7 a) Dependence of MIS intensity on time after cut using the same unirradiated sample before and after additional cut. The same sample demonstrates a MIS that is about twice more intensive after each additional cut but with a very similar evolution with time. Solid lines show exponential fits of the experimental data, with a time constant of $T=1.05\pm0.05$ hr that was found the same before and after additional cut; b) Similar as a) but for the BKS component. Again, the signal intensity is about twice more intensive after each additional cut but with a very similar evolution with time, and the time constants of the exponential fits (solid lines) was found to be the same before and after additional cut, e.g. $T=1.1\pm0.1$ hr.

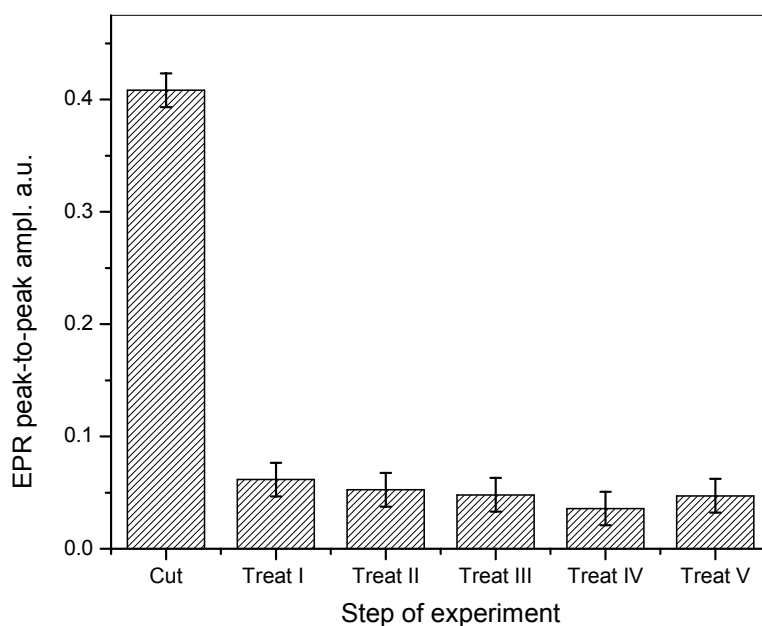


Fig. 8 Changes of the peak-to-peak amplitude of the EPR signal in an unirradiated fingernail sample, shortly after cut and after five consequent five-minute water treatments.

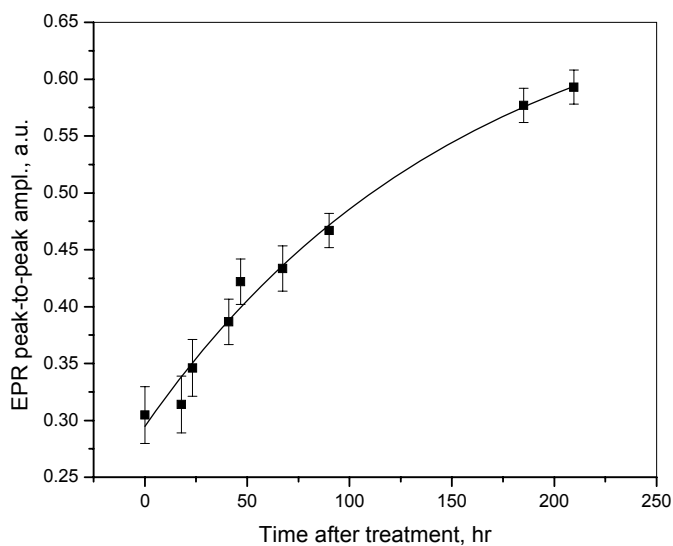


Fig. 9 Growth of BKS in water-treated fingernails with time after treatment.

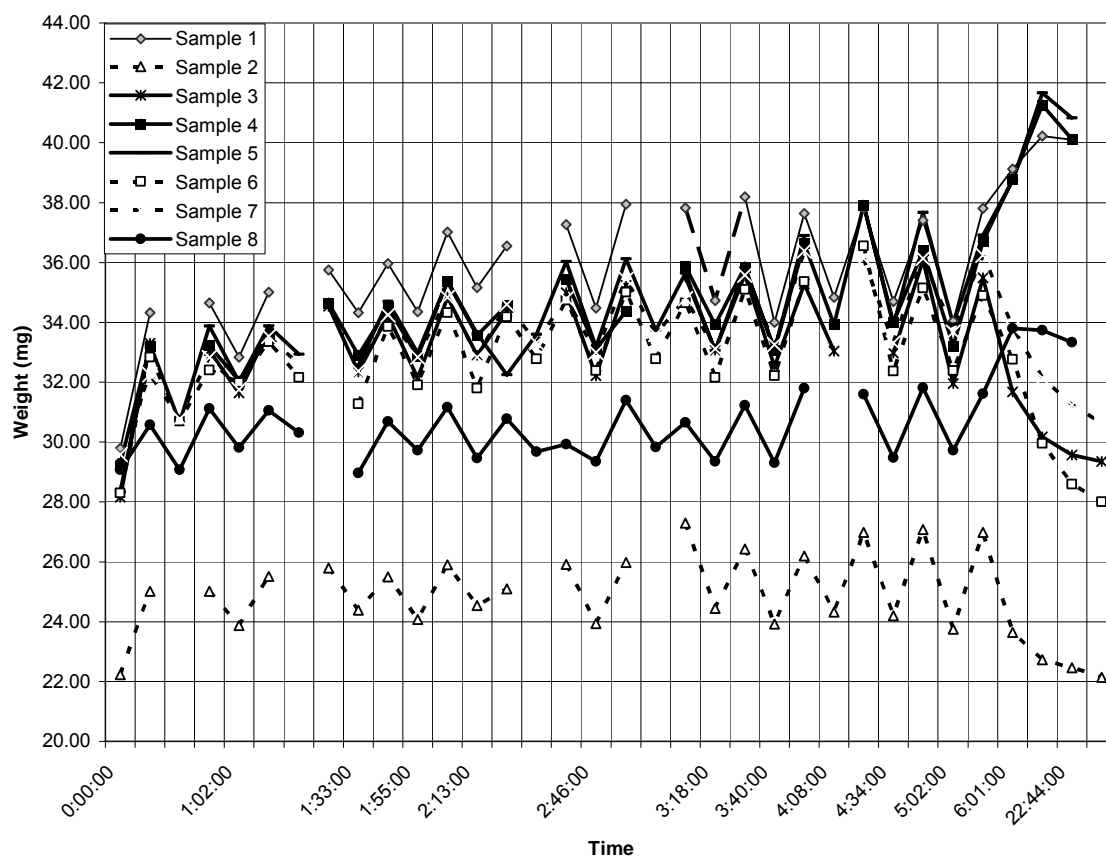


Fig. 10 Weight change of fingernail samples after periodical soaking in water and weighting after a short drying period. At the end of this procedure, samples 1, 4, 5, and 8 were left in the water bath, while samples 2, 3, 6 and 7 were left dry. For all samples, the weights were subsequently measured three to four times.

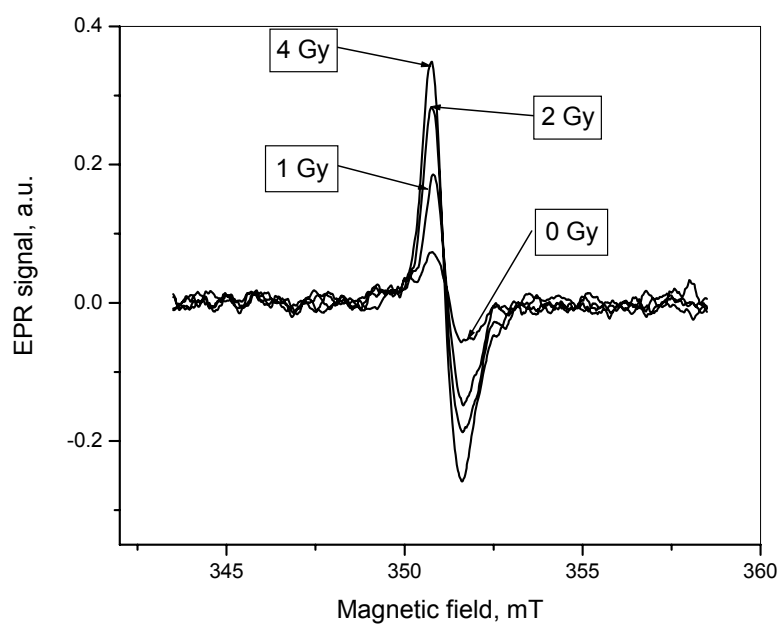


Fig. 11 EPR spectra in water-treated fingernails exposed to different radiation doses.

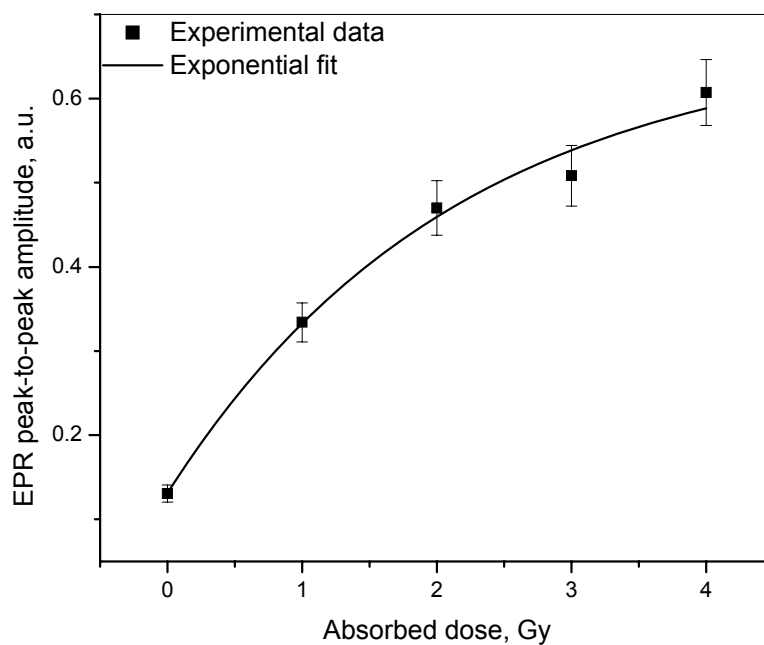


Fig. 12 Dose dependence of the EPR signal in a water-treated fingernail sample.

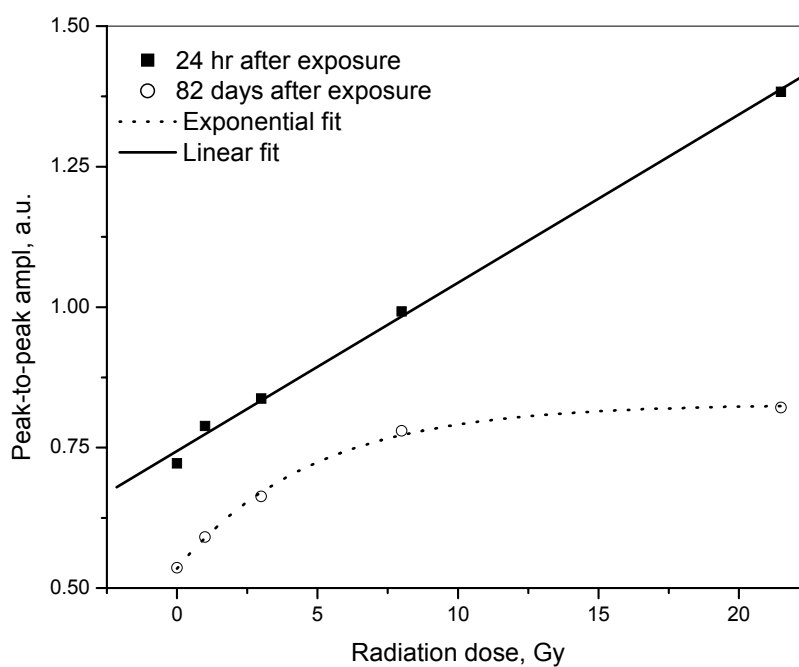


Fig. 13 Dose dependence of the RIS component in untreated fingernails with time. Solid squares: results obtained on five untreated fingernail samples from the same volunteer at the same time, irradiated and measured 24 hours after cut; Solid line: linear regression of the dose dependence data; Open circles: results obtained on the same samples, after an 82 day storage period at -20°C ; Dashed line: exponential regression of the dose dependence data after the 82 day storage.

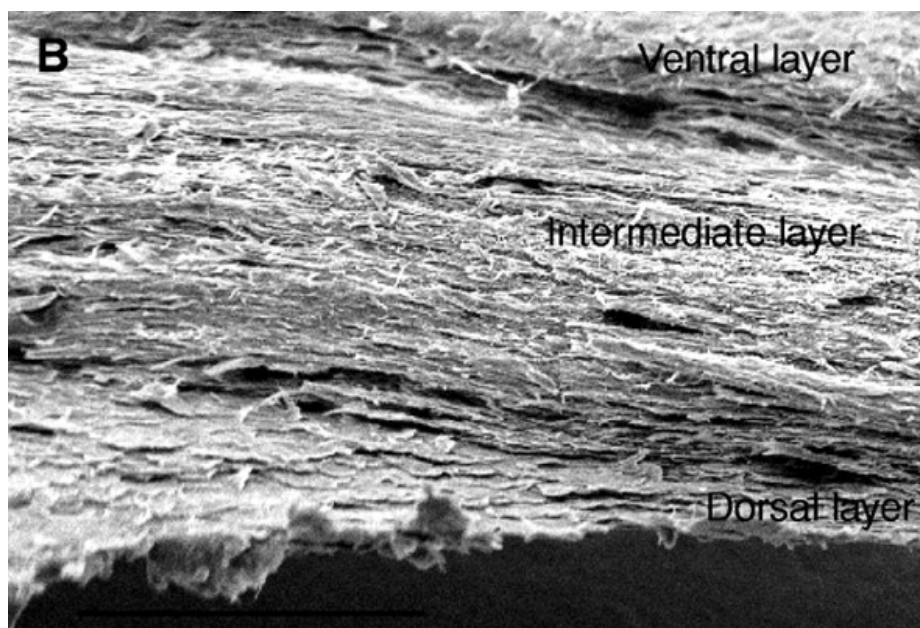


Fig. 14 Scanning electron micrographs of the fracture surfaces of torn nail clippings [10] (reproduced with permission of the Company of Biologists).

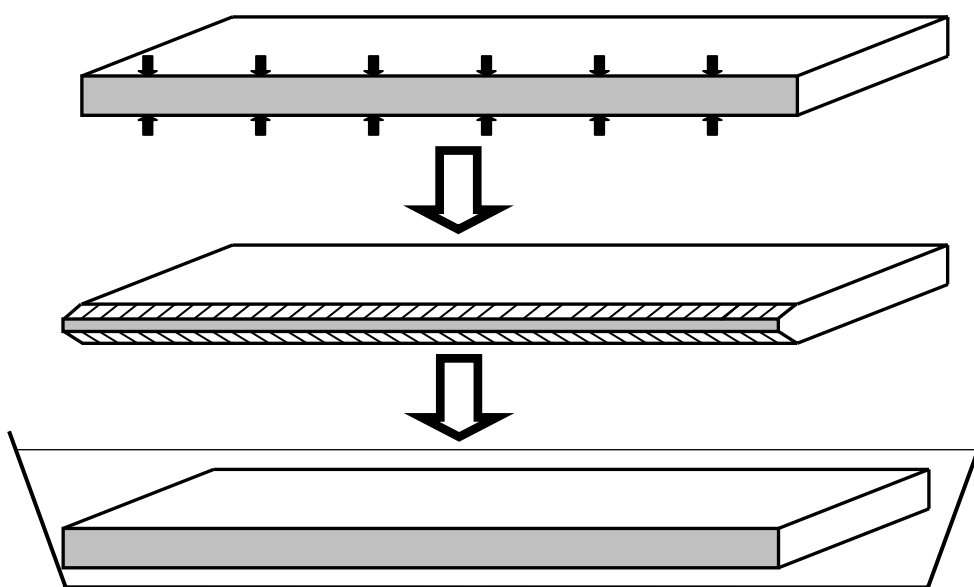


Fig. 15 Schematic model of the deformation of fingernails at the edge of a cut and subsequent restoration of its shape while soaking in water.

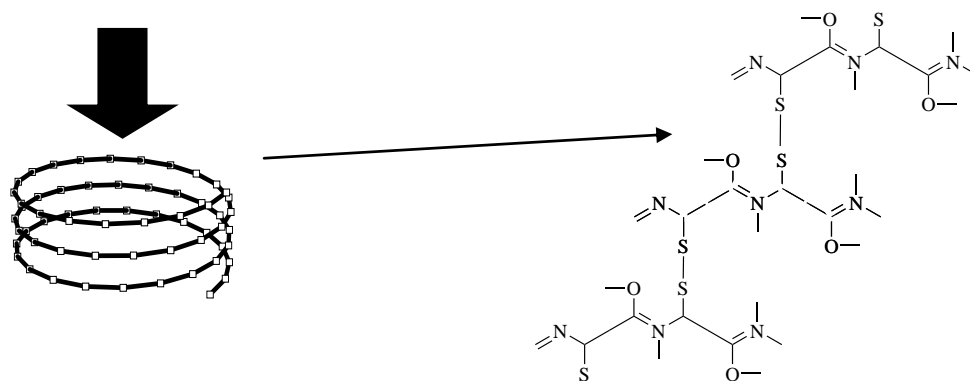


Fig. 16 Schematic picture of two possible types of fingernail deformation. Left: deformation of the keratin helix as whole (plastic deformation), which is supposedly the source of the MIS2 (formerly BKS) component; Right: deformation of S – S bridges connecting the three left-twisted backbone peptide chains (elastic deformation) which is supposedly responsible for the MIS1 (formerly MIS) component.

CHAPTER 4

“EPR dose dependence in fingernails: Variability and possibilities of initial dose assessment”

R.A. Reyes¹, A. Romanyukha^{1,2}, C. Olsen¹, F. Trompier³, L.A. Benevides²

¹Uniformed Services University of the Health Sciences, Bethesda, MD, USA

²Naval Dosimetry Center, Bethesda, MD, USA

³Institut de Radioprotection et de Sûreté Nucléaire, Fontenay-aux-roses, France

ABSTRACT

Results of an extensive study of dose dependence variability in fingernail samples are presented. Five different groups of samples were selected and studied based on the time of fingernails collections, the level of mechanical stress in them, and their number and size of clippings: 1) recently (<24 hr) cut, irradiated, and measured with EPR without any treatment of samples and with rigorous control of size and number of clippings (stressed-fresh, controlled); 2) recently (<24 hr) cut, irradiated, and measured with EPR after application of a special treatment (10 min water soaking, 5 min drying time) to reduce the mechanical stress caused by cutting samples and with rigorous control of size and number of clippings (unstressed-fresh, controlled); 3) previously (>24 hr) cut, stored at room temperature, additionally cut into small pieces immediately prior to study, irradiated and measured with EPR without any treatment of samples and with rigorous control of size and number of clippings (stressed-old, controlled); 4) previously (>24 hr) cut, stored at room temperature, additionally cut into small pieces immediately prior to study, irradiated and measured with EPR after application of a special treatment to reduce mechanical stress caused by cut and with rigorous control of size and number of clippings

(unstressed-old, controlled); and 5) recently (<24 hr) cut, irradiated, and measured with EPR after the application of a special treatment to reduce the mechanical stress caused by cut and without rigorous control of size and number of clippings (unstressed-fresh, uncontrolled). Except for the fifth selected group, variability of the dose dependence inside all groups was found to be statistically insignificant although the variability between the different groups was significant. Comparison of the mean dose dependences, obtained for each group, allowed selecting key factors responsible for radiation sensitivity (dose response per unit of mass and dose) and the shape of dose dependence in fingernails. The major factor responsible for radiation sensitivity of fingernails was identified as their water content, which can affect radiation sensitivity up to 35%. The major factor responsible for shape of the radiation sensitivity was identified as the mechanical stress. At a significant level of mechanical stress, the shape of dose dependence is linear in the studied dose range (<20 Gy), and in lesser-stressed samples, it is of an exponential growth with saturation type which depends on the degree of mechanical stress. Recommendations on the appropriate ways of doing dose measurements in fingernails are discussed and presented.

Key words: accidental dosimetry, EPR, ESR, fingernails, external exposure, radiation dose reconstruction

INTRODUCTION

The use of fingernails as EPR radiation dosimeters offers the advantages of having measurements with an estimated relatively low dose limit (1-2 Gy)¹⁻³ and simple sampling processing, which makes it possible to complete dose assessments in less than 10-15 minutes. Moreover, dose measurements in fingernails can potentially be done at the site of a radiological accident/incident. This makes EPR fingernail dosimetry an attractive complementary methodology for dose evaluations during mass casualty events involving radioactive sources.

Fingernails are mostly composed of alpha-keratin. The molecule of this protein consists of three, long α -helical peptide chains that are twisted together in a left-handed coil and strengthened by S-S (sulfur-sulfur) bridges that are formed from adjacent cystine groups. It is known that radiation exposure induces radicals in finger- and toe-nails and that these radicals can be measured by electron paramagnetic resonance (EPR). The radiation-induced EPR signal (RIS) is persistent and proportional to the radiation dose. If necessary, this signal can be preserved for long time (months) by storage at low temperatures (on ice or in freezer). However, there is a known problem: the presence of two non-radiation signals in the EPR spectra of fingernails. The first non-radiation signal had been identified as a mechanically-induced signal (MIS) because it is generated by the clipping of fingernails at sampling.^{4,5} Until recently, the origin of the second non-radiation signal in the EPR spectrum of a fingernail was unknown and this signal had

been labelled as a background signal (BKS).⁵ Last year, specially-designed experiments showed that this signal is similar to the MIS, caused by the mechanical stress at the time of fingernails cut.⁶ Therefore, it was suggested to rename the background signal as mechanically-induced signal type 2 (MIS2) and the original MIS as MIS1. These signals overlap the radiation response at doses below 10 Gy and their intensities are time dependent and vary for different samples, which makes it difficult to account for their contributions during dose assessments. In Reyes et al.,⁶ in order to explain the origin and behaviour of the non-radiation signals, the sponge model was proposed. According to this model, a fingernail can be described as having spongy tissue, which is significantly deformed at the time of fingernails cutting. Then, the MIS1 can be interpreted as a signal from the electron dipoles formed at the S-S bridges after elastic deformation, and the MIS2 as a signal from the electron dipoles or holes located in cystine backbone chains and originated from their plastic deformation at the time of fingernails cutting. By definition, after elastic deformation of a material, in our case fingernails, this restores its original shape with time without the application of any additional force and that is exactly what is seen with the MIS1, which is very intensive immediately after fingernails' cut and then it disappears after approximately 20-24 hours. A plastic deformation is stable with time and needs some external force for the restoration of the object's original shape, and that is exactly what is seen in the case of the MIS2, which is very stable with time.^{5,6} In the framework of the sponge model, the observed effect of the MIS1 elimination and the MIS2 significant reduction at several applied chemical^{2,4} or water treatments,³ could be explained by the known property of the sponge tissue of restoring its original shape when liquid fills its pores. This means that soaking fingernails in water shortly after

cutting effectively restores their original *in vivo* properties. This important understanding brings at least two new questions:

- 1) Does the deformation at fingernails clipping significantly modify their radiation properties so that deformed (clipped or cut) fingernails do not represent fully dosimetric properties of *in vivo* fingernails?
- 2) How significant can the variation of dosimetric properties of fingernails, collected from the same individuals at different times and collected from different persons at the same time be?

The answers to these and to some other related questions can be obtained as a result of the comparison of the radiation dose dependences of EPR signals in stressed and unstressed fingernail samples, collected from different same individuals. Stressed fingernail samples are considered nail clippings that have been recently cut, either during the initial cut from a donor's finger or during the sample preparation process, when samples are cut to a recommended size for analysis. These samples have gone through a mechanical stress that has inferred a permanent physical deformation. After cutting, they show a typical mechanically induced EPR signal, which decays in approximately 20-24 hours after cutting. According to Reyes et al.,⁶ unstressed samples are samples that have been treated by soaking in water for 10 minutes to completely eliminate the MIS1 and significantly reduce the MIS2. Treatment physically restores these samples.

This present paper includes the study of 83 dose dependences of the EPR radiation induced signals, obtained from different fingernail samples collected from different and

same individuals. The main purpose of the study was the evaluation of variability of the dose dependences in fingernails. Studied samples were conditionally divided in five different groups:

- 1) recently (<24 hr) cut, irradiated, and measured with EPR without any treatment of samples and with rigorous control of size and number of clippings (stressed-fresh, controlled);
- 2) recently (<24 hr) cut, irradiated, and measured with EPR after application of a special treatment to reduce the mechanical stress caused by cutting samples and with rigorous control of size and number of clippings (unstressed-fresh, controlled);
- 3) previously (>24 hr) cut, stored at room temperature, additionally cut into small pieces immediately prior to study, irradiated and measured with EPR without any treatment of samples and with rigorous control of size and number of clippings (stressed-old, controlled);
- 4) previously (>24 hr) cut, stored at room temperature, additionally cut into small pieces immediately prior to study, irradiated and measured with EPR after application of a special treatment to reduce mechanical stress caused by cut and with rigorous control of size and number of clippings (unstressed-old, controlled); and
- 5) recently (<24 hr) cut, irradiated, and measured with EPR after the application of a special treatment to reduce the mechanical stress caused by cut and without rigorous control of size and number of clippings (unstressed-fresh, uncontrolled).

Statistical evaluation of the data was performed using SPSS v. 12.0.1 and nQuery Advisor v. 7.0 software packages. The correlation between the EPR radiation induced

signals and the added radiation dose were evaluated and all statistical results were used to support the use of fingernails as biological samples in EPR dosimetry.

MATERIALS AND METHODS

All of the donors used in this study were civilian and military personnel from the Department of Defense between the ages of 21 and 53. Out of 150 samples, 75 were randomly selected. Since our pilot data showed a difference in EPR signal behavior in freshly-cut versus previously cut samples, we separated the samples into two sets of freshly-cut samples (collected within 24 hours of the study, set 1, n=31) and older samples (collected longer than 24 hours of study, set 2, n=44). Out of these, 20 fresh and 20 old samples were selected based on having the most volume (minimum of 60 mg). Each sample was further split in two approximately equal sub-samples of the same donor (n=40 stressed, n=40 unstressed).

During sample collection, nails were cut using a sharp scissors. Typical amounts of nail parings for one person are up to 120 mg for fingernails and up to 160 mg for toenails. Sample requirements for fingernails are summarized in Table I. These were derived during preliminary studies for determining the most effective size and weight, without the compromising of sensitivity in measurements, for fingernail EPR dosimetry. The inner diameter of the EPR sample tubes used in this study, 3.5 mm, was also taken into consideration when deriving the required size of the sample clippings. The Bruker ELEXSYS 500 (Bruker BioSpin) spectrometer, equipped with a super-high-Q resonator

ER 4123SHQE in the X-band (9-10 GHz) was used for measurements. Table II shows the recording settings. In order to eliminate the residual MIS2 contribution subtraction of the spectra recorded at 2 different microwave powers, e.g. 1 and 16 mW were applied, as described in Reyes et al.⁶ Each sample in this study was measured three times at five different added doses: 0, 2, 5, 10, and 15 Gy. A ^{137}Cs irradiator (Atomic Energy of Canada Limited Gammacell 40) with a dose rate of 0.7 Gy/min was used for irradiations.

This study includes the examination of the EPR RIS in stressed and unstressed fingernail samples. In order to eliminate (significantly reduce) the mechanical stress caused by cutting fingernails prior EPR measurements these samples were soaked in water for 10 min and dried on paper towels for 5 min.⁶ Previously collected samples (>24 hrs) do not exhibit a noticeable MIS1. However, if further cutting takes place during sample preparation, the use of water treatment is required to eliminate this added mechanically induced signal prior to measurements. Egawa et al. documented that there is a slight correlation between water content in fingernails and nail thickness.⁷ That means that, as with older fingernails samples, fingernails that are noticeably thicker may also require an additional treatment to restore their original physical state. To examine the thickness of the fingernail samples is difficult and may require the use of an electrometer and microscope. As a general guidance, fingernails that exhibit a weight of more than 4 mg/clipping (12 mg per three clippings) of the same size (width and length), as that described in Table I, can be considered thick and therefore, a second treatment is recommended. Added water treatments that are not necessary will not affect the magnitude of the RIS EPR signal, unless a remainder MIS1 was present (physical

restoration of sample is not completed = signal decrease with added treatment), or the sample is too wet (sample not dried enough and water is absorbing microwave power = signal decrease with higher noise spectrum). Therefore, the applicability of additional water treatment may be adapted by centers desiring to have a standard protocol for all fingernail samples.

Fingernail clippings used for the study of stressed samples were prepared by further cutting them to make them similar in size, as that shown in Table I. All stressed samples were made of 8 clippings with an average weigh of 30.51 mg (± 0.95 mg), 3.81 mg/clipping. Samples were labeled as “fresh” when they were recently cut (< 2 hr) and “old” when they had been previously collected. Samples were kept at freezing temperatures during experiments because the RIS signal persists with no noticeable fading at low temperatures for at least 6 months.

The general experimental steps are delineated below (Fig. 1) and illustrated in flow chart (Fig. 2). Step 2, for sample preparation in experiments that supported the study of dose dependency using stressed fingernail samples, only required sub-steps 2.a.-2.d. The remaining sub-steps, 2.e.-2.g., were used for those experiments in support of the study of the dose dependency using unstressed samples. Samples that have different characteristics than those in Table I may require a modification of treatment (longer time, never less than 10 min with drying time no less than 5 min), a preferably second treatment (10 min water bath/5 min drying time), and normalization to weight. During step 3, measurements are repeated at least three times to derive the standard deviation. An

alternate method for deriving statistical variations is to obtain the signal to noise ratio from the spectrometer after the collection of each spectra. On step 4, every spectra obtained at 16 mW is multiplied by $(1/16)^{1/2}$ and subtracted from that obtained a 1 mW.⁶ On step 5, we record the value of the peak-to-peak amplitude, which helps us quantify the amount of electron spins that is proportional to the radiation induced radicals and therefore, the radiological dose. The recording of EPR spectra prior to and right after treatment was selectively performed to document changes in the signal, as previously done in preliminary studies.

Generally in our experiments, two types of dose dependence were observed in fingernails. In stressed (untreated) fingernails, the dose dependence was close to a linear response, similar to Refs. 1 and 5.^{1,5} In this case the linear fit model was applied for the primary statistical analysis during the variability study. In unstressed (treated) samples the dose dependence was found to be non-linear^{2,6,8} with saturation at 10-20 Gy. In this case, the exponential fit model as described in Refs. 2, 6, and 8, was applied.^{2,6,8}

The mean value (peak-to-peak amplitude of EPR signal) of the two split samples for each added dose was used with both linear and exponential fit models for stressed and unstressed samples respectively. In order to evaluate how well the two models fit the data, we assessed all individual plotted lines using the coefficient of determination (R^2). The R^2 is the square of the Pearson product moment correlation coefficient through data points in the amplitude of the EPR signals and corresponding added radiation dose. It represents the proportion of the variance in the signal which is attributable to the variance

in added dose. We tested both sets of slopes for freshly-cut and older samples using F and t statistics and assumed that both variables, EPR signal and dose, were normally distributed. The interpersonal variability in measurements for each dose was assessed by looking at the standard deviation of the averaged (over split samples) values obtained for each added dose, 0, 2, 5, 10, and 15 Gy. The intrapersonal variability in measurements was computed by looking at the standard deviation in measurements from each donor and estimating the overall variance at each added dose. The best estimate for this within-subject variability is to use the variances for all of the measurements (not their standard deviations), average them, and then use the square root of the average to estimate the intrapersonal variability (within-subject standard deviation).⁹

In order to estimate the significance of having rigorous requirements on the number and size of clippings in a sample (Table I), additional EPR dose response dependence was further studied in two other experiments. The first experiment consisted of measurements of dose dependence in eight fresh fingernail samples where there was no strict control over the number and size of fingernail clippings. However, all fingernails were cut right before study (fresh fingernails) and treated in the same way by soaking in water for 10 minutes and following drying on a paper towel for 5 minutes. These samples were measured and irradiated in the exactly the same way as the four other types of the studied samples.

In the second experiment, 100 mg of fingernails were collected from the same donor, split into 3 portions, and prepared in 3 different ways:

- Sample 1 was frozen in liquid nitrogen and crushed into powder, sample mass: 45 mg;
- Sample 2 consisted of 8 small equal pieces, sample mass: 26 mg; and
- Sample 3 consisted of 3 relatively large equal pieces, sample mass: 20 mg.
- All samples were simultaneously irradiated to a dose of 5 Gy in 4 steps, e.g. 1 Gy, 1 Gy, 1 Gy and 2 Gy.
- After each step, the EPR spectrum was recorded from each sample.

RESULTS

EPR dose response in stressed samples

The first set of 20 samples (stressed) showed a RIS dependence on added dose that can be fitted well by linear regression (see Figure 3). The EPR dose response of fingernails that were older is distinct from that of freshly-cut fingernails samples. Principally, the time-since-cut is proportional to the MIS1 contribution for freshly-cut samples (much larger right after cut, within 24 hours), or to the MIS2 contribution from the state of dryness/deformation of the samples (older samples are more dry than freshly-cut ones). Other factors affecting the signal, such as temperature of storage and sample preparation were controlled by treating all samples the same way. The slopes of the linear regressions of EPR dose responses were comparable for each set of samples but different for freshly- and previously- cut fingernails (see Figure 4).

Tables III.A and III.B show the peak to peak amplitudes of the EPR signals in both freshly-cut and older samples in response to added doses of 0, 2, 5, 10 and 15 Gy. Variations within these groups are potentially due to the factors mentioned above and the intrapersonal variability of samples. The average signal amplitude after sample preparation (cut of clippings to equal 8 clippings of size that would meet Table I specifications and no treatment) and after a 24 hour delay was $0.4449 (\pm 0.0388)$ and $0.7907 (\pm 0.0668)$ for freshly-cut and older samples respectively. The average slope of the dose response curves were $0.0281 (\pm 0.0017)$ and $0.0387 (\pm 0.0008)$ for freshly-cut and older samples respectively. The average dose offset, which is mostly due to the MIS2 contribution, is (15.8 ± 2.5) Gy and (20.5 ± 2.1) Gy for freshly-cut and older samples respectively. The square of the Pearson correlation coefficient, R^2 , showed that there is a strong positive correlation (linear) between the EPR RIS amplitude and the average radiation dose ($R^2 = 0.997$ and $= 0.998$ for freshly-cut and older samples respectively).

Since slopes were generally larger for older samples, we looked at the correlation between the slopes and the time since-cut. This time is an indicator of the state of dryness of the samples, as fingernail samples dry out with time much like a sponge, as described in Reyes et al. ⁶ Figures 5 (a) and (b) illustrate the slopes variation in EPR with added radiation dose versus the time-since-cut for each sample ($n=40$) in freshly-cut and older samples respectively. There was an apparent small increase of the slope with time-since-cut for both sets of samples, which were analyzed and plotted separately because of the large difference in times (x-axis in Fig. 5). Both freshly-cut and old samples showed a significant correlation (less significant in older samples) of 0.618 ($p=0.004$) and 0.445

($p=0.049$) respectively. Putting both sets of data together and running the statistical software gave us a correlation between slope and time-since-cut for all stressed samples of 0.808 ($p<0.001$) (see Fig. 6, SPSS output).

The statistical evaluation of the data obtained for the stressed samples indicates that there is a strong linear correlation between EPR radiation induced signal and added dose for both sets of fresh and old fingernail samples ($R^2=0.9998$) and that the slopes of these curves are numerically close. However, when comparing the slopes of both sets of samples using the t-test, these are significantly different ($p<0.001$).

Figure 7 shows the interpersonal and intrapersonal variability for each added dose. The interpersonal variability was computed by using the variance of both sets of samples, freshly-cut and old, and determining the standard deviation of their averaged values⁹. The quantities used for the intrapersonal variability were not the averaged values for each added dose but that of each split sample from each donor ($n=40$, 200 measurements). The interpersonal variability was higher than the intrapersonal variability in stressed samples. Older samples generally showed a larger variability than freshly-cut samples. However, t-test of data sets for all split samples showed that there is no statistically significant difference in EPR measurements between (interpersonal) or within (intrapersonal) samples (we could not reject the null hypothesis that the measurements were the same with $p>>0.05$ for all data sets). For these computations, each array of data was compared with the average values for each dose across all donors and added dose.

EPR dose response in unstressed (treated by soaking in water) samples

The same distinct response between the freshly-cut and older samples was observed when measurements were taken after one treatment of samples. Older fingernail samples may require additional treatments (10 min soak in water with 5 min drying time minimum) to eliminate the strong effect of the residual EPR MIS2 (signal effect from the plastic deformation of the fingernail spongy tissue). Table IV shows the weight difference after treatment of samples (first set of split samples $n=20$) and the time since cut (time between clipping and right before treatment). The average weight increase for all samples was 2.20 mg (± 0.84 mg). The average weight increase for freshly-cut and older samples was 1.51 mg (± 0.52 mg) and 2.90 mg (± 0.39 mg) respectively. Older samples showed higher water absorption than freshly-cut ones in general. Freshly-cut nails that were more dried (having longer times since cut) generally absorbed more water than those that were less dried (shorter times since cut). The same seemed to be applicable to the older fingernail samples. This can be explained with the sponge model, as nails that are less dried require less water for their physical restoration.

Figure 8 shows the plot of weight increase versus time since cut, plotted separately for both freshly-cut (a) and older (b) fingernails samples because of the large difference in time-since-cut. Fresh samples gained less weight than old ones under the same water treatment conditions. As samples are less dry, as in the case of freshly-cut fingernails, they require less water to restore their physical shape. Older samples were drier and required more water to be restored, much like a sponge, as described in Reyes et al.⁶ A

strong correlation was found between weight gains (direct indication of water absorption) and time-since-cut (indicator of state of dryness of sample), 0.807 ($p < 0.001$) (see Fig. 9, SPSS output results).

Table V shows the dose response in treated (unstressed) samples for freshly-cut and older fingernail samples and the correlation for each data set. A strong positive correlation between added dose and EPR signal ($N = 120$, 20 sets of 6, $p < 0.001$) is shown. Figure 10 illustrates this dose dependency in unstressed samples (Fig. 10 (a)) and a plot of the average values for both sets of freshly-cut and older samples (Fig. 10(b)). Data from pilot studies of freshly-cut fingernail samples, taken in the last two years, was plotted to fit the curve of the average values for the freshly-cut samples.

In general, old samples displayed a higher response than freshly-cut ones and this was made apparent at the end of the exercise and after the data analysis. Therefore, in order to confirm the hypothesis that the difference in the signal was mostly due to the difference in MIS2, we gave the samples a second water treatment after the last irradiation of 20 Gy (added dose) and measured the EPR signal after this treatment. We suspected that the MIS2 was due to the state of dryness of the old samples and knew from pilot studies that treatment would not affect the RIS. The resulting reduction of the signal for each sample is shown in Figure 11. In average, the signal before and after the second treatment were 0.5889 a.u. (± 0.0281) and 0.3709 a.u. (± 0.0209) respectively, with an average decrease in the signal amplitude of 0.2180 a.u. (± 0.0369). The resulting average of 0.3709 a.u. (± 0.0209) is very close to the average signal from fresh samples irradiated at the same 20 Gy, 0.3624 a.u. (± 0.0189), confirming our stated theory. Therefore, it may

be possible reduce the MIS2 as much as possible prior to performing EPR dosimetry in old fingernail samples by having additional water treatments.

Figure 12 shows the interpersonal and intrapersonal variability for each added dose for unstressed samples, computed in the same way as with stressed samples. As with stressed samples, the interpersonal variability was higher than the intrapersonal variability in unstressed samples and older samples had a higher variability than freshly-cut ones. Results of the t-test of the data sets for all split samples also showed that there was no statistical significant difference in EPR measurements between (interpersonal) or within (intrapersonal) samples (we could not reject the null hypothesis that the measurements were the same with $p \gg 0.05$ for all data sets and with a 95% CI). Variability was smaller in unstressed samples than in stressed samples (see Figures 7 and 12).

Effect of variation in size and number of fingernail clippings in unstressed samples

Figure 13 shows the dose dependences for the first experiment in the investigation of the effect of size and number of clippings in eight samples. One can see that in difference from previous cases, where number and size of clips were rigorously controlled; there is strong variation in dose dependence appearance. From this figure, one can see that variability of the dose dependence became significant if there is no control over the clippings' size and number. The residual and saturation doses, D_E and D_0 can be

significantly different for such samples.

Figure 14 shows the EPR dose response obtained from the second experiment for testing the effect of having strict requirements on the size and number of clippings using weight-normalized dose dependences. Although all three dose dependences seemed to have a similar appearance, the exponential fit using Grun formula gave very different results for D_E and D_0 for the same fingernail samples that were prepared differently

DATA ANALYSIS AND DISCUSSION

A distinctive radiation-induced signal (RIS) is seen within the EPR spectra of fingernails for all the investigated fingernail samples in this present study. Generally, the RIS integral intensity should be used as a measure of absorbed dose because this dose is proportional to the concentration of radiation-induced radicals. However, in most cases the EPR integral intensity (double integral of EPR signal) is strongly affected by a choice of baseline position and possible contributions from non-radiation-induced unresolved signals. Therefore, in all existing applications of EPR dosimetry (alanine and tooth enamel) the peak-to-peak amplitude of the first derivative is used as a measure of the absorbed dose. A peak-to-peak amplitude was selected as a measure of radiation dose response for fingernails for the same reasons (baseline uncertainty and the presence of overlapping non-radiation signals) as done for other EPR dosimetry applications.^{1,10}

For all the investigated samples, the peak-to-peak amplitude of the RIS signal was proportional to the radiation dose and the RIS is stable for more than 6 months if irradiated fingernail samples are stored at low temperatures (water in fingernails is frozen at temperatures $< 0^{\circ}\text{C}$). The first four groups (types) of the studied fingernail samples with the implementation of precise controls for size and number clippings – stressed-fresh, unstressed-fresh, stressed-old, and unstressed-old demonstrated having relatively low (insignificant) variability of dose dependence inside each group; whereas, the differences were statistically significant between the studied groups. The intensity of the EPR signals per unit of mass and dose for older fingernail samples was significantly higher than for freshly-cut samples in stressed and unstressed fingernails, even after normalization to EPR standard had taken place. The main difference between old and fresh fingernails is their water content; older samples are more dried. Fig. 11 shows that water treatment causes about 35% reduction of the RIS in irradiated samples. The difference in the slope of linear regression of the dose dependences (in other words, radiation sensitivity) for old and fresh stressed samples was also about 30% (5% bias can be explained by water squeezing out from the cutting edge of stressed fingernails). A comparison of the radiation sensitivity (dose response per 1 Gy of dose) of treated old and fresh samples showed a similar enhancement of sensitivity in old samples for about 35% (see Figs. 10 (a) and (b)). Thus, a comparison of the radiation sensitivity in old and fresh samples together, with a 35% reduction effect of a second treatment of irradiated unstressed samples, clearly indicates that water content is responsible for radiation sensitivity in both stressed and unstressed fingernail samples. Therefore, a general

recommendation for fingernail dosimetry is either to preserve the water content in fingernails by keeping them at low temperatures ($<0^{\circ}\text{C}$) when water is frozen, or to repeat water treatments to restore the original water content and to have the same (or close enough) radiation sensitivity as for *in vivo* samples.

A significant difference between the shape of dose dependence in stressed and unstressed samples of fingernails has been found. Stressed fingernails demonstrate a quasi-linear dose dependence in the investigated dose range ($< 20\text{ Gy}$) with a large dose offset (up to 20 Gy). The term quasi-linear has been used because as it is well known, all “linear” dose responses become non-linear at a certain level of dose and fit better with an exponential function⁸. Whereas, unstressed samples in the same dose range, show non-linear dose dependence with much smaller dose offset ($0.5 - 5\text{ Gy}$) and various values of saturated dose ($10 - 50\text{ Gy}$). Older fingernail samples are more sensitive to radiation than freshly-cut ones but have a higher dose offset (MIS2 contribution). As previously mentioned, the main difference between stressed and unstressed samples is the degree of mechanical stress in the fingernail sample and its water content. The degree of mechanical stress is determined by the number of clippings in the sample, their size and water content. This water content varies for different individuals and depends on the time-since-cut and storage conditions. The most possible reason for the observed low variability inside each group is a tight requirement for sample on size, time-after-cut, and number of clippings (Table I), which provides more or less the same level of mechanical stress in samples of the same group. In absence of the above control, there is a significant variation of dose dependence (Fig. 13). Thus, the degree of mechanical stress in

fingernail samples is responsible for the shape (quasi-linear or non-linear) of the dose dependence.

The problem of dose dependence variations in fingernails is complex because of two main factors responsible for radiation sensitivity its shape: water content, and the level of mechanical stress. Radiation sensitivity is not really independent, e.g., drier samples have higher mechanical stress in it.

The standard way of doing a dose assessment in EPR dosimetry consists of using the back extrapolation of the dose dependence, obtained by irradiation of samples under investigation to a set of known doses, to a zero EPR radiation-induced signal (dose, x-axis intercept). In case of stressed fingernails, the dose dependence is close to a linear model in the investigated dose range (<20 Gy). Variation of the parameters of linear fit (including the slope of dose dependence and dose offset) was found to be insignificant ($p < 0.01$) inside both studied (old and fresh) groups of stressed fingernail samples (see Figs. 3-4). This means that in principle, an universal dose calibration can be applied for these types of samples, similar to EPR dosimetry in tooth enamel. In contrast, unstressed fingernails demonstrate non-linear dose dependence with saturation that can be fitted with an exponential function. According to the sponge model [6], properties of unstressed fresh samples are most close to those of *in vivo* fingernails. Cardinal change of the dose dependence after deformation of fingernails makes the use of stressed samples to measure radiation dose (dose obtained in an unstressed state) difficult if not impossible. Certainly, there should be some critical (acceptable) level of deformation, which does not destroy

the radiation-induced radicals in fingernails; therefore, dose measurements would still be possible. Based on the results of present study, one can conclude that the parameter of the stress level in fingernails is the peak-to-peak amplitude of the MIS2, which we believe is the main contributor of dose offset. Indeed, the highest values of dose offset were found for stressed samples, (20.5 ± 2.1) Gy and (15.8 ± 2.5) Gy for older and freshly-cut fingernails respectively. The values of dose offset, D_E , and saturation dose, D_0 , determined from the fit of experimental data using the Grun formula⁸ for three differently stressed samples, prepared from the same fingernails (Fig. 14), are given in the Table VI.

It is interesting to note that small pieces are the mostly stressed type of samples, followed by large pieces, and that powder samples are the least stressed. Such behaviour is probably explained by understanding that although powder samples are expected to be mostly stressed during crushing, water-soaking of these samples is most effective in reducing stress in their small powder particles (highest surface area). In small pieces, treatment is not as effective and large pieces end up having the least stress. One can see that there is a correlation between D_E and D_0 (Fig. 15), e.g. the higher D_E is, the higher D_0 .

All 83 obtained dose dependences, including the quasi-linear dose dependences observed in stressed samples can generally be fitted by using the exponential function (Grun formula). As it was shown in Ref. 8,⁸ the use of an exponential fit gives a more accurate dose assessment than a linear fit of the same data. Fig. 16 shows the results of the correlation between D_0 and D_E for all (stressed and unstressed) measured samples.

The existence of a correlation between cystine chains and radiation radicals can be explained based on the sponge model in following way. Dose offset, D_E , is proportional to the mechanical stress exerted on the cystine chains. Then, the higher the stress (larger MIS_2), the easier it is to make a hole (radiation defect) in a cystine molecule. Then a more intensive RIS at the same dose exposure and a saturation RIS at a higher dose D_0 will be achieved. In other words, one can speculate that the mechanical stress in cystine chains produces traps for radiation defects in fingernails.

In a real-life scenario, a significant variation in dose dependence could significantly affect the accuracy and precision of dose measurements in fingernail samples. There are at least two ways to reduce the effect of possible changes in dose dependence during the sampling (cutting) of fingernails and their dose measurements:

- 1) Application of a meticulous procedure for fingernail sampling in which all samples would have the same size and number of clippings together with the treatment of soaking in warm water prior cutting. In this case, the mechanical stress and variation of dose dependence in the collected samples will be minimized. It would then be feasible (for this case) to develop an “universal” calibration curve and determine the dose in the samples being measured without additional irradiations; and
- 2) If collection of the “standard” type of sample is not possible, an alternate approach can be applied. After cutting and soaking the collected fingernail clippings, these unstressed samples (or parts of it) should be irradiated to 3-5 known doses. Similar to the additive dose method, the EPR signal should be measured after each irradiation. A fit of the obtained results using the Grun formula will allow to determine D_0 and D_E

($D_E = D_x + D_{E0}$), where D_x is the dose to be determined and D_{E0} is dose offset caused by mechanical stress. Fig. 16 facilitates the estimation of D_{E0} from D_0 , $D_{E0} = D_E - D_x$.

Applying these methods would allow the development of a consensus/universal type of dose calibration curve when we implement strict controls in sample preparation and measurements or a self-standard type of calibration curve when we do not, and the use an EPR fingernail dosimetry protocol as depicted in Fig. 16. A modified version of the provisional EPR biodosimetry protocol for use in radiation incidents and accidents delineated in Alexander et al., Appendix E (ref. 10) can be implemented to inspect samples without restrictions from hand washing, which was proposed when water was thought to reduce the RIS. Since water only affects the non-radiation signals, hand washing is in fact recommended. In order to avoid a reduction of water content in the samples, it is recommended to store them between measurements at low temperatures (keeping sample in a frozen state). In some cases, the original water content (and original dose dependence) in fingernails can be restored by additional soakings of the samples in water. Preparation and measurements are to be done as explained above. Data analysis will include regression of calibration curves to predict accidental dose, which may be modified by available specific information about exposure incident prior to assigning a radiation dose.

CONCLUSIONS

Fingernails form stable free radicals when subjected to ionizing radiation. These yield an EPR signal that is dose dependant with low interpersonal and intrapersonal variability, making possible EPR dosimetry in fingernails. Some of the advantages of fingernail biodosimetry are the sensitivity of its measurements, its non-invasive sample collection approach, easy sample preparation methods, its reproducibility (inter-laboratory and potentially using a field deployable unit) and its standardization and expansion (adaptation potential) capabilities.

However, highly-stressed fingernail samples are not suitable for dose assessments. These assessments need the application of strict requirements for fingernails collection and preparation. Fingernail samples should be cut with minimally invasive stress, e.g. after soaking in warm water and using sharp scissors. EPR signals and added radiation dose have a non-linear relationship for unstressed samples. The Grun formula, which was suggested for dose assessment in tooth enamel at high dose levels, seems to be well suited for unstressed fingernails. There is a significant variation of the dose dependence at different levels of mechanical stress in fingernail samples. Therefore, a special care should be taken for either having a highly reproducible dose dependence using rigorous controls for the number and size of clippings in samples being measured, or pin pointing the right dose dependence for a particular sample using the found correlation between the saturation dose, D_0 , and the residual dose offset, D_{E0} (Fig. 17).

With a starting dose (accidental dose), the additive method offers us the tool to have at least 3 irradiations (for example 2, 5, 10Gy) and use the Grun model in unstressed samples. We recommend that EPR fingernail dosimetry is done in unstressed (treated) samples, which give us a more stable signal. The application of the Grun model for predicting the dose of these samples is advisable. However, even though we see a non-linear response of the RIS in unstressed fingernail samples, it is important to notice that the portion of the curves at the range of radiation doses which may be of most interest for human exposures (categories below expectant in emergency radiological casualties or below the LD₅₀) is linear and its slope may still be useful in predicting the accidental dose.

Biodosimetry is based on the estimation of radiation dose by measuring radiation-induced changes in the body using a biological dosimeter. These should be easily obtained fluids or tissues that must change as a function of dose with a high signal-to-noise ratio. The measured effect has to be largely specific for ionizing radiation and evaluation should be easy, rapid, or capable of automation. Fingernail biodosimetry meets these qualifications and therefore is a promising emerging method in EPR dosimetry. The results of fingernail EPR dosimetry can be combined with that of other methods, such as teeth EPR dosimetry, for predicting a whole-body dose during triage, as recommended in Alexander et al.¹⁰ At the current stage of this research, we can use this method as complementary to other biodosimetry techniques.

The methodology described in this study can be applied to readily available off-the-shelf transportable EPR spectrometers with the appropriate software for fingernail dosimetry. A specific protocol for use of fingernail clippings as biological samples can place these on the list of physical dosimeters to be used in radiological emergencies with the advantage of having accurate measurements in a very short period of time (approximately 5-10 min). The challenges that we may encounter when adapting the protocol developed at our laboratory to a smaller field unit arise from the need for re-evaluating spectrum parameters, sample preparation procedures that would facilitate high sensitivity measurements ($< 1\text{Gy}$), and field environmental conditions that may affect spectrometers / EPR signals.

ACKNOWLEDGEMENTS

This study is part of a larger investigational project in EPR dosimetry: Center for Biophysical Assessment and Risk Management Following Irradiation – EPR Dosimetry. Approval for this research study design and recruitment of donors was obtained from the Institutional Review Board of the Uniformed Services University of the Health Sciences.

REFERENCES

- ¹ B.G. Dalgarno and J.D. McClymont, "Evaluation of ESR as a radiation accident dosimetry technique," *Appl Radiat Isot* **40**, 1013-1020 (1989).
- ² A. Romanyukha, F. Trompier, B. LeBlanc, C. Calas, I. Clairand, C. Mitchell, Smirniotopoulos J.G., and H.M. Swartz, "EPR dosimetry in chemically treated fingernails," *Radiation Measurements* **42**, 1110-1113 (2007).
- ³ F. Trompier, Kornak L., C. Calas, A. Romanyukha, B. LeBlanc, I. Clairand, C. Mitchell, and H.M. Swartz, "Protocol for emergency EPR dosimetry in fingernails," *Radiation Measurements* **42**, 1085-1088 (2007).
- ⁴ H. Chandra and M. C. Symons, "Sulphur radicals formed by cutting alpha-keratin," *Nature* **328** (6133), 833-834 (1987).
- ⁵ M.C. Symons, H. Chandra, and J.L. Wyatt, "Electron paramagnetic resonance spectra of irradiated finger-nails: A possible measure of accidental exposure," *Radiat Prot Dosimetry* **58** (No. 1), 11-15 (1995).
- ⁶ R.A. Reyes, A. Romanyukha, F. Trompier, C.A. Mitchell, I. Clairand, De T., L.A. Benevides, and H. M. Swartz, "Electron Paramagnetic Resonance in Human Fingernails: The Sponge Model Implication," *Radiation and Environmental Biophysics* (2008).
- ⁷ M. Egawa, Y. Ozaki, and M. Takahashi, "In vivo measurement of water content of the fingernail and its seasonal change," *Skin Res Technol* **12** (2), 126-132 (2006).
- ⁸ R. Grun, "Errors in dose assessment introduced by the use of the "linear part" of a saturating dose response curve," *Radiation Measurements* **26** (2), 297-302 (1996).

- ⁹ G.W. Snedecor and W.G. Cochran, *Statistical Methods*. (Iowa State University Press, 1989), Eighth ed.
- ¹⁰ George A. Alexander, Harold M. Swartz, Sally A. Amundson, William F. Blakely, Brooke Buddemeier, Bernard Gallez, Nicholas Dainiak, Ronald E. Goans, Robert B. Hayes, Patrick C. Lowry, Michael A. Noska, Paul Okunieff, Andrew L. Salner, David A. Schauer, Francois Trompier, Kenneth W. Turteltaub, Phillipe Voisin, Albert L. Wiley Jr, and Ruth Wilkins, "BiodosEPR-2006 Meeting: Acute dosimetry consensus committee recommendations on biodosimetry applications in events involving uses of radiation by terrorists and radiation accidents," *Radiation Measurements* **42** (6-7), 972-996 (2007).

TABLES

Table I. Practical sample requirements for fingernail EPR dosimetry.

Category	Require
Appearance	Healthy without polish
Cut	Recently for accident response or previously for retrospective studies
Clip size (width x length)	1-2 mm by 4-7 mm
Number of cuts in sample	8
Weight range	15 -20 mg

Table II. EPR recording conditions – Spectrometer settings.

Parameter	Value
HF modulation	100 kHz
Amplitude of HF modulation	0.5 mT (5 G)
Microwave power	Variable
Receiver gain	60 db
Time constant	81.92 ms
Converse time	40.96 ms
Number of points	1024
Sweep time	41.96 s
Number of scans	10
Total recording time	7 min
Central field	351 mT (3510 G)
Sweep field	15 mT (150 G)

Table III.A. Peak to peak amplitude of EPR signals in stressed fresh fingernail samples (within 24 hours of clipping) at 0, 2, 5, 10, and 15 Gy added radiation dose, slope for each sample, and R^2 [average slope = 0.0281 (± 0.0017), average $R^2 = 0.9982$ (± 0.0013)].

Dose (Gy)	Sample ID									
	Fresh 1	Fresh 2	Fresh 3	Fresh 4	Fresh 5	Fresh 6	Fresh 7	Fresh 8	Fresh 9	Fresh 10
0	0.4614	0.4352	0.4460	0.3960	0.4200	0.4740	0.4080	0.4060	0.5090	0.4930
2	0.5162	0.4940	0.5070	0.4420	0.4880	0.5310	0.4700	0.4570	0.5680	0.5436
5	0.5862	0.5827	0.5700	0.5240	0.5600	0.6110	0.5600	0.5410	0.6720	0.6536
10	0.7390	0.7049	0.6910	0.6610	0.7130	0.7520	0.6860	0.6760	0.8060	0.7840
15	0.9120	0.8590	0.8360	0.7890	0.8840	0.8990	0.8170	0.7980	0.9490	0.9390
Slope	0.0299	0.0278	0.0254	0.0265	0.0305	0.0282	0.0270	0.0263	0.0293	0.0297
R^2	0.9954	0.9985	0.9973	0.9996	0.9974	0.9997	0.9985	0.9994	0.9985	0.9980

Table III.B. Peak to peak amplitude of EPR signals in stressed old fingernail samples (after 24 hours of clipping) at 0, 2, 5, 10, and 15 Gy added radiation dose, slope for each sample, and R^2 [average slope = 0.0387 (± 0.0008), average $R^2 = 0.9987$ (± 0.0015)].

Dose (Gy)	Sample ID									
	Old 1	Old 2	Old 3	Old 4	Old 5	Old 6	Old 7	Old 8	Old 9	Old 10
0	0.7600	0.7790	0.8140	0.7380	0.7430	0.7170	0.7237	0.8920	0.8890	0.8510
2	0.8260	0.8600	0.8920	0.8360	0.8290	0.8000	0.8020	0.9850	0.9540	0.9350
5	0.9310	0.9680	1.0100	0.9390	0.9410	0.9340	0.9200	1.1020	1.0650	1.0469
10	1.1160	1.1540	1.2000	1.1180	1.1430	1.1200	1.1100	1.2870	1.2400	1.2282
15	1.3280	1.3630	1.4000	1.3030	1.3310	1.3110	1.2950	1.4950	1.4780	1.4470
Slope	0.0378	0.0385	0.0390	0.0370	0.0392	0.0395	0.0381	0.0396	0.0389	0.0391
R^2	0.9980	0.9992	0.9999	0.9985	0.9997	0.9989	0.9999	0.9992	0.9979	0.9986

Table IV. Weight difference after treatment of samples and time after cut for first set of treated samples. Fresh samples were collected within 24 hours prior to measurements; whereas, old samples were measured after 24 hours post collection.

Sample	Weight before treatment (mg)	Weight after treatment (mg)	Weight diff. (mg)	Time since cut (hh:mm)
Fresh 1-1	30.92	31.71	0.79	0:09
Fresh 2-1	29.72	31.28	1.56	4:05
Fresh 3-1	29.92	31.12	1.20	1:52
Fresh 4-1	30.66	32.59	1.93	10:19
Fresh 5-1	30.57	32.55	1.98	11:27
Fresh 6-1	29.79	31.88	2.09	20:48
Fresh 7-1	30.17	31.11	0.94	0:48
Fresh 8-1	30.52	32.40	1.88	5:12
Fresh 9-1	29.35	31.20	1.85	7:45
Fresh 10-1	30.28	31.11	0.83	0:21
Old 1-1	29.21	31.45	2.24	65:59
Old 2-1	30.73	33.45	2.72	1366:40
Old 3-1	30.98	33.58	2.60	984:32
Old 4-1	29.38	32.53	3.15	4466:35
Old 5-1	30.47	33.50	3.03	2200:43
Old 6-1	29.88	33.22	3.34	5605:30
Old 7-1	30.55	33.63	3.08	3169:30
Old 8-1	30.44	33.74	3.30	4412:40
Old 9-1	30.15	33.29	3.14	2585:14
Old 10-1	30.21	32.56	2.35	145:15
Average	30.20	32.40	2.20	
SD	0.52	0.97	0.84	

Table V. Dose response in treated (unstressed) samples (each value is the average obtained from split samples, two samples per donor, n=40).

Added Dose (Gy)	Fresh 1	Fresh 2	Fresh 3	Fresh 4	Fresh 5	Fresh 6	Fresh 7	Fresh 8	Fresh 9	Fresh 10
0	0.0885	0.1000	0.1178	0.1209	0.1300	0.1360	0.1084	0.1173	0.1052	0.0974
2	0.1318	0.1430	0.1485	0.1569	0.1645	0.1745	0.1408	0.1448	0.1446	0.1380
5	0.1850	0.2010	0.1906	0.2080	0.2130	0.2230	0.1870	0.2050	0.1920	0.1860
10	0.2570	0.2740	0.2571	0.2800	0.2930	0.2960	0.2600	0.2860	0.2670	0.2580
15	0.2977	0.3237	0.3100	0.3367	0.3421	0.3467	0.3038	0.3300	0.3161	0.3008
20	0.3337	0.3610	0.3520	0.3834	0.3788	0.3888	0.3406	0.3690	0.3710	0.3459
Correlation	0.9813	0.9841	0.9952	0.9936	0.9883	0.9907	0.9887	0.9853	0.9940	0.9889

Added Dose (Gy)	Old 1	Old 2	Old 3	Old 4	Old 5	Old 6	Old 7	Old 8	Old 9	Old 10
0	0.1950	0.1935	0.1913	0.2297	0.1859	0.2051	0.1798	0.2130	0.1840	0.1900
2	0.2609	0.2746	0.2420	0.3017	0.2588	0.2879	0.2550	0.2920	0.2450	0.2453
5	0.3144	0.3466	0.3161	0.3636	0.3356	0.3559	0.3407	0.3550	0.3280	0.3042
10	0.4128	0.4407	0.4280	0.4674	0.4500	0.4733	0.4585	0.4630	0.4339	0.4033
15	0.4927	0.5200	0.5124	0.5558	0.5380	0.5651	0.5448	0.5500	0.5314	0.5035
20	0.5440	0.5770	0.5680	0.6170	0.5960	0.6200	0.6119	0.6060	0.5890	0.5600
Correlation	0.9904	0.9847	0.9909	0.9914	0.9878	0.9868	0.9877	0.9881	0.9905	0.9950

Table VI. Dose offset, D_E , and saturation dose, D_0 , determined from the fit of experimental data of three samples made of powder, large and small pieces using the Grun formula.

Sample	D_E	D_0
Powder	1.0813	9.5838
Large pieces	2.1418	20.316
Small pieces	2.9065	34.850

FIGURES AND LEGENDS

1. Sample Collection
 - a. Examine donor fingernails to be sampled.
 - i. Look for a natural look with no evidence of illness.
 - ii. Clean off any polish that may be on fingernail.
 - b. Collect sample from donor (initial cut) using sharp scissors.
 - c. Record time of cutting.
 2. Sample Preparation
 - a. Cut sample to size that would fit EPR sampling tube (approximately 1-2 mm by 4-7 mm).
 - b. Weight sample (>15 mg).
 - c. Record number of clippings.
 - d. Record sample weight.
 - e. Treatment. Place sample in water bath for 10 minutes and allowed at least 5 minutes of drying time before measurement.
 - f. Weight sample.
 - g. Record sample weight.
- NOTE: For “older” (previously cut > 24 hours) fingernails, steps 2e, 2f, and 2g may need repetition.
3. Collect sample spectra at 1mW and 16 mW (repeat at least three times to derive statistical standard deviation).
 4. Multiply spectrum obtained at 16 mW by $(1/16)^{1/2}$ and subtract it from that obtained a 1 mW.
 5. Record amplitude of the signal.
 6. Irradiate samples in increase dose steps at 2Gy, 3 Gy, and 5Gy (5Gy step may be repeated 2-3 times).
- NOTE: Sample weights are measured and recorded prior to each measurement.
7. Repeat steps 3-5 after each irradiation and collect data for the collective doses of 2Gy, 5Gy, 10Gy, and 15Gy, and 20Gy if a third 5Gy irradiation is done.
 8. Normalize and record the average measurement for each dose and corresponding standard deviation.
 9. Plot data of the EPR dose response curve (if linear, compute slope).
 10. Obtain the correlation coefficient.
 11. Use statistical software for variability evaluation of data.
 12. Use plotted data (Amplitude vs Dose) and perform fit [linear for untreated and exponential growth (Grun model) for treated samples].

FIG. 1. Experimental steps for the assessment of radiological doses using fingernails as biodosimeters.

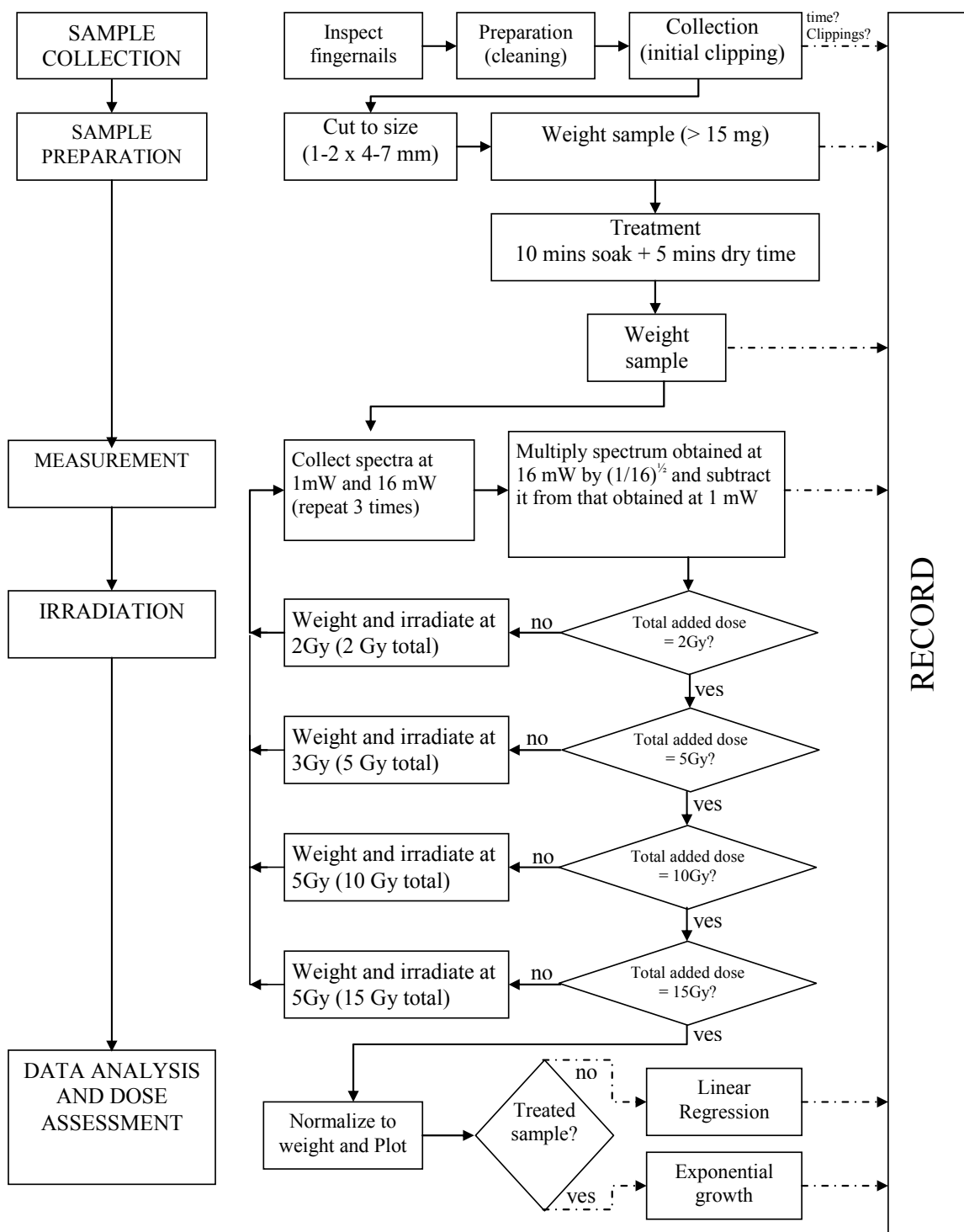


FIG. 2. Flow chart illustrating experimental steps for the assessment of radiological doses using fingernails as biophysical dosimeters.

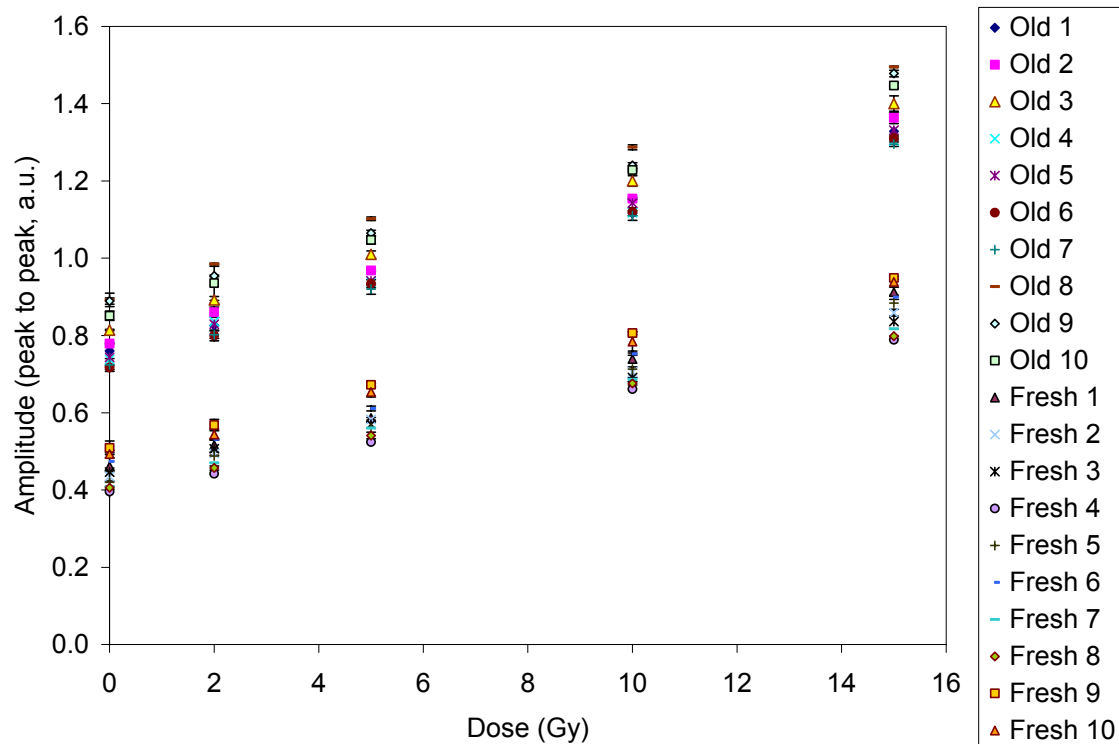


FIG. 3. EPR Signal dose response in stressed (untreated) fingernails (30 mg / 8 clippings). Symbols represent the mean value of 3 measurements, 10 scans each. Error bars represent 1 standard deviation.

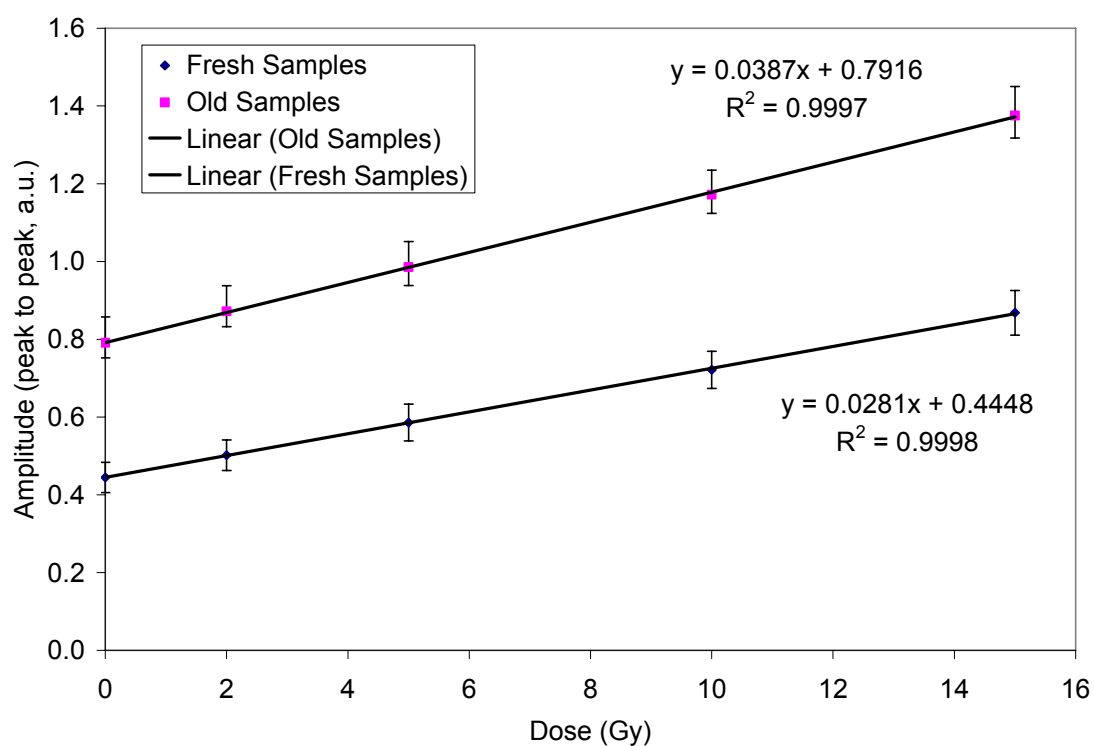
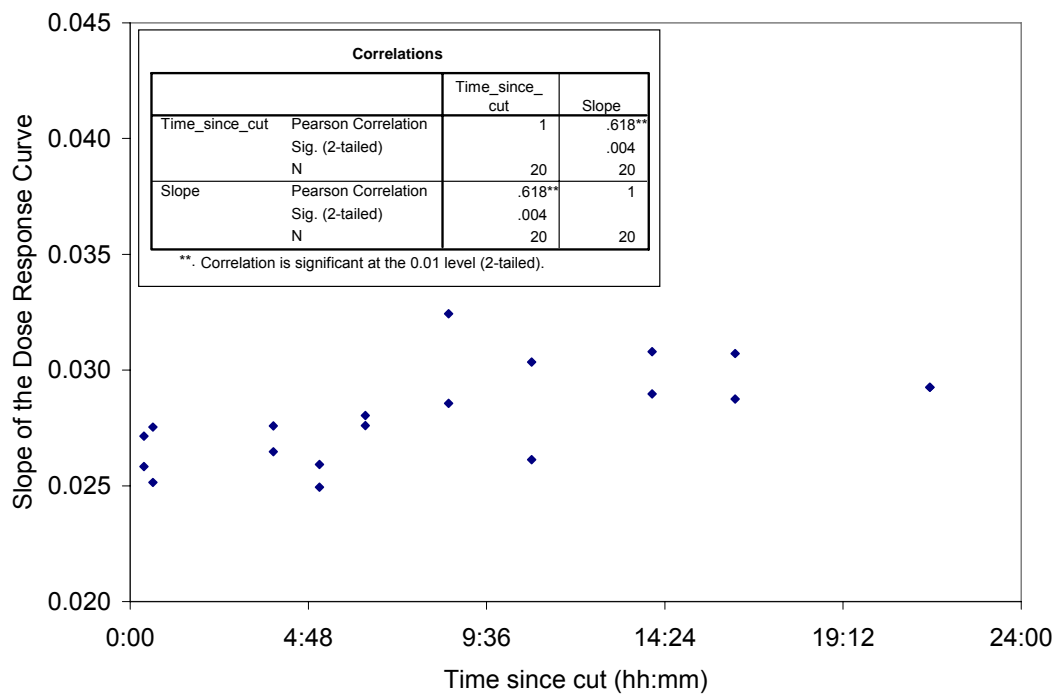
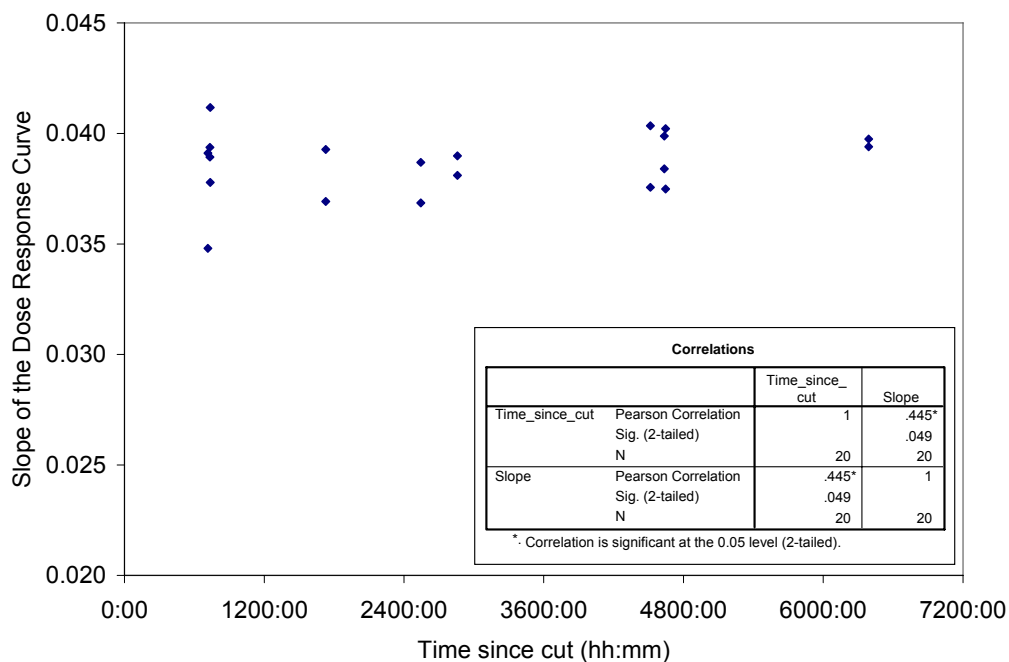


FIG. 4. Average EPR dose response in freshly (“fresh”) and previously cut (“old”) fingernail samples at 0, 2, 5, 10, and 15 Gy added radiation dose (30 mg / 8 clippings, n=40). Error bars represent 1 standard deviation.



(a)



(b)

FIG. 5. Slope variation in EPR added radiation dose response in freshly-cut (a) and old (b) fingernails (values are the average for each donor' split sample).

Correlations

		Time_since_ cut	Slope
Time_since_cut	Pearson Correlation	1	.808**
	Sig. (2-tailed)		.000
	N	40	40
Slope	Pearson Correlation	.808**	1
	Sig. (2-tailed)	.000	
	N	40	40

** . Correlation is significant at the 0.01 level (2-tailed).

FIG. 6. SPSS output showing the correlation between the slope of the dose curve and the time-since-cut for all stressed (untreated) samples.

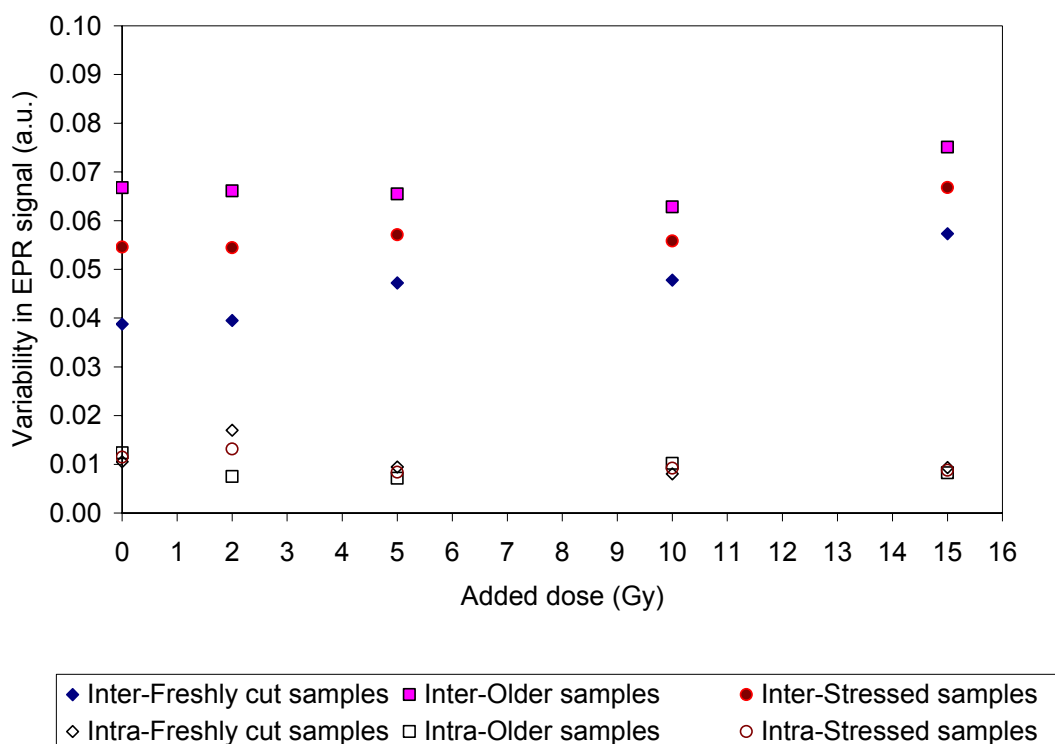
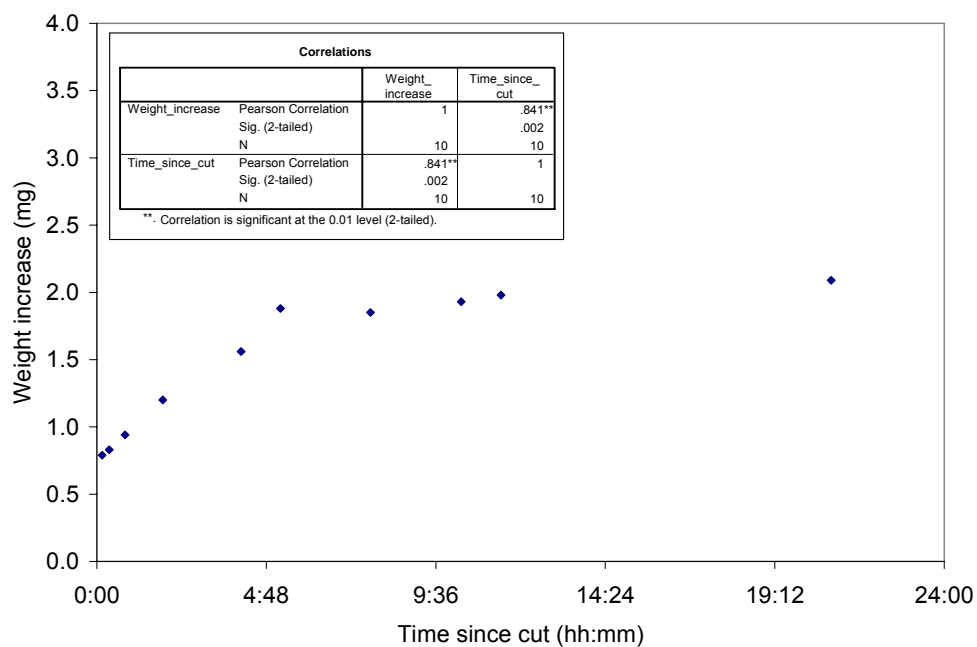
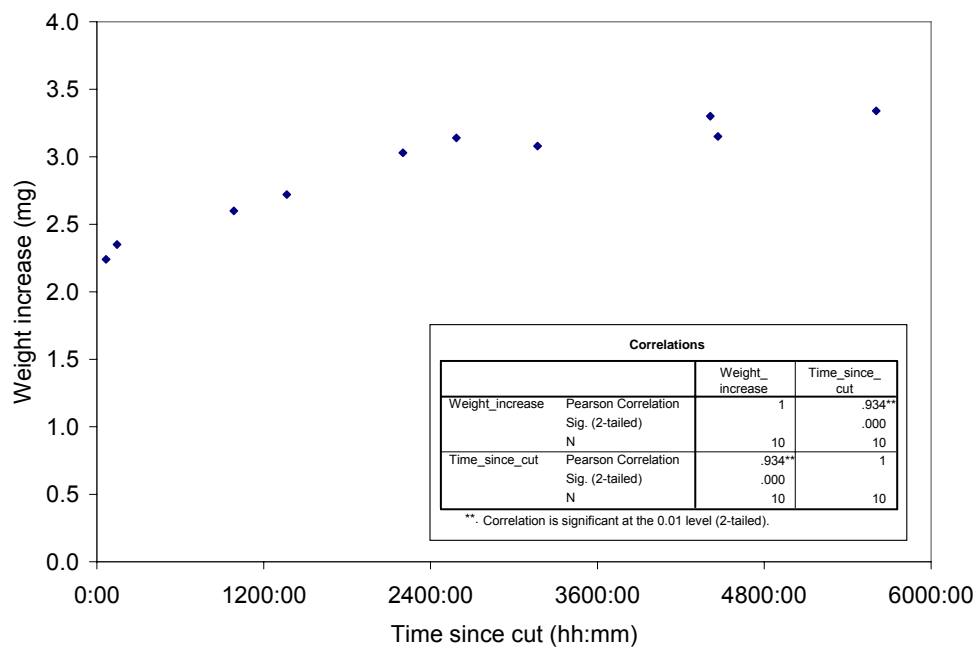


FIG. 7. Interpersonal and intrapersonal variability of EPR radiation dose response (peak-to-peak amplitude) for added dose values of 0, 2, 5, 10, and 15 Gy for freshly-cut, older samples, and for all stressed samples. The interpersonal variability was assessed using the standard deviation of the averaged (over split samples) values obtained for each added dose and the intrapersonal variability by using the standard deviation in measurements from each donor (not averaged) and estimating the overall variance at each added dose.



(a)



(b)

FIG. 8. Weight increase after 10 min treatment with water versus time since cut for fresh (a) and old (b) fingernail samples (values are from the first sample of each donor' split set).

Correlations

		Time_since_ cut	Weight_ increase
Time_since_cut	Pearson Correlation	1	.807**
	Sig. (2-tailed)		.000
	N	20	20
Weight_increase	Pearson Correlation	.807**	1
	Sig. (2-tailed)	.000	
	N	20	20

** . Correlation is significant at the 0.01 level (2-tailed).

FIG. 9. SPSS output showing the correlation between the weight increase in unstressed (treated) fingernails and the time-since-cut.

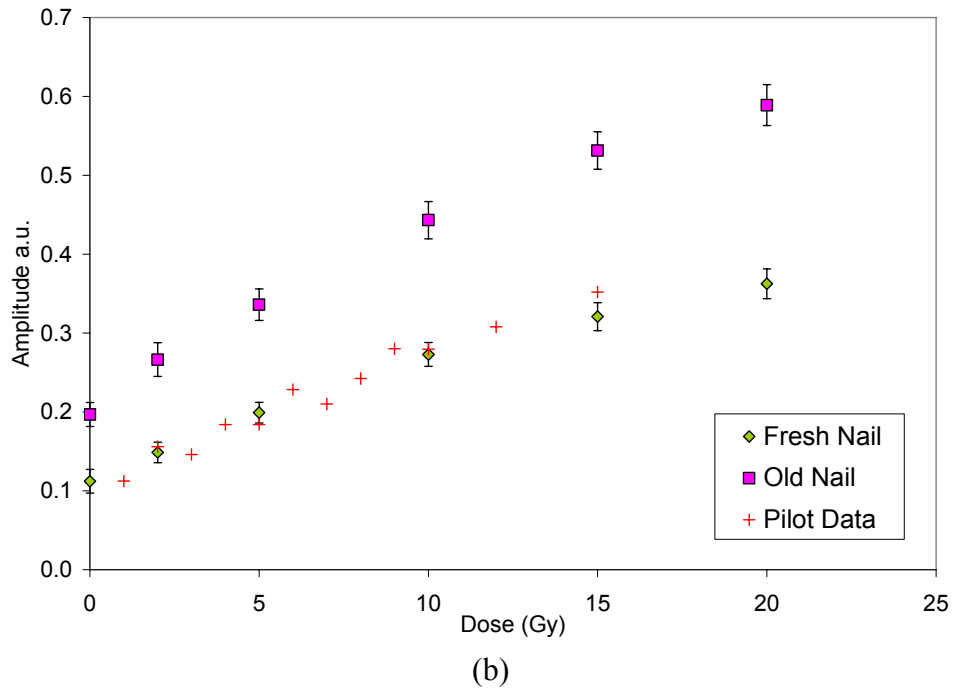
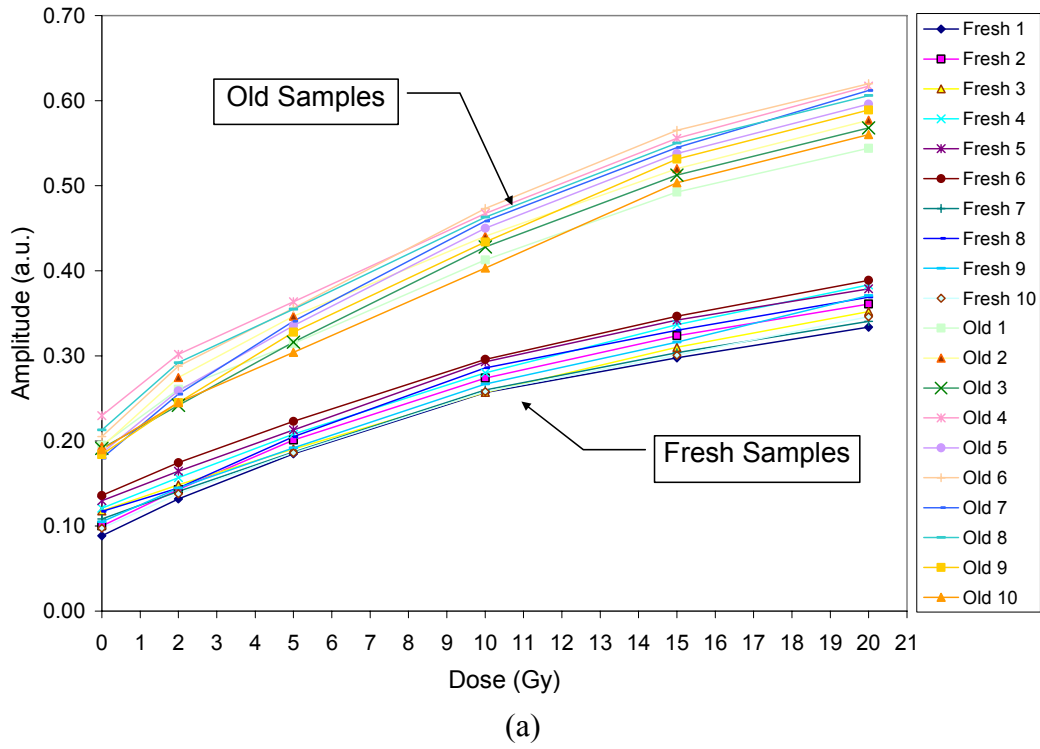


FIG. 10. Dose dependence in unstressed (treated) fingernail samples; (a) shows the data for 20 donors and (b) shows the average for freshly-cut and older samples, $n=40$ (plus-sign represent pilot data fitted to plot). Error bars represent 1 standard deviation, 95 % confidence interval.

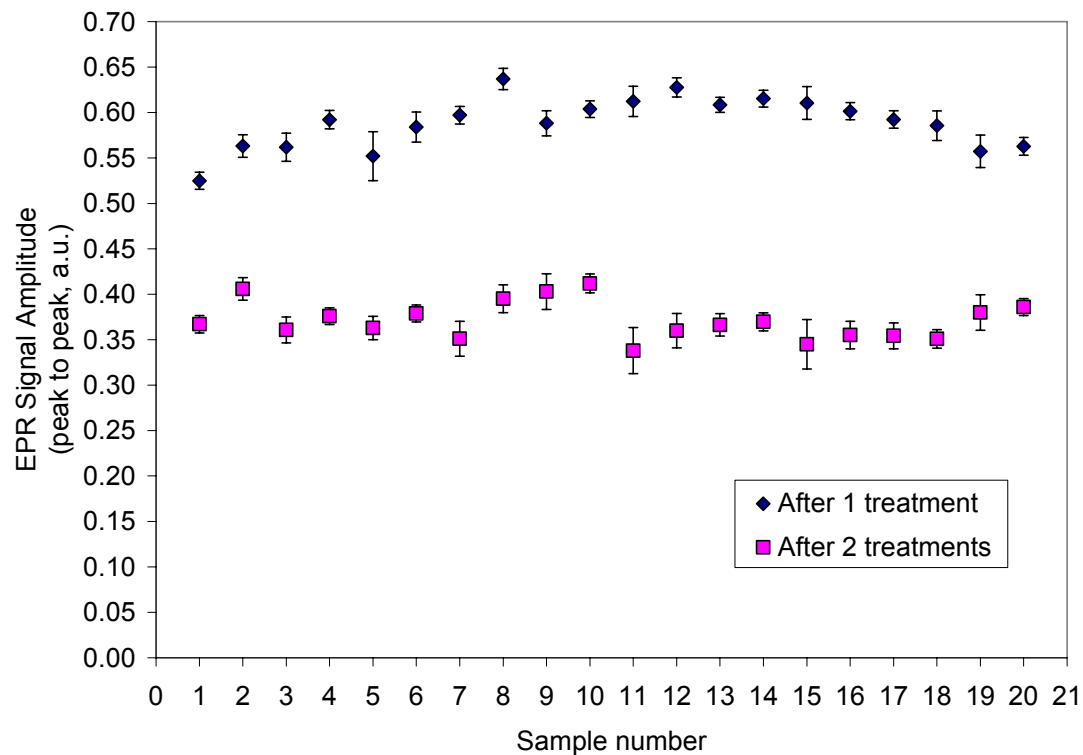


FIG. 11. Signal reduction for 20 old unstressed samples after last irradiation of 20 Gy (cumulative). Error bars represent 1 standard deviation, 95 % confidence interval.

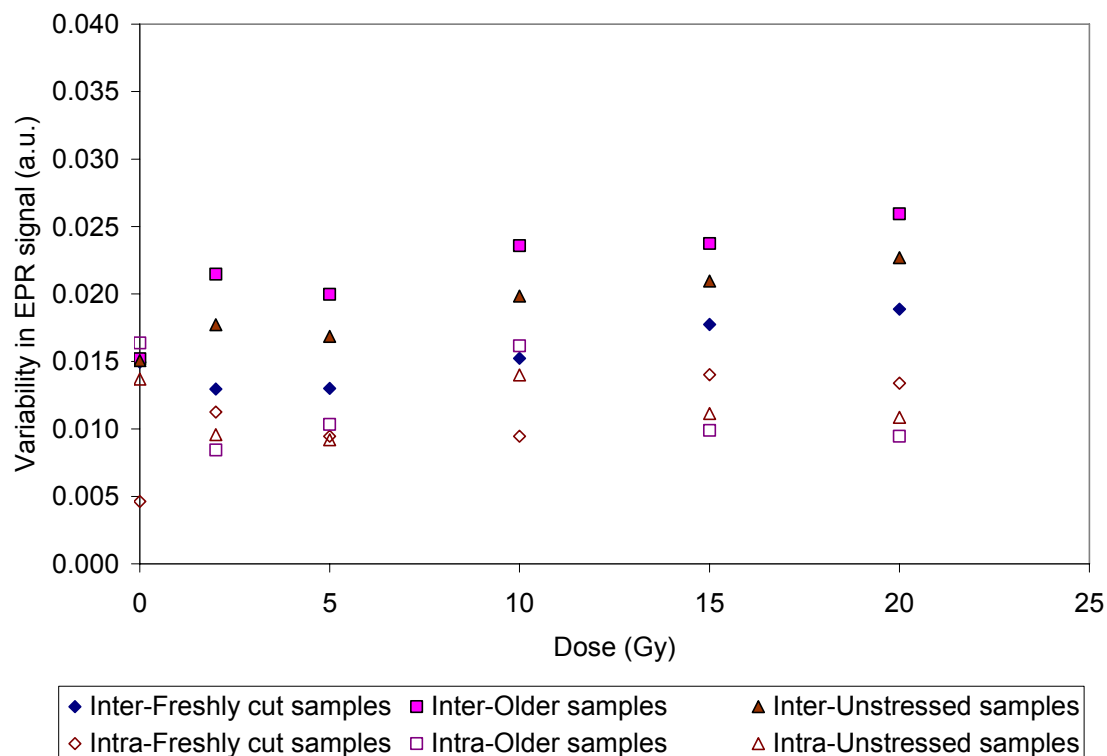


FIG. 12. Interpersonal and intrapersonal variability of EPR radiation dose measurements for added dose values of 0, 2, 5, 10, 15, and 20 Gy for freshly-cut, older samples, and for all unstressed samples. The interpersonal variability was assessed using the standard deviation of the averaged (over split samples) values obtained for each added dose and the intrapersonal variability by using the standard deviation in measurements from each donor (not averaged) and estimating the overall variance at each added dose.

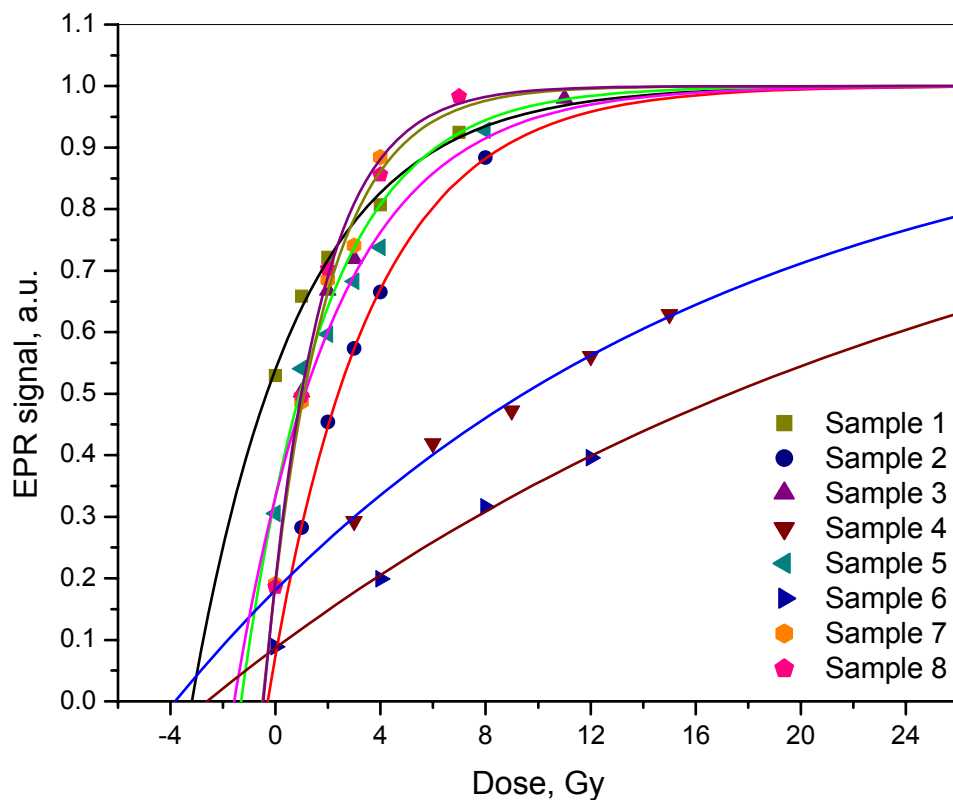


FIG. 13. Dose dependences for treated fingernail samples with different number of clippings and size. The solid lines show the fit of the experimental results using Grun formula: $A = I_{\max} (1 - \exp(-(D + D_E)/D_0))$,⁸ where A is the EPR dose response, I_{\max} is the maximum EPR dose response (saturation level), D is the variable dose, D_0 is the characteristic saturation dose, and D_E is the dose to be determined. All results were normalized on I_{\max} .

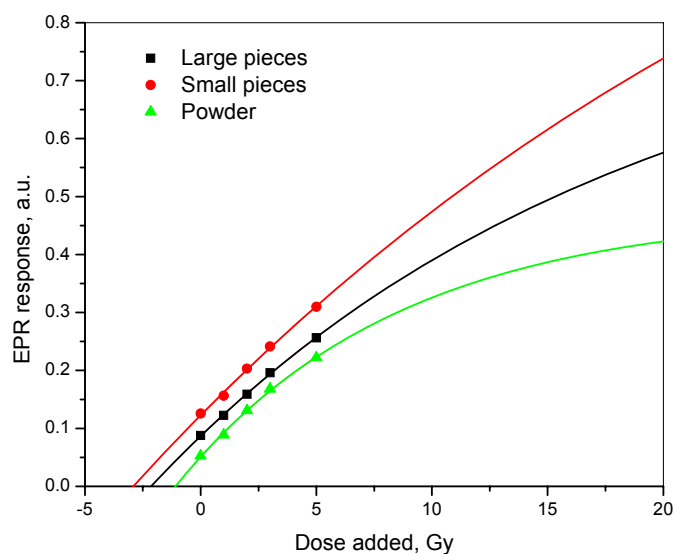


FIG. 14. Dose dependences for samples from fresh fingernails, collected from the same person, at the same time, but prepared differently. The triangle symbols represent the dose dependence values for the powder sample, the square symbols represent the dose dependence values for the sample with large pieces, and the round symbols represent the dose dependence values for the sample with small pieces. The solid lines are the results of the exponential fit of the data using the Grun formula.

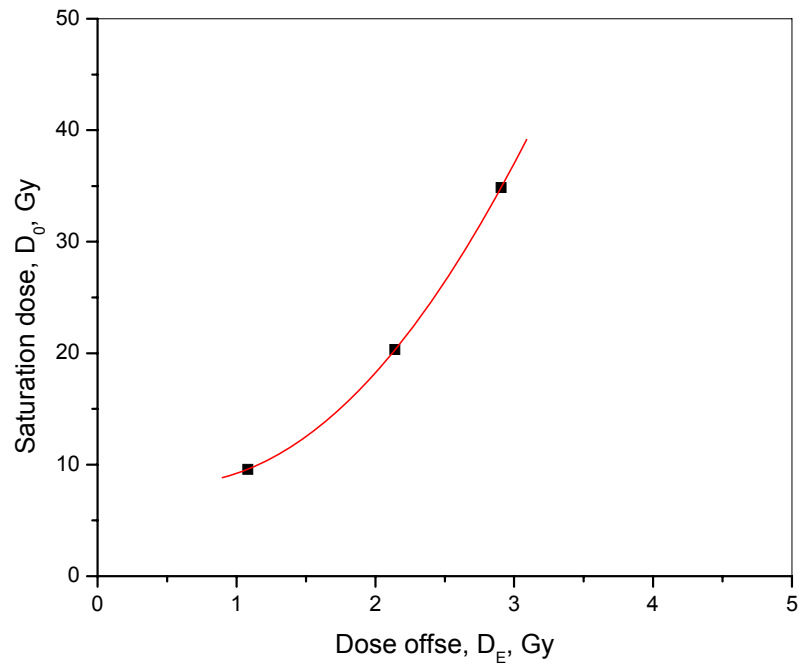


FIG. 15. Saturation dose versus dose offset for three samples with different size and number of clippings in the sample.

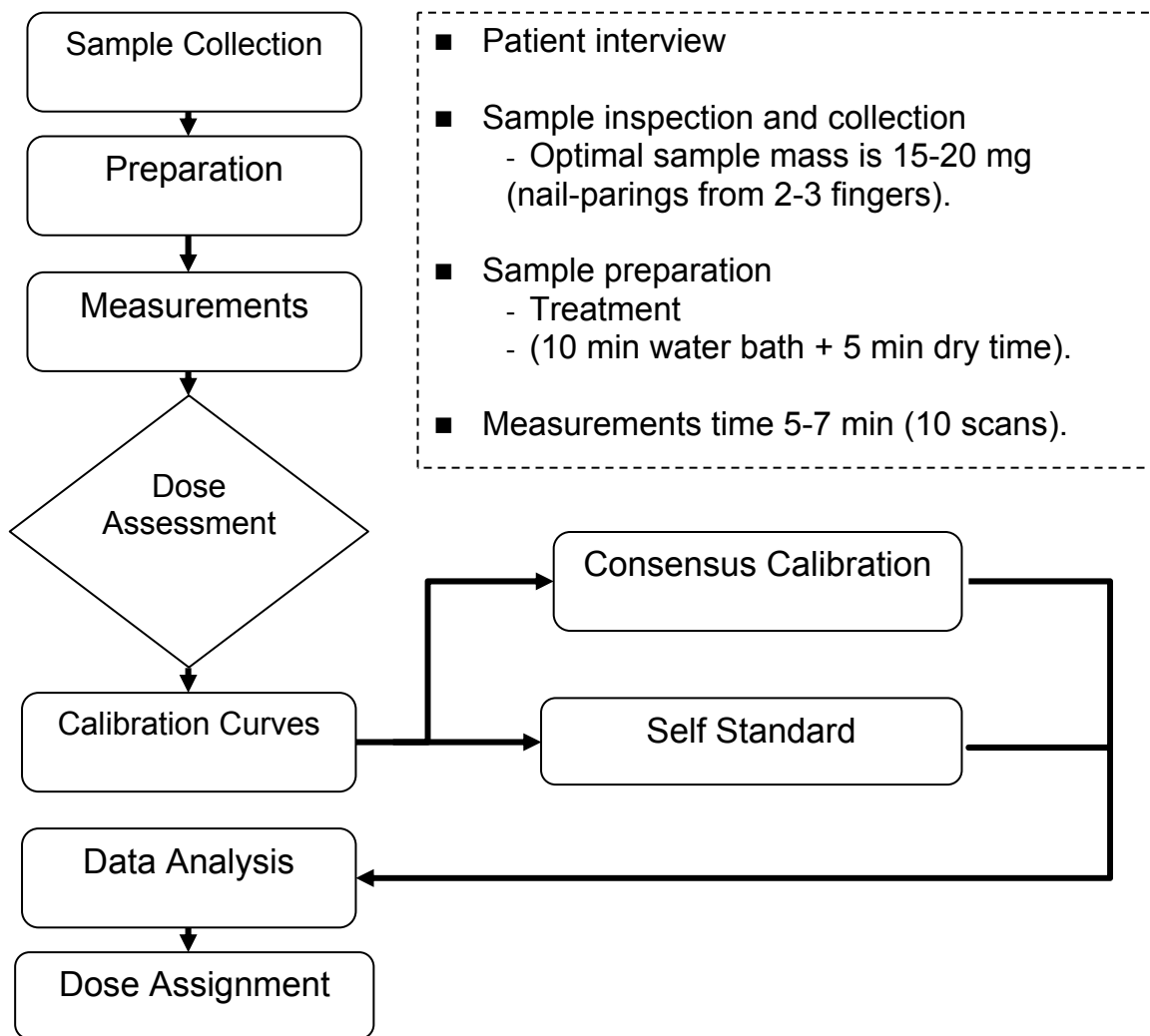


FIG. 16. EPR fingernail dosimetry protocol for use in radiation incidents and accidents.

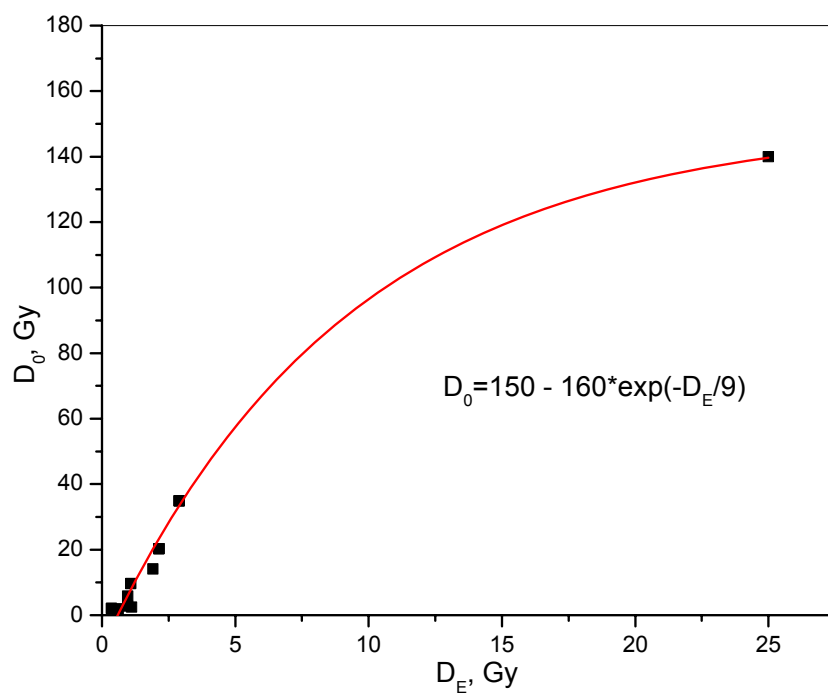


FIG. 17. Correlation between D_0 and D_E in stressed and unstressed fingernails samples.

CHAPTER 5

CONCLUSION

5.1. DISCUSSION OF RESEARCH FINDINGS

The hypothetical situation presented in this study included demonstrating that our null hypothesis (H_0 : Fingernail clippings CANNOT be used as biodosimeters of suspected radiological casualties using EPR/ESR dosimetry technology) could be rejected by addressing all identified factors that affect the EPR signals, evaluating the correlation of these signals with radiation dose, and the sources of uncertainty that affect them. The identified factors included weight, number of clippings, spectrometer settings, sample collection and preparation, temperature, and the presence of other signals. We controlled for samples weight, number of clippings, spectrometer settings, and temperature by normalizing all data to weight in the same fashion, matching samples with the same number of clippings, keeping the same spectrometer settings during all measurements, and handling samples under the same temperature conditions (at low temperatures – in freezer $\approx -20^\circ\text{C}$ in between measurements) respectively. All samples were prepared in the same way using sample preparation techniques described in chapter 2 and illustrated in chapters 3 and 4 that allowed us to get closer to a realistic exposure-to-fingernail scenario, in which nails are as hydrated as in their *in vivo* stage. By using this technique, we can avoid mistakes found in previous studies, in which fingernails were stressed and showed a behavior not representative of their true life phase.

The non-radiation induced signals, described in chapters 1-4, were handled using methods shown in chapter 3. The MIS1, originated during the initial clipping and cutting during sample preparation, was eliminated by allowing it to decay with time (≈ 24 hrs) or with water treatment. The MIS2, which originates during the plastic deformation at cutting and while sample is drying, was also significantly reduced with treatment. This MIS2 was identified and corrected-for by using measurements at two different microwave powers (1 and 16 mW) and subtracting the spectrum collected at 16 mW (algebraically modified by using a multiplication factor, $(1/16)^{1/2}$) from that collected at 1 mW, as described in chapters 2-4. A strong positive correlation of the EPR signals in fingernails and added radiation was found in all samples with minimal variability (both interpersonal and intrapersonal) in measurements, as reported in chapter 4. Therefore, our study showed enough evidence to prove that fingernails are great candidates as biomarkers in EPR dosimetry that can be used as complementary assessments to other already established physical dosimetric techniques. However, in order to recommend its use as an accurate dose assessment methodology, such as teeth dosimetry, further investigations of our sampling procedures and their effect on the RIS need to take place.

In chapter 3 the most significant problems in fingernail EPR dosimetry were investigated as been related to the presence of signals of non-radiation origin. These are the MIS, which would decay in a 20-24 period and the BKS, which has a mechanical component that grows with time. This chapter characterized these signals and showed a methodology for isolating and correcting for their combined effect on the EPR spectra, as explained above. Due to the mechanical properties of these signals the MIS was identified as the MIS1, associated with the break of the S-S bridges between the peptide

chains that form electron dipoles after elastic deformation, and the MIS2, associated with the deformation of the keratin helix at sample cutting and as the sample dries out with time. The most contributing fact offered in this chapter was the association of the mechanical behavior of fingernails with that of a sponge (the sponge model implication). By doing this, it was possible to explain the behavior of the non-radiation conflicting signals and their isolation from the RIS. In this chapter the development of the water treatment for the restoration of the spongy tissue of fingernails that would not affect the RIS is explained and recommended for dosimetry studies in unstressed samples. These would be samples that have been physically restored and free of mechanical stress from clipping, cutting, and the natural drying process; therefore, having minimal to null effect on the RIS. The resulting dose response curves using these samples were non-linear.

Chapter 4 showed the evaluation of the variability of the dose dependence in fingernails using stressed and unstressed samples and confirmed that not only these have different dose response behavior, linear and non-linear respectively, but also that the magnitude of the signals in freshly-cut samples (<24 hrs) was significantly smaller than in older samples (previously collected). The level of stress in the spongy tissue of fingernail samples, which would affect the magnitude of the MIS1 and MIS2 contribution to the spectra, was not quantified here. However, it was confirmed that they are caused by the processes of clipping, cutting, and drying of this spongy tissue.

It is proposed that treated samples be used in fingernail EPR dosimetry because they show more stable signals than untreated ones and have lower interpersonal and intrapersonal variability. A strong positive correlation between the RIS and added dose was reported as well as a positive correlation between the slopes and time-since-cut (time

between clipping/cutting and measurement) in stressed samples and water absorption and time-since-cut in unstressed samples. The use of this time-since-cut factor was justified as that this would be an indicator of the state of dryness and physical (plastic) deformation of the keratin helix of the samples that would go beyond the 24 hour period, after which the MIS2 would dominate the mechanical induced contribution to the EPR signal. The interpersonal and intrapersonal variability, as a potential source of uncertainty in measurements was evaluated and the result showed that these were very small.

The major factor responsible for radiation sensitivity of fingernails was identified as their water content, which can affect radiation sensitivity up to 35%. The major factor responsible for shape of the radiation sensitivity was identified as the mechanical stress. At a significant level of mechanical stress, the shape of dose dependence is linear in the studied dose range (<20 Gy), and in lesser-stressed samples, it is of an exponential growth with saturation type which depends on the degree of mechanical stress. This manuscript showed the possibility for developing universal dose response curves in samples in which strict controls for weight, number of clippings, and time-since-cut are taken and offered recommendations on the appropriate ways of doing dose measurements in fingernails.

5.2. PUBLIC HEALTH RELEVANCE

The public health significance of this study was addressed in chapter 1. The method developed here accommodates a simple non-invasive way to collect and prepare samples and make accurate EPR measurements to predict accidental radiation doses. This method is a rapid assessment of individual radiation doses using fingernails as biodosimeters and serves as the foundation for the development of emergency response protocols using fingernail EPR dosimetry. This has a larger impact when individual results are applied to others who have been exposed to the same radiological sources, in the same location, and for the same period of time. Therefore, avoiding the need for further individual measurements in a mass casualty scenario and allowing health care providers to promptly assess prognosis during the triage of exposed patients and recommend treatment based on few individual results.

This study offers the main tools for adapting the method we developed in a laboratory setting to a possible field-deployable unit. For example, a smaller scale off-the-shelf EPR spectrometer, currently available for use with other sample media, can be adapted for use with finger- and toe- nails. This unit can then be taken to the site of a radiological accident/incident or to an area where military operations would deal with radiation sources, where samples would be collected, prepared, and immediately measured for rapid dosimetry assessment.

5.3. RECOMMENDATIONS FOR FUTURE RESEARCH

The research included in this dissertation sets a benchmark for performing fingernail EPR dosimetric studies. At this current stage of research, we cannot conclude that we have a totally true representation of an *in vivo* scenario involving fingernails. However, we have gotten a step much closer to a realistic situation in fingernail behavior under both mechanical and radiation-induced stressors. Our approach sets the stage for performing future dosimetry assessments.

This dissertation shows that fingernails can be used as biodosimeters of suspected radiological casualties using EPR technology. However, before this technique can be recommended for dose assessment, there must be more investigations of the effects of our developed sampling and treatment protocols on the radiation induced signals and the persistence of these signals.

The next generation of experiments should include the further investigation of the persistence of the signals at both low temperatures, where the RIS is being known to persist, and at ambient temperature, where the behavior of the RIS has not been documented, and a set of tests in which:

- 1) samples are (1) treated, (2) irradiated, and then (3) cut (at this point samples have had an acute dose). A step (4) for dose assessment would be step-added-irradiation, as described in step 6 (experimental step in chapter 4) and illustrated in Figure 1 and flow chart in chapter 4. One would expect the cutting of the samples to induce an MIS1; therefore, making them stressed samples;
- 2) samples are (1) cut, (2) treated, and then (3) irradiated (at this points samples have

had an acute dose). A step (4) for dose assessment would be step-added-irradiation, as described in step 6 (experimental step and flow chart in chapter 4). One would expect samples to be unstressed, as treatment took place after cutting, drastically reducing or eliminating the induced MIS1; and

3) a variation of 1) is done in which samples are (1) treated on hand prior to cutting (reduction of the original MIS), (2) cut, (3) treated (reduction of additionally induced MIS), and then (4) irradiated (at this point samples have had an acute dose). A step (5) for dose assessment would be step-added-irradiation, as described in step 6 (experimental step in chapter 4) and illustrated in Figure 1 and flow chart in chapter 4. One would expect these to be unstressed samples, closer to an *in vivo* scenario.

These experiments would then be performed under various conditions and evaluation would take into account changes in storage temperatures, time-since-cut, and other potential confounding factors.

5.4 CONCLUSION

This study has given a physical/mechanical explanation to the behavior of EPR signals in fingernail dosimetry by modeling fingernails as a sponge and studying its behavior under different stress conditions. Since previous work was performed using stressed (untreated) samples, they do not represent the realistic behavior of unstressed (treated) fingernails. The fingernail is modeled as a sponge, physically stressed during the initial clipping in sample collection and preparation, and drying with time. Both processes cause elastic and plastic deformational stresses on the fingernail tissue that are

the cause of the mechanical EPR signals, MIS1, and MIS2, observed in fingernail spectra.

The MIS1 is believed to originate from the electron dipoles formed at the S-S bridges after elastic deformation and the MIS2 originates from the plastic deformation of keratin helix, as electron dipoles or holes form in the cystine backbone chains of the sample when cut and as it dries with time, as described in chapters 1 and 3. The MIS1 fades with time and the MIS2 slightly increases with time until it is relatively stable, as reported in chapter 3. This ongoing combined effect on the EPR signal makes it impossible to use stressed (untreated) fingernails for emergency dosimetry assessment.

The developed water treatment eliminates the combined effect of these signals to allow us use finger- and toe- nail samples in EPR dosimetry. As nail samples are physically restored with treatments, are not stressed, and display a response closer to that of *in vivo* specimens. Therefore, using dose assessment techniques on these treated samples, such as the additive dose method, would result in a more realistic assessment of the radiation dose. The MIS2 signal, believed to also be originated at cutting, is algebraically corrected using the two microwave powers, 1 and 16 mW, as described in chapter 3. However, as the sample dries out this signal increases to a saturation value. Once we have reduced or eliminated the combined effect of these signals the remaining EPR signal from an irradiated sample is the RIS. The RIS originates from the radiation radicals induced during the ionization in the sample, as described in chapter 1. This signal is proportional to the radiation dose and shows a linear dose response in stressed samples and non-linear dose response in unstressed samples. These are recommended for EPR dosimetry using a saturating exponential model (grun model) for predicting residual

or accidental radiological dose.

The interpersonal and intrapersonal variability of fingernail samples are very low compared to the magnitude of the signals but generally and slightly higher for older samples. It is proposed that treated samples be used in EPR dosimetry because they show more stable signals (without the uncertainties induced from the MIS1 and MIS2) than untreated ones and have lower variability (mainly due to its water content). Practical conditions of sample collection, preparation, and measurements at an accident site can be met with techniques illustrated in this study.

This research identified water content as the factor responsible for sensitivity of fingernails in EPR dosimetry measurements and the stress level of the fingernail samples (mechanical stress was not quantified) as responsible for the shape of the radiation sensitivity. It showed the possibility for developing universal dose response curves in samples in which strict controls for weight, number of clippings, and time-since-cut are taken. It was also identified that more work needs to be done in order to recommend fingernail EPR dosimetry as an independent assessor of the radiation dose in an emergency scenario. The use of treated fingernail samples is a more realistic representation of an *in vivo* exposure and therefore is recommended. One can further say that fingernail EPR dosimetry is a sensitive enough technique for the dose range of interest in emergency responses that can currently be used as a complementary methodology to other established physical dosimetric techniques, such as teeth and bone EPR dosimetry, and other dose assessment modalities.

The success of using fingernails EPR dosimetry brings afloat a technology that offers expedience in sample processing and precision in measurements. By having finger

or toe-nails as biological samples (easy to collect radiation biomarkers), this technique offers the opportunity to perform dose assessment during the triage phase of a radiological incident on site. The possible adaptation of the methods illustrated in this study to field deployable EPR units accentuates the potential of fingernail EPR dosimetry for its use in radiological emergency responses and the management of radiological casualties.

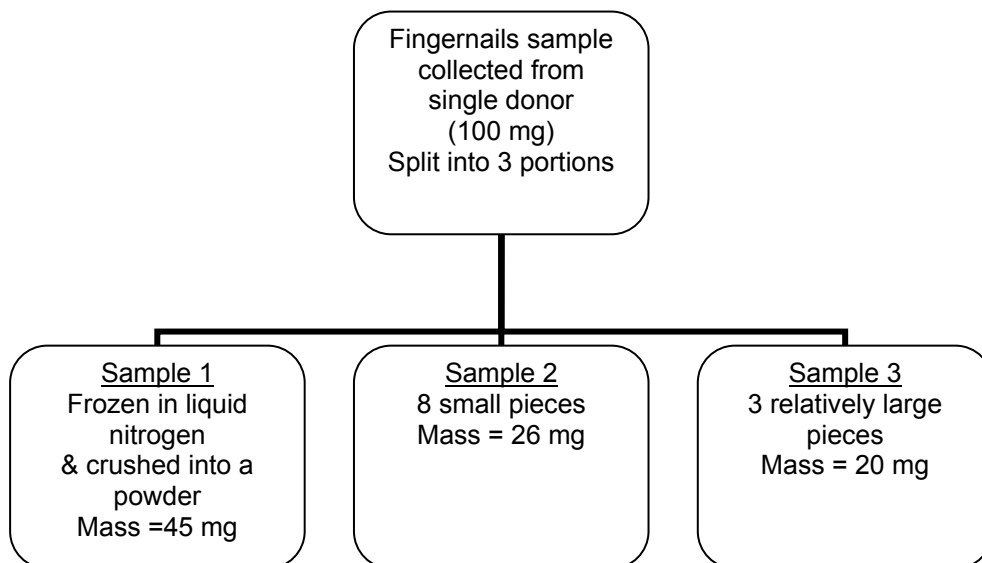
APPENDIX A

Effect of “sample number of cuts” on radiation dose dependence in fingernails dosimetry

A-1. EXPERIMENT GOAL: To investigate how sample collection (number of cuts and size of fingernail clippings) and sample preparation can affect EPR signals and radiation dose measurements.

A-2. EXPERIMENTAL DESIGN:

- (1) Sample is cut and the MIS and BKS are measured.
- (2) The same sample is cut into two parts and the MIS and BKS are measured again.
- (3) Samples are prepared as shown in diagram below:



- (4)** EPR spectra is collected for every sample using standard protocol.
 - a)** Sample 1 (measured shortly after grounding)
 - b)** Samples 2 and 3 (measured shortly after cut)
- (5)** Samples are treated and dried using standard procedure.
 - a)** Sample 1 (powder dried in vacuum for 30 min at room temperature)
 - b)** Samples 2 & 3 (air dry)
- (6)** Samples are re-measured using standard protocol.
- (7)** Samples are irradiated to a dose of 5 Gy.
 - a)** Simultaneous irradiation of all samples
 - b)** Step irradiation (4 steps): 1 Gy, 1 Gy, 1 Gy and 2 Gy
- (8)** EPR spectra is collected for every sample (after each irradiation step) using standard protocol.

A-3. RESULTS

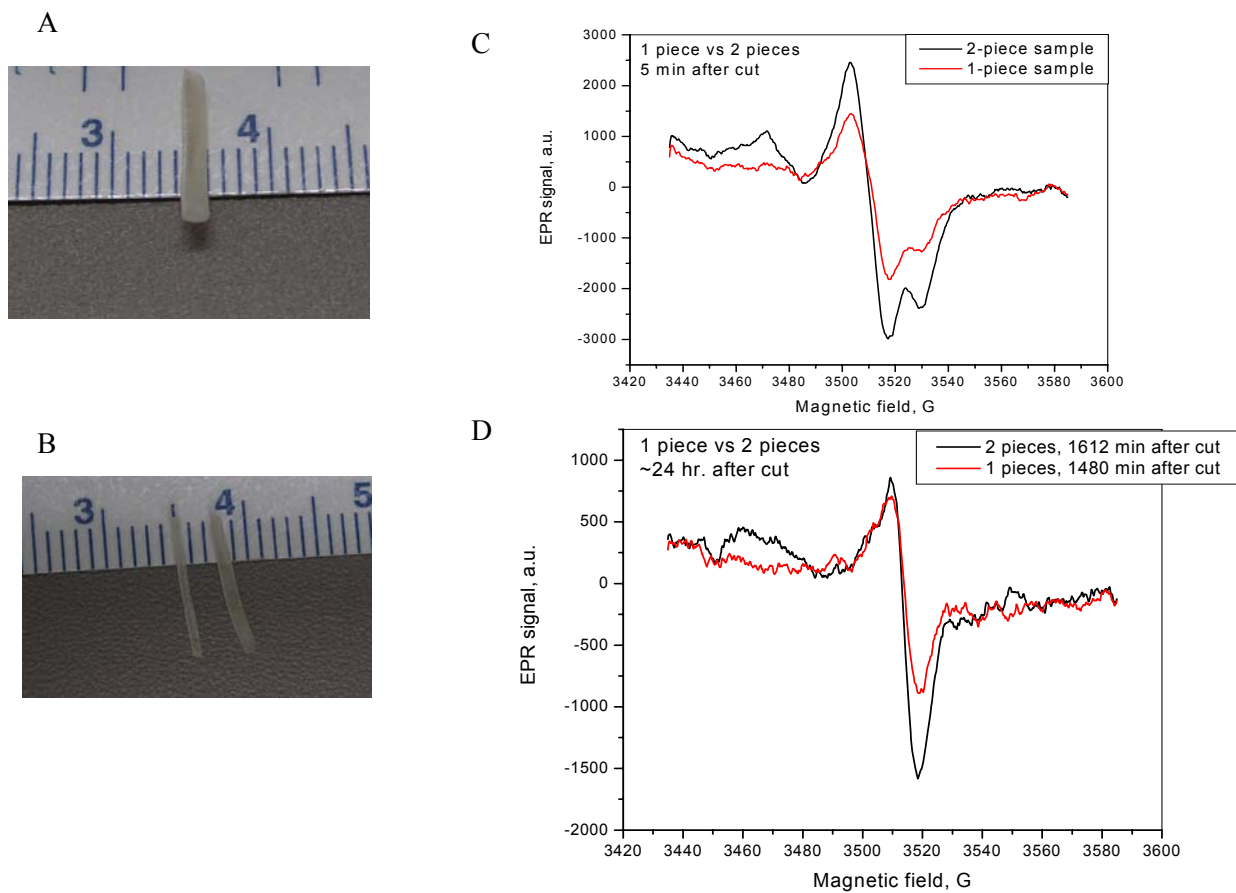


Figure A-1. MIS and BKS size dependence. (A) One piece sample, (B) the same piece cut into 2 parts, 2 days later, (C) MIS intensity in the same sample with 1 and 2 cuts, 5 minutes after cut, and (D) BKS intensity in the same sample with 1 and 2 cuts, 24 hours after cut.

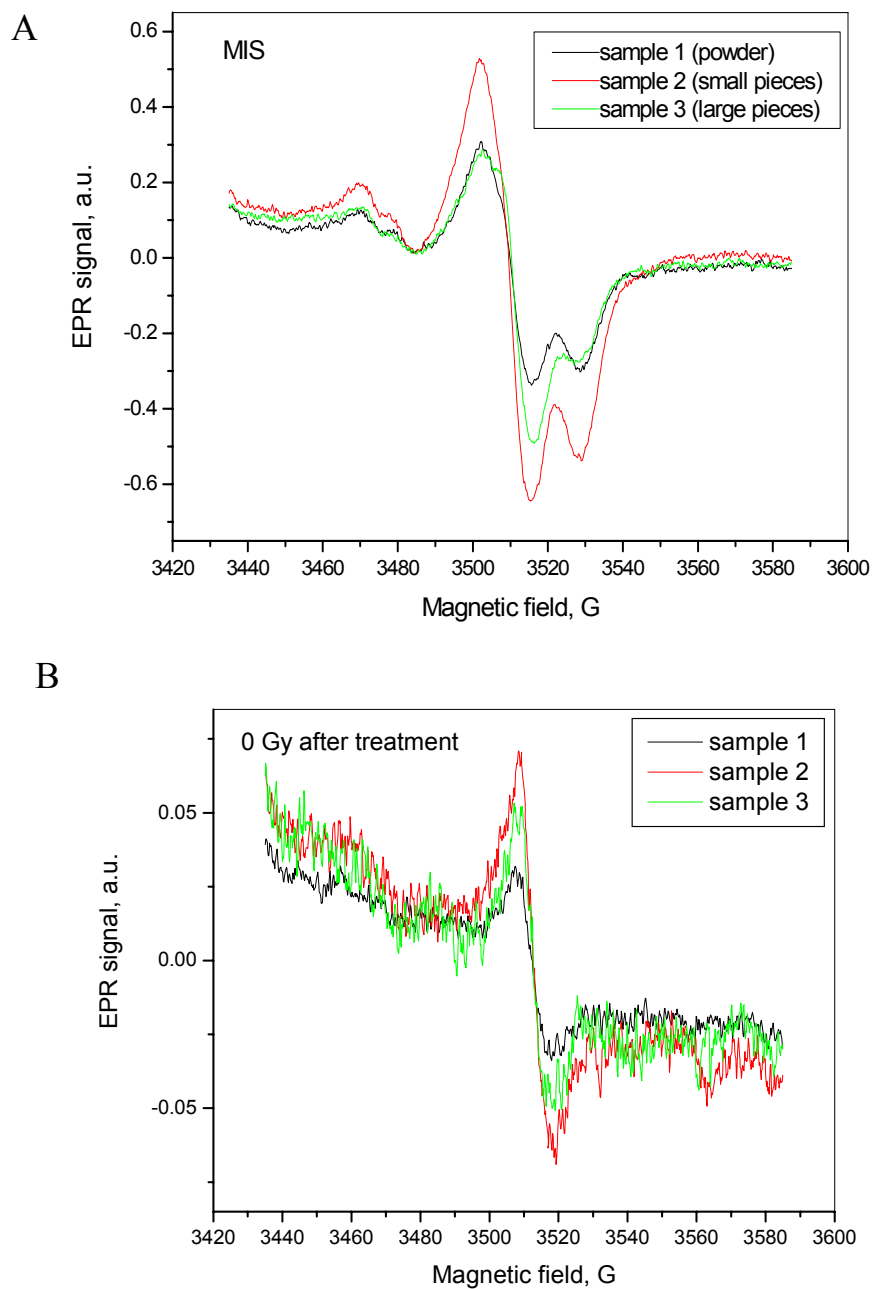


Figure A-2. EPR spectra after cut (A) and treatment (B).

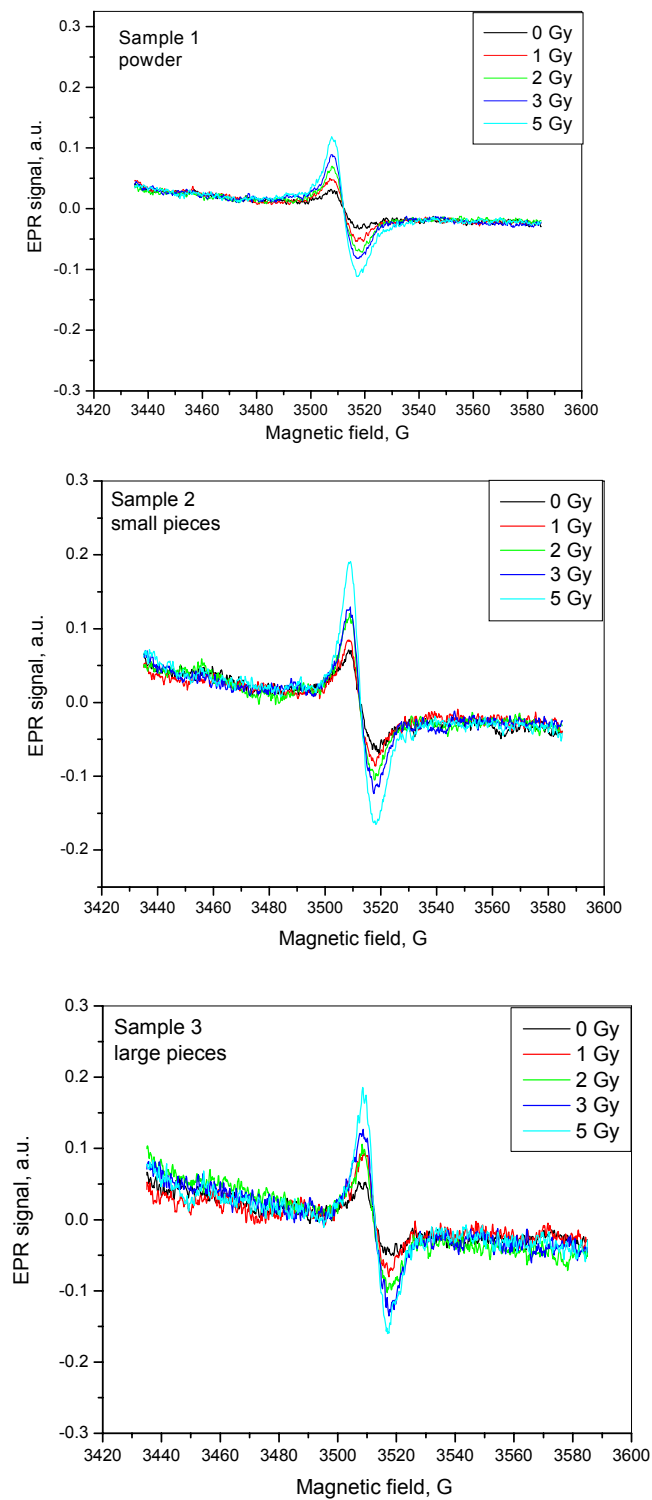


Figure A-3. Spectra progression with radiation (normalization to 20 mg).

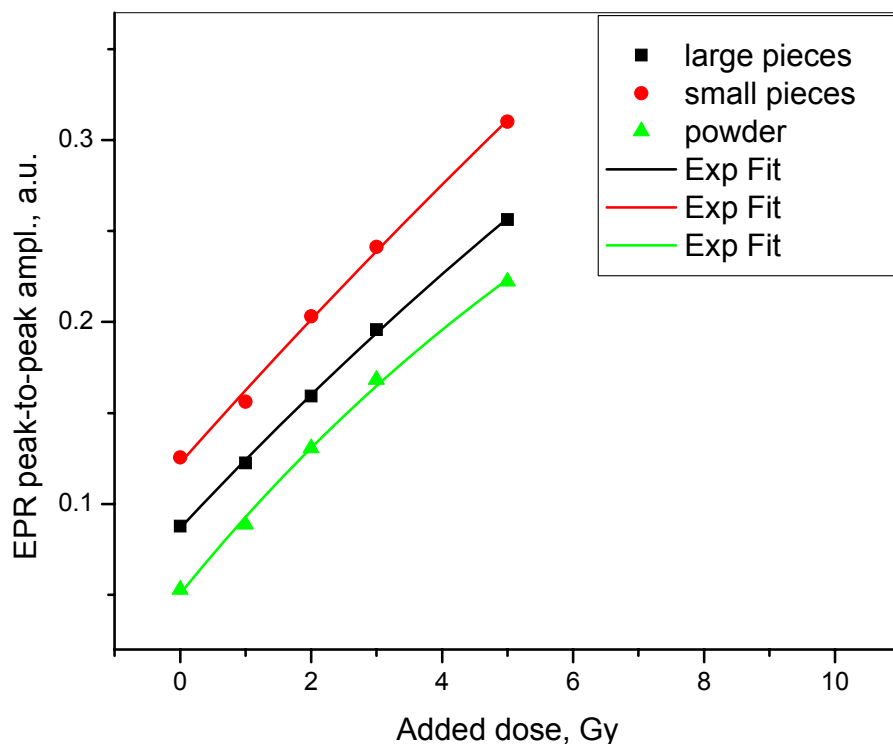


Figure A-4. Dose dependences for samples from fresh fingernails, collected from the same person, at the same time, but prepared differently. The triangle symbols represent the dose dependence values for the powder sample, the square symbols represent the dose dependence values for the sample with large pieces, and the round symbols represent the dose dependence values for the sample with small pieces. The solid lines are the results of the exponential fit of the data using the Grun formula.

A-4. EXPERIMENT CONCLUSIONS

(1) Number of cuts in the fingernail samples:

- a)** does not significantly affect radiation sensitivity (parallel dose dependences for all samples); and
- b)** affects residual dose in the sample [in line with preliminary experimental results of BKS (MIS2) dependence on number of cuts].

(2) Small pieces sample showed highest residual dose (MIS2), which means that this is the worst type of the fingernail sample for dose measurements.

(3) Powder seemed to be the best type of fingernail sample for dose measurements.

APPENDIX B

Development of saturation curve lines for finger nails in support of proposed treatment of nails for EPR measurements and the sponge behavior theory

B-1. INTRODUCTION

By knowing the rate of water absorption and reduction by evaporation in fingernails, we can evaluate the time factor of water baths of nail clippings for an effective and practical treatment time and drying time. Water was originally used to simulate hand washing and mainly because of its effect on the EPR signals.

The original goal of this experiment was to be able to develop quick water absorption curves for finger nail samples and reach saturation within 2-3 hours. The second original goal was to develop drying curves for the same samples. There was a higher rate of evaporation than absorption of water in the nail samples. Therefore, saturation was not achieved within the predicted time frame (5 min water soaking - 5 min drying intervals) and the experiment was modified to saturate samples with a longer water treatment (10 min water soaking – 5 min drying intervals). These were then let to dry, and time and weight measurements were recorded.

B-2. MATERIALS AND METHODS

Fingernails previously and recently collected as biosamples for use in EPR project and water at room temperature was used to determine the rate of water saturation of nail samples. Preliminary measurements using distilled or de-ionized water did not show a difference in EPR measurements that used tap water. Moreover, in the event of an emergency, having access to clean tap water would ease the sample treatment process. The samples used were at least 20 mg and with 3 to 5 clippings. The scaled used was a Mettler Toledo, Model AG 285.

B-3. DESCRIPTION OF SAMPLES (SEE TABLE B-1)

- (1) The first eight samples can be broken into 4 pairs of samples (1-2, 3-4, 5-6, 7-8) from the same donors, collected at different times.
- (2) Samples 5, 6, 9 and 10 were collected from the same volunteer at the same cut time.
- (3) Samples 2 and 8 were recently cut, prior to start of experiment.

Table B-1. Samples information.

Sample	Cut time	Clips (#)	Gender	Age group
1	10/30/06 23:00	4	M	43-47
2	3/22/07 10:12	5	M	43-47
3	1/26/07 17:00	4	F	23-27
4	3/6/07 17:00	4	F	23-27
5	1/27/07 19:00	3	M	43-47
6	3/16/07 23:00	3	M	43-47
7	3/3/07 22:00	3	M	33-37
8	3/22/07 10:45	3	M	33-37
9	3/16/07 23:00	3	M	43-47
10	3/16/07 23:00	3	M	43-47

B-4. DESCRIPTION OF EXPERIMENT

(1) Samples 1-8

- a) Samples were first weighted and start time was recorded.
- b) We then did 11 treatments of these samples with water baths for 5 minutes and letting the nail clippings dry for another 5 minutes.
- c) Time and weight of the samples were recorded after each step.

Since water saturation was not clearly apparent in the samples, due to the fact that there was an apparent higher rate of evaporation than absorption of water in the nail samples, we decided to increase the water treatment times.

- d) Four more water treatments were done using 10 minute water baths and 5 minute drying times.
- e) Time and weight of the samples were recorded after each step.

Since the rate of saturation seemed to be closer for some samples and not for all and the end of the working day was approaching, samples were either left in their water baths

or left to dry over night in order to: (1) see if saturation can be reached, and (2) see if data could be collected for the rate of water evaporation.

- f) Samples 1, 4, 5, and 8 were then left in the water baths and measurements of times and weights were recorded three to four times more.
- g) Samples 2, 3, 6, and 7 were then left to dry and measurements of times and weights were recorded three to four times more.

(2) Samples 9 – 10

These samples were collected with the intent of having similar samples to those previously treated and to see if we could reach water saturation faster, using a longer water treatment without drying.

- a) Samples 9 and 10 were placed in water baths for 2 consecutive $\frac{1}{2}$ hour intervals.
- b) After weighting, sample 9 was left in water bath and sample 10 was left to dry.
- c) Three to four more recordings were taken for both samples.

B-5. RESULTS

Data set tables B-2-a, B-2-b, and B-2-c at the end of this appendix show the measurement results raw data, including the treatment type, time of treatment, elapsed time between treatment and weight measurements, and corresponding weights in mg. A code of W and D represent water and drying respectively. W-5 and W-10 represent water treatments for 5 and 10 minutes respectively, and D-5 is drying time of 5 minutes. The

tabulated values are represented graphically in Figures B-1 and B2 below.

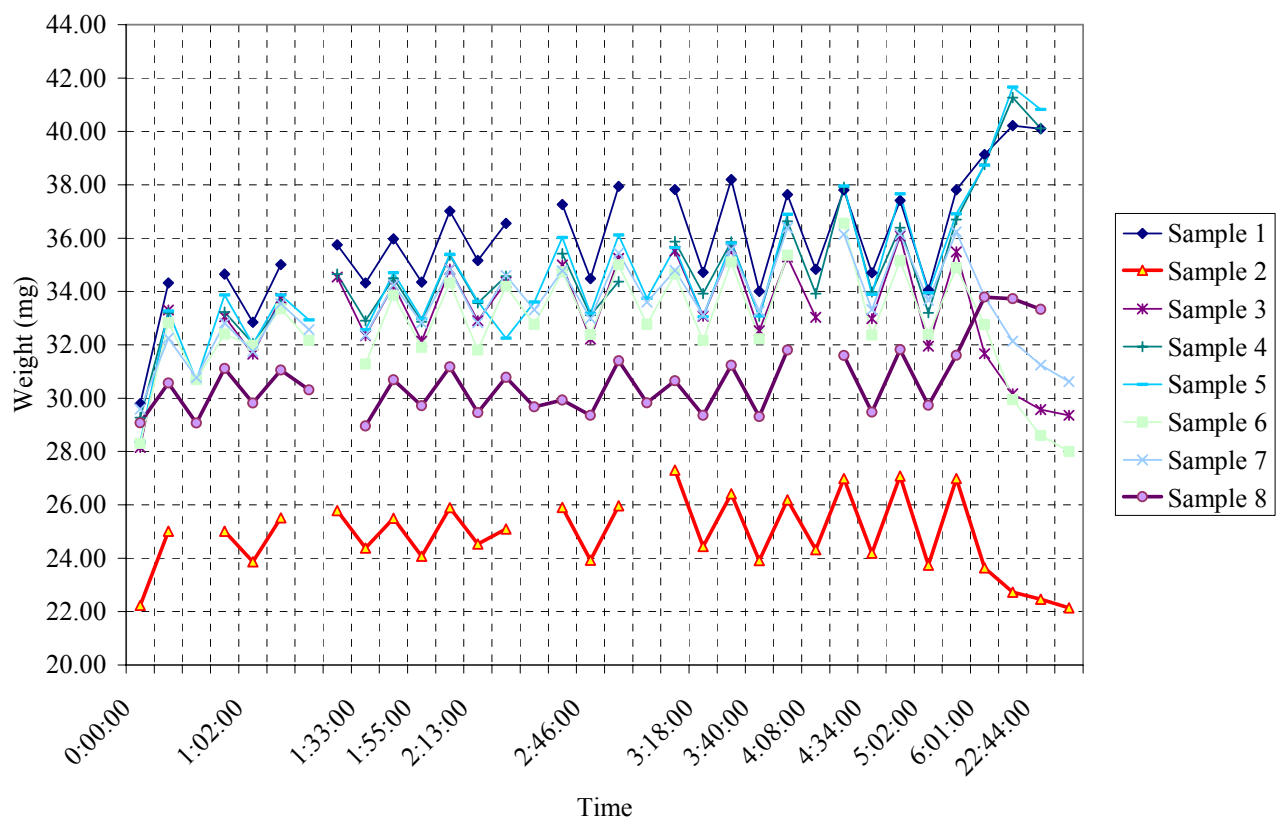


Figure B-1. Plot of water absorption curves for fingernail samples 1-8.

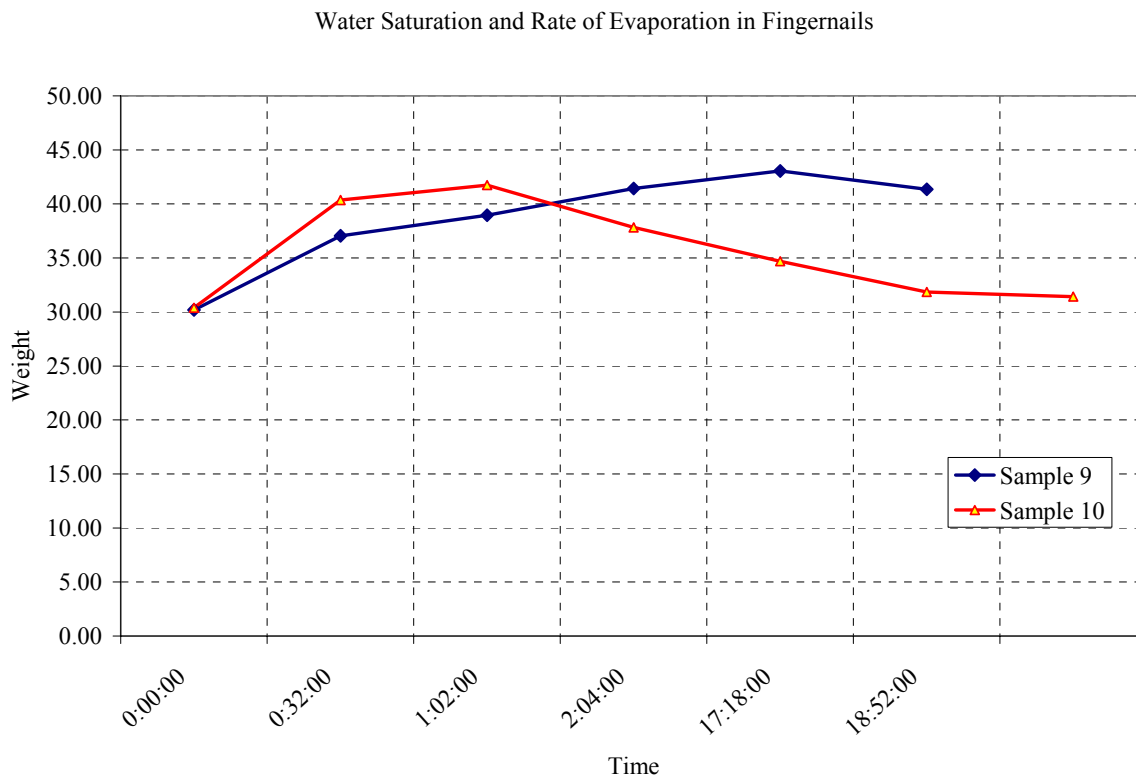


Figure B-2. Plot of water absorption curves for fingernail samples 9-10.

B-6. ANALYSIS OF DATA AND CONCLUSION

- (1) In order to calculate the rate of saturation, only data points taken right after water treatment were considered. In contrast, the rate of evaporation could only be calculated by looking at the data taken after the last water treatment, and using those samples left to dry and considering that drying is still an ongoing physical process by the end of this experiment.
- (2) The true rate of saturation in nail samples would require a more precise technique for measuring and recording the time and weight of samples.

- (3) The elapsed time since cutting, as a factor of the state of dryness of the nails, seems to affect the rate nails absorb water and dry. However, this relation cannot be proven quite clearly because samples were kept inside plastic ziplog bags, in which evaporation rate may be less than nails in ambient air.
- (4) Samples 2 and 8 were freshly cut fingernail clippings and they seem to absorb water at a slower rate than the rest. Perhaps this is because they would have an “initial” higher water content than the rest.
- (5) It is apparent that the rate of evaporation is higher than the rate of water absorption and therefore it is difficult to measure the true rate of absorption as the samples are drying between treatments. If we look at samples 9 and 10 we can tell that both samples have similar rates of saturations. Sample 10 was left in the water slightly longer than sample 9. The drying rate of sample 10 was faster than the saturation rate of sample 9.
- (6) The specific structure of the nails, double-layered thickness, surface area (geometrical factor due to the shape of nail clipping), and general thickness may be confounders of the data.

B-7. DATA SET TABLES

Table B-2-a. Data set for samples 1-4.

Treatment Sample 1				Weight				Weight				Weight-mg				Weight-mg			
	Time	Elapsed time		Sample 1	Treatment Time	Elapsed Time		Sample 2	Treatment Time	Elapsed Time		Sample 3	Treatment Time	Elapsed Time		Sample 4	Treatment Time	Elapsed Time	
1 W-5min	3/22/07 11:24	0:00:00	29.79		3/22/07 11:27	0:00:00	22.23		3/22/07 11:30	0:00:00	28.16		3/22/07 11:32	0:00:00	29.27		3/22/07 11:32	0:00:00	29.27
D-5min	3/22/07 12:02	0:38:00	34.32	1 W-5min	3/22/07 12:03	0:36:00	25.01	1 W-5min	3/22/07 12:05	0:35:00	33.30	1 W-5min	3/22/07 12:06	0:34:00	33.20		3/22/07 12:06	0:34:00	33.20
2 W-5min	3/22/07 12:20	0:56:00	34.65	2 W-5min	3/22/07 12:21	0:54:00	25.01	2 W-5min	3/22/07 12:21	0:51:00	33.06	2 W-5min	3/22/07 12:22	0:50:00	33.23		3/22/07 12:22	0:50:00	33.23
D-5min	3/22/07 12:26	1:02:00	32.84	D-5min	3/22/07 12:26	0:59:00	23.87	D-5min	3/22/07 12:27	0:57:00	31.65	D-5min	3/22/07 12:27	0:55:00	32.05		3/22/07 12:27	0:55:00	32.05
3 W-5min	3/22/07 12:36	1:12:00	35.01	3 W-5min	3/22/07 12:36	1:09:00	25.51	3 W-5min	3/22/07 12:37	1:07:00	33.75	3 W-5min	3/22/07 12:38	1:06:00	33.52		3/22/07 12:38	1:06:00	33.52
D-5min				D-5min				D-5min				D-5min					3/22/07 12:38		
4 W-5min	3/22/07 12:51	1:27:00	35.75	4 W-5min	3/22/07 12:52	1:25:00	25.79	4 W-5min	3/22/07 12:53	1:23:00	34.54	4 W-5min	3/22/07 12:53	1:21:00	34.65		3/22/07 12:53	1:21:00	34.65
D-5min	3/22/07 12:57	1:33:00	34.32	D-5min	3/22/07 12:58	1:31:00	24.38	D-5min	3/22/07 12:58	1:28:00	32.34	D-5min	3/22/07 12:59	1:27:00	32.90		3/22/07 12:59	1:27:00	32.90
5 W-5min	3/22/07 13:13	1:49:00	35.97	5 W-5min	3/22/07 13:13	1:46:00	25.50	5 W-5min	3/22/07 13:14	1:44:00	34.23	5 W-5min	3/22/07 13:14	1:42:00	34.50		3/22/07 13:14	1:42:00	34.50
D-5min	3/22/07 13:19	1:55:00	34.35	D-5min	3/22/07 13:20	1:53:00	24.07	D-5min	3/22/07 13:20	1:50:00	32.14	D-5min	3/22/07 13:21	1:49:00	32.86		3/22/07 13:21	1:49:00	32.86
6 W-5min	3/22/07 13:30	2:06:00	37.01	6 W-5min	3/22/07 13:31	2:04:00	25.90	6 W-5min	3/22/07 13:31	2:01:00	34.84	6 W-5min	3/22/07 13:32	2:00:00	35.36		3/22/07 13:32	2:00:00	35.36
D-5min	3/22/07 13:37	2:13:00	35.16	D-5min	3/22/07 13:37	2:10:00	24.53	D-5min	3/22/07 13:38	2:08:00	32.90	D-5min	3/22/07 13:38	2:06:00	33.57		3/22/07 13:38	2:06:00	33.57
7 W-5min	3/22/07 13:47	2:23:00	36.55	7 W-5min	3/22/07 13:47	2:20:00	25.10	7 W-5min	3/22/07 13:48	2:18:00	34.35	7 W-5min	3/22/07 13:49	2:17:00	34.57		3/22/07 13:49	2:17:00	34.57
D-5min				D-5min				D-5min				D-5min					3/22/07 13:49		
8 W-5min	3/22/07 14:02	2:38:00	37.26	8 W-5min	3/22/07 14:03	2:36:00	25.91	8 W-5min	3/22/07 14:03	2:33:00	34.99	8 W-5min	3/22/07 14:04	2:32:00	35.42		3/22/07 14:04	2:32:00	35.42
D-5min	3/22/07 14:10	2:46:00	34.48	D-5min	3/22/07 14:10	2:43:00	23.93	D-5min	3/22/07 14:13	2:43:00	32.21	D-5min	3/22/07 14:13	2:41:00	33.11		3/22/07 14:13	2:41:00	33.11
9 W-5min	3/22/07 14:20	2:56:00	37.94	9 W-5min	3/22/07 14:22	2:55:00	25.97	9 W-5min	3/22/07 14:22	2:52:00	35.24	9 W-5min	3/22/07 14:23	2:51:00	34.37		3/22/07 14:23	2:51:00	34.37
D-5min				D-5min				D-5min				D-5min					3/22/07 14:23		
10 W-5min	3/22/07 14:34	3:10:00	37.82	10 W-5min	3/22/07 14:35	3:08:00	27.30	10 W-5min	3/22/07 14:36	3:06:00	35.51	10 W-5min	3/22/07 14:37	3:05:00	35.87		3/22/07 14:37	3:05:00	35.87
D-5min	3/22/07 14:42	3:18:00	34.72	D-5min	3/22/07 14:43	3:16:00	24.44	D-5min	3/22/07 14:43	3:13:00	33.07	D-5min	3/22/07 14:44	3:12:00	33.92		3/22/07 14:44	3:12:00	33.92
11 W-5min	3/22/07 14:52	3:28:00	38.20	11 W-5min	3/22/07 14:54	3:27:00	26.42	11 W-5min	3/22/07 14:54	3:24:00	35.60	11 W-5min	3/22/07 14:55	3:23:00	35.86		3/22/07 14:55	3:23:00	35.86
D-5min	3/22/07 15:04	3:40:00	34.00	D-5min	3/22/07 15:04	3:37:00	23.91	D-5min	3/22/07 15:05	3:35:00	32.53	D-5min	3/22/07 15:05	3:33:00	33.07		3/22/07 15:05	3:33:00	33.07
12 W-10 min	3/22/07 15:24	4:00:00	37.63	12 W-10 min	3/22/07 15:25	3:58:00	26.19	12 W-10 min	3/22/07 15:25	3:55:00	35.29	12 W-10 min	3/22/07 15:26	3:54:00	36.63		3/22/07 15:26	3:54:00	36.63
D-5 min	3/22/07 15:32	4:08:00	34.83	D-5 min	3/22/07 15:32	4:05:00	24.32	D-5 min	3/22/07 15:33	4:03:00	33.03	D-5 min	3/22/07 15:34	4:02:00	33.92		3/22/07 15:34	4:02:00	33.92
13 W-10 min	3/22/07 15:49	4:25:00	37.80	13 W-10 min	3/22/07 15:50	4:23:00	26.99	13 W-10 min				13 W-10 min	3/22/07 15:51	4:19:00	37.91		3/22/07 15:51	4:19:00	37.91
D-5 min	3/22/07 15:58	4:34:00	34.70	D-5 min	3/22/07 15:59	4:32:00	24.19	D-5 min	3/22/07 16:00	4:30:00	32.98	D-5 min	3/22/07 16:00	4:28:00	33.99		3/22/07 16:00	4:28:00	33.99
14 W-10 min	3/22/07 16:13	4:49:00	37.41	14 W-10 min	3/22/07 16:14	4:47:00	27.08	14 W-10 min	3/22/07 16:15	4:45:00	36.08	14 W-10 min	3/22/07 16:17	4:45:00	36.39		3/22/07 16:17	4:45:00	36.39
D-5 min	3/22/07 16:26	5:02:00	34.05	D-5 min	3/22/07 16:26	4:59:00	23.74	D-5 min	3/22/07 16:27	4:57:00	31.95	D-5 min	3/22/07 16:27	4:55:00	33.20		3/22/07 16:27	4:55:00	33.20
15 W-10 min	3/22/07 16:40	5:16:00	37.81	15 W-10 min	3/22/07 16:42	5:15:00	26.99	15 W-10 min	3/22/07 16:45	5:15:00	35.49	15 W-10 min	3/22/07 16:45	5:13:00	36.70		3/22/07 16:45	5:13:00	36.70
W	3/22/07 17:25	6:01:00	39.13	D	3/22/07 16:56	5:29:00	23.64	D	3/22/07 16:57	5:27:00	31.67	W	3/22/07 17:28	5:56:00	38.76		3/22/07 17:28	5:56:00	38.76
W	3/23/07 8:39	21:15:00	40.22	D	3/22/07 17:26	5:59:00	22.73	D	3/22/07 17:27	5:57:00	30.17	W	3/23/07 8:42	21:10:00	41.26		3/23/07 8:42	21:10:00	41.26
W	3/23/07 10:08	22:44:00	40.10	D	3/23/07 8:40	21:13:00	22.46	D	3/23/07 8:41	21:11:00	29.57	W	3/23/07 10:13	22:41:00	40.11		3/23/07 10:13	22:41:00	40.11
				D	3/23/07 10:09	22:42:00	22.14	D	3/23/07 10:11	22:41:00	29.36								

Table B-2-b. Data set for samples 5-8.

Weight-mg				Weight-mg				Weight-mg				Weight-mg			
Treatment	Time	Elapsed Time	Sample 5	Treatment	Time	Elapsed Time	Sample 6	Treatment	Time	Elapsed Time	Sample 7	Treatment	Time	Elapsed Time	Sample 8
	3/22/07 11:35	0:00:00	28.35		3/22/07 11:38	0:00:00	28.30		3/22/07 11:40	0:00:00	29.59		3/22/07 11:47	0:00:00	29.08
1 W-5min	3/22/07 12:08	0:33:00	33.27	1 W-5min	3/22/07 12:08	0:30:00	32.83	1 W-5min	3/22/07 12:09	0:29:00	32.25	1 W-5min	3/22/07 12:10	0:23:00	30.57
D-5min	3/22/07 12:14	0:39:00	30.66	D-5min	3/22/07 12:15	0:37:00	30.70	D-5min	3/22/07 12:16	0:36:00	30.77	D-5min	3/22/07 12:16	0:29:00	29.07
2 W-5min	3/22/07 12:24	0:49:00	33.87	2 W-5min	3/22/07 12:24	0:46:00	32.40	2 W-5min	3/22/07 12:25	0:45:00	32.82	2 W-5min	3/22/07 12:25	0:38:00	31.11
D-5min	3/22/07 12:29	0:54:00	32.02	D-5min	3/22/07 12:29	0:51:00	31.98	D-5min	3/22/07 12:30	0:50:00	31.75	D-5min	3/22/07 12:31	0:44:00	29.82
3 W-5min	3/22/07 12:42	1:07:00	33.87	3 W-5min	3/22/07 12:42	1:04:00	33.35	3 W-5min	3/22/07 12:43	1:03:00	33.54	3 W-5min	3/22/07 12:43	0:56:00	31.05
D-5min	3/22/07 12:47	1:12:00	32.93	D-5min	3/22/07 12:47	1:09:00	32.16	D-5min	3/22/07 12:48	1:08:00	32.57	D-5min	3/22/07 12:49	1:02:00	30.31
4 W-5min				4 W-5min				4 W-5min				4 W-5min			
D-5min	3/22/07 13:01	1:26:00	32.56	D-5min	3/22/07 13:02	1:24:00	31.28	D-5min	3/22/07 13:02	1:22:00	32.37	D-5min	3/22/07 13:07	1:20:00	28.96
5 W-5min	3/22/07 13:17	1:42:00	34.70	5 W-5min	3/22/07 13:17	1:39:00	33.86	5 W-5min	3/22/07 13:17	1:37:00	34.24	5 W-5min	3/22/07 13:18	1:31:00	30.69
D-5min	3/22/07 13:22	1:47:00	32.97	D-5min	3/22/07 13:23	1:45:00	31.91	D-5min	3/22/07 13:23	1:43:00	32.83	D-5min	3/22/07 13:24	1:37:00	29.72
6 W-5min	3/22/07 13:34	1:59:00	35.39	6 W-5min	3/22/07 13:35	1:57:00	34.32	6 W-5min	3/22/07 13:36	1:56:00	34.84	6 W-5min	3/22/07 13:36	1:49:00	31.17
D-5min	3/22/07 13:40	2:05:00	33.63	D-5min	3/22/07 13:42	2:04:00	31.80	D-5min	3/22/07 13:43	2:03:00	32.83	D-5min	3/22/07 13:43	1:56:00	29.46
7 W-5min	3/22/07 13:52	2:17:00	32.25	7 W-5min	3/22/07 13:52	2:14:00	34.19	7 W-5min	3/22/07 13:53	2:13:00	34.60	7 W-5min	3/22/07 13:53	2:06:00	30.78
D-5min	3/22/07 13:57	2:22:00	33.60	D-5min	3/22/07 13:57	2:19:00	32.77	D-5min	3/22/07 13:58	2:18:00	33.31	D-5min	3/22/07 13:59	2:12:00	29.67
8 W-5min	3/22/07 14:06	2:31:00	36.02	8 W-5min	3/22/07 14:07	2:29:00	34.74	8 W-5min	3/22/07 14:08	2:28:00	34.78	8 W-5min	3/22/07 14:12	2:25:00	29.93
D-5min	3/22/07 14:15	2:40:00	33.18	D-5min	3/22/07 14:15	2:37:00	32.38	D-5min	3/22/07 14:16	2:36:00	32.99	D-5min	3/22/07 14:17	2:30:00	29.36
9 W-5min	3/22/07 14:29	2:54:00	36.12	9 W-5min	3/22/07 14:30	2:52:00	35.00	9 W-5min	3/22/07 14:30	2:50:00	35.44	9 W-5min	3/22/07 14:31	2:44:00	31.40
D-5min	3/22/07 14:37	3:02:00	33.74	D-5min	3/22/07 14:38	3:00:00	32.77	D-5min	3/22/07 14:39	2:59:00	33.60	D-5min	3/22/07 14:39	2:52:00	29.83
10 W-5min	3/22/07 14:48	3:13:00	35.64	10 W-5min	3/22/07 14:48	3:10:00	34.65	10 W-5min	3/22/07 14:50	3:10:00	34.79	10 W-5min	3/22/07 14:50	3:03:00	30.65
D-5min	3/22/07 14:55	3:20:00	33.05	D-5min	3/22/07 14:56	3:18:00	32.12	D-5min	3/22/07 14:57	3:17:00	33.12	D-5min	3/22/07 14:57	3:10:00	29.40
11 W-5min	3/22/07 15:09	3:34:00	35.82	11 W-5min	3/22/07 15:10	3:32:00	35.10	11 W-5min	3/22/07 15:11	3:31:00	35.58	11 W-5min	3/22/07 15:11	3:24:00	31.23
D-5min	3/22/07 15:18	3:43:00	33.08	D-5min	3/22/07 15:19	3:41:00	32.22	D-5min	3/22/07 15:19	3:39:00	33.26	D-5min	3/22/07 15:20	3:33:00	29.81
12 W-10 min	3/22/07 15:36	4:01:00	36.89	12 W-10 min	3/22/07 15:37	3:59:00	35.36	12 W-10 min	3/22/07 15:38	3:58:00	36.38	12 W-10 min	3/22/07 15:39	3:52:00	31.30
D-5 min				D-5 min				D-5 min				D-5 min			
13 W-10 min	3/22/07 15:54	4:19:00	37.95	13 W-10 min	3/22/07 15:55	4:17:00	36.55	13 W-10 min	3/22/07 15:57	4:17:00	36.14	13 W-10 min	3/22/07 15:57	4:10:00	31.60
D-5 min	3/22/07 16:06	4:31:00	33.89	D-5 min	3/22/07 16:06	4:28:00	32.37	D-5 min	3/22/07 16:07	4:27:00	33.32	D-5 min	3/22/07 16:07	4:20:00	29.98
14 W-10 min	3/22/07 16:21	4:46:00	37.66	14 W-10 min	3/22/07 16:22	4:44:00	35.15	14 W-10 min	3/22/07 16:23	4:43:00	36.14	14 W-10 min	3/22/07 16:24	4:37:00	31.82
D-5 min	3/22/07 16:30	4:55:00	33.94	D-5 min	3/22/07 16:30	4:52:00	32.39	D-5 min	3/22/07 16:33	4:53:00	33.67	D-5 min	3/22/07 16:33	4:46:00	29.73
15 W-10 min	3/22/07 16:48	5:13:00	36.91	15 W-10 min	3/22/07 16:52	5:14:00	34.89	15 W-10 min	3/22/07 16:53	5:13:00	36.24	15 W-10 min	3/22/07 16:54	5:07:00	31.61
W	3/22/07 17:30	5:55:00	38.73	D	3/22/07 16:58	5:20:00	32.76	D	3/22/07 16:58	5:18:00	33.81	W	3/22/07 17:32	5:45:00	33.79
W	3/23/07 8:43	21:08:00	41.66	D	3/22/07 17:30	5:52:00	29.95	D	3/22/07 17:31	5:51:00	32.14	W	3/23/07 8:46	20:59:00	33.73
W	3/23/07 10:15	22:40:00	40.82	D	3/23/07 8:44	21:06:00	28.60	D	3/23/07 8:45	21:05:00	31.24	W	3/23/07 10:18	22:31:00	33.33
				D	3/23/07 10:16	22:38:00	28.00	D	3/23/07 10:17	22:37:00	30.62				

Table B-2-c. Data set for samples 9-10.

	V6-wet			# Clips 3	V6-dry				# Clips 3
	Cut Time	3/16/07 23:00		Weight (mg)		Cut Time	3/16/07 23:00		Weight (mg)
	Treatment	Time	Elapsed time	Sample 9		Treatment	Time	Elapsed time	Sample 10
		3/22/07 15:29	0:00:00	30.20			3/22/07 15:46	0:17:00	30.39
1	W-30min	3/22/07 16:01	0:32:00	37.04	1	W-30min	3/22/07 16:18	0:49:00	40.35
2	W-30min	3/22/07 16:31	1:02:00	38.96	2	W-30min	3/22/07 16:49	1:20:00	41.74
	W	3/22/07 17:33	2:04:00	41.43		D	3/22/07 17:00	1:31:00	37.82
	W	3/23/07 8:47	17:18:00	43.05		D	3/22/07 17:33	2:04:00	34.70
	W	3/23/07 10:21	18:52:00	41.36		D	3/23/07 8:47	17:18:00	31.85
						D	3/23/07 10:21	18:52:00	31.41

APPENDIX C

Evaluation of dose buildup during irradiation of samples

C-1. EXPERIMENT GOAL: To investigate if there is any buildup during irradiation of samples using the Gammacell 40 Cesium 137 irradiator.

C-2. EXPERIMENTAL DESIGN:

- 1) Several thermoluminescent detectors (TLDs), DT-702/PD, were irradiated at different doses using a Cs 137 irradiator. The DT-702 has four chips for monitoring photon, beta, and neutron personnel exposures. The TLD card for this dosimeter is formed from Teflon encapsulated LiF:Mg,Cu,P phosphors that are mounted on an aluminum substrate [1]. It was used in this experiment because it is the same TLD currently employed by the National Dosimetry Center (NDC). The NDC uses this DT-702/PD, a Harshaw 8840 holder and 8842 card, which is described elsewhere [1-3]. We did not use the holders in this experiment.
- 2) Table C-1 shows the irradiation plan for a set of six TLDs (5 sets = 30 TLDs total). The first two columns show the target dose in rad and Gray respectively. It would have required a time, such as that shown on the third column, to accomplish this exact dose. However, irradiation timing setting is set to automatically measure time in the

order of tenths of a minute. Therefore, we used the timing shown in column 4 and delivered a dose shown in column 5.

Table C-1. Dose range for experimental plan of TLDs.

Target Dose, Gray (rad)	Timer required (min)	Real time (min)	Dose, Gray (rad) (delivered)
0.0720 (7.2)	0.1001	0.1	0.0719 (7.19)
0.1440 (14.4)	0.2002	0.2	0.1439 (14.39)
0.288 (28.8)	0.4004	0.4	0.2877 (28.77)
0.576 (57.6)	0.8007	0.8	0.5755 (57.55)
1.152 (115.2)	1.6015	1.6	1.151 (115.1)

3) Figure C-1 illustrates the irradiation geometry for all samples. Technical specs for this irradiator state that irradiation is uniform in the irradiation cavity [4].

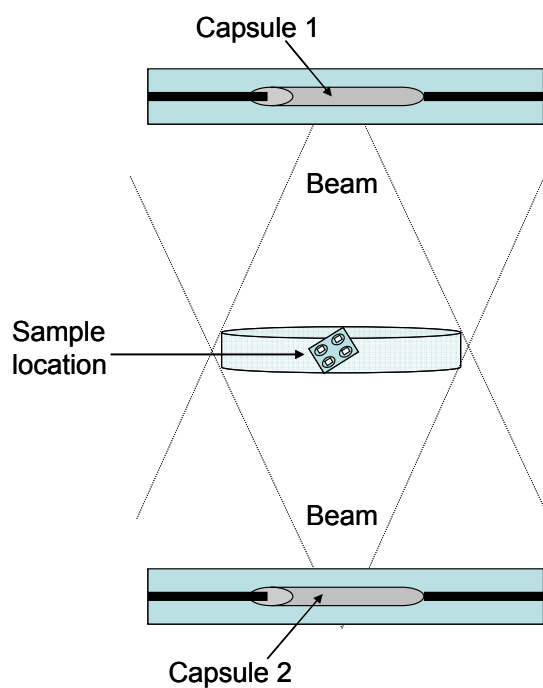


Figure C-1. Illustration of geometric location of the irradiated samples in irradiation cavity.

- 4) Table C-2 shows the list of serial numbers for the irradiated dosimeters and the planned thickness of shielding / buildup material (plexiglass). Five dosimeters were used as control. The plexiglass thicknesses were 2 , 4 , 6, and 8 mm, which were placed between the radiation sources and the TLDs. The ID numbers listed on table C-2 are used to match given doses to the dose results from the NDC.

Table C-2. Irradiation plan for dosimeters with no shielding and four thicknesses of plexiglass (2mm, 4mm, 6mm, and 8 mm).

Dose, Gray (Rad) (delivered)	Dosimeter ID number					Controls (no dose)
	No shielding	2 mm plxgls	4 mm plxgls	6 mm plxgls	8 mm plxgls	
0.0719 (7.19)	170085	172249	174085	176331	168500	179093
0.1439 (14.39)	170225	172267	174280	176640	168709	179345
0.2877 (28.77)	170645	172561	174285	169118	178941	179562
0.5755 (57.55)	170716	172805	177023	169916	173378	179594
1.151 (115.1)	175666	175835	177030	169131	177968	175970

C-3. RESULTS

- 1) Table C-3 shows the results obtained from the NDC for all TLDs, as compared with the given dose using the Cs 137 irradiator and plexiglass thickness of 2, 4, 6, and 8 mm.
- 2) Figure C-2 shows the plot of the reported NDC dose versus the delivered dose using the Cs 137 irradiator.
- 3) Figures C-3 and C-4 are the plot of the reported NDC doses of all 4 chips of each irradiated TLD dosimeter and the plot of the average NDC dose respectively.

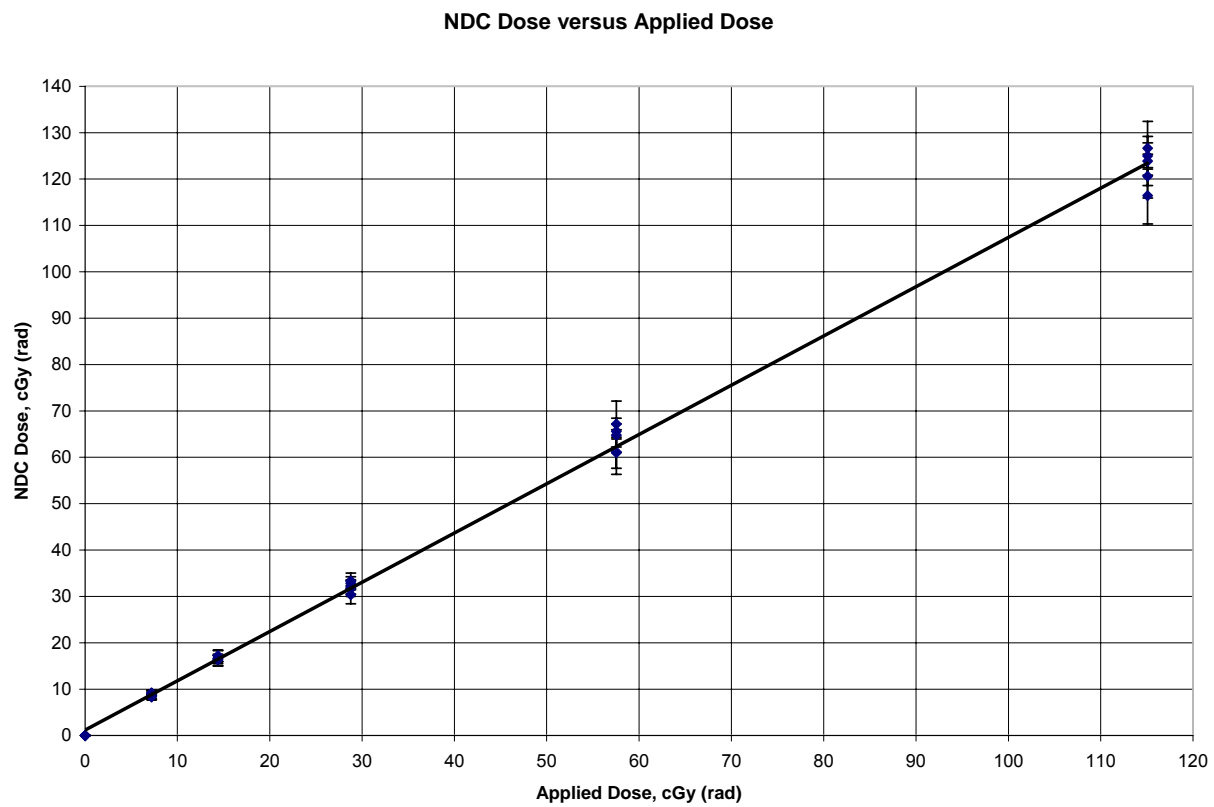


Figure C-2. Plot of NDC dose versus delivered dose.

Table C-3. Data obtained from the NDC for all TLDs at thicknesses 0, 2, 4, 6, and 8 mm.

Time on 20080114	ID number	Applied Dose (cGy)	Shield thickness (mm)	NDC Dose Results (cGy)						BU
				P1	P2	P3	P4	Mean	SD	
102055	175970	0	0	0.0081	0.0075	0.0104	0.0070	0.0083	0.0015	
102607	179345	0	0	0.0083	0.0093	0.0100	0.0077	0.0088	0.0010	
102843	179093	0	0	0.0084	0.0112	0.0110	0.0074	0.0095	0.0019	
101911	179594	0	0	0.0088	0.0109	0.0118	0.0080	0.0099	0.0018	
101725	179562	0	0	0.0098	0.0105	0.0113	0.0083	0.0100	0.0013	
102003	170085	7.19	0	8.6	8.7	7.5	8.3	8.2889	0.5558	
103142	172249	7.19	2	9.0	9.0	7.8	8.3	8.5266	0.5691	1.029
103842	174085	7.19	4	9.1	9.6	8.4	9.6	9.1720	0.5437	1.107
102516	176331	7.19	6	9.1	9.7	7.6	8.2	8.6645	0.9415	1.045
101632	168500	7.19	8	9.2	9.6	8.3	9.6	9.1746	0.6394	1.107
101818	170225	14.39	0	16.5	17.9	14.9	15.8	16.3010	1.2534	
103605	172267	14.39	2	16.7	18.8	14.7	16.4	16.6484	1.6434	1.021
102751	174280	14.39	4	16.9	17.1	15.5	16.9	16.5933	0.7116	1.018
103657	176640	14.39	6	17.1	16.6	15.1	16.8	16.3899	0.8672	1.005
101300	168709	14.39	8	17.3	18.8	15.8	17.2	17.2386	1.2251	1.058
102332	170645	28.77	0	31.6	32.2	27.8	29.8	30.3922	1.9768	
102659	172561	28.77	2	31.7	32.4	29.4	33.2	31.6700	1.6474	1.042
103329	174285	28.77	4	31.9	34.2	31.5	30.6	32.0459	1.5448	1.054
103237	169118	28.77	6	32.7	34.9	31.8	31.9	32.8293	1.4270	1.080
101356	178941	28.77	8	35.2	34.3	32.3	31.6	33.3596	1.6882	1.098
102240	170716	57.55	0	63.1	64.6	57.7	58.5	60.9936	3.3680	
103421	172805	57.55	2	64.5	67.5	64.0	66.3	65.5912	1.6315	1.075
102935	177023	57.55	4	64.6	69.8	60.9	63.8	64.7701	3.6949	0.987
103750	169916	57.55	6	64.7	63.5	54.1	62.3	61.1322	4.8159	0.944
101448	173378	57.55	8	69.3	72.3	60.7	66.4	67.1788	4.9511	1.099
102424	175666	115.10	0	120.2	121.8	108.3	115.4	116.4082	6.0645	
102147	175835	115.10	2	122.1	126.6	116.1	117.7	120.6152	4.7419	1.036
103513	177030	115.10	4	122.7	129.1	124.0	124.1	125.0006	2.8206	1.036
101016	169131	115.10	6	128.4	127.4	116.7	123.0	123.8823	5.2951	0.991
101540	177968	115.10	8	130.3	132.4	119.6	124.3	126.6425	5.8161	1.022

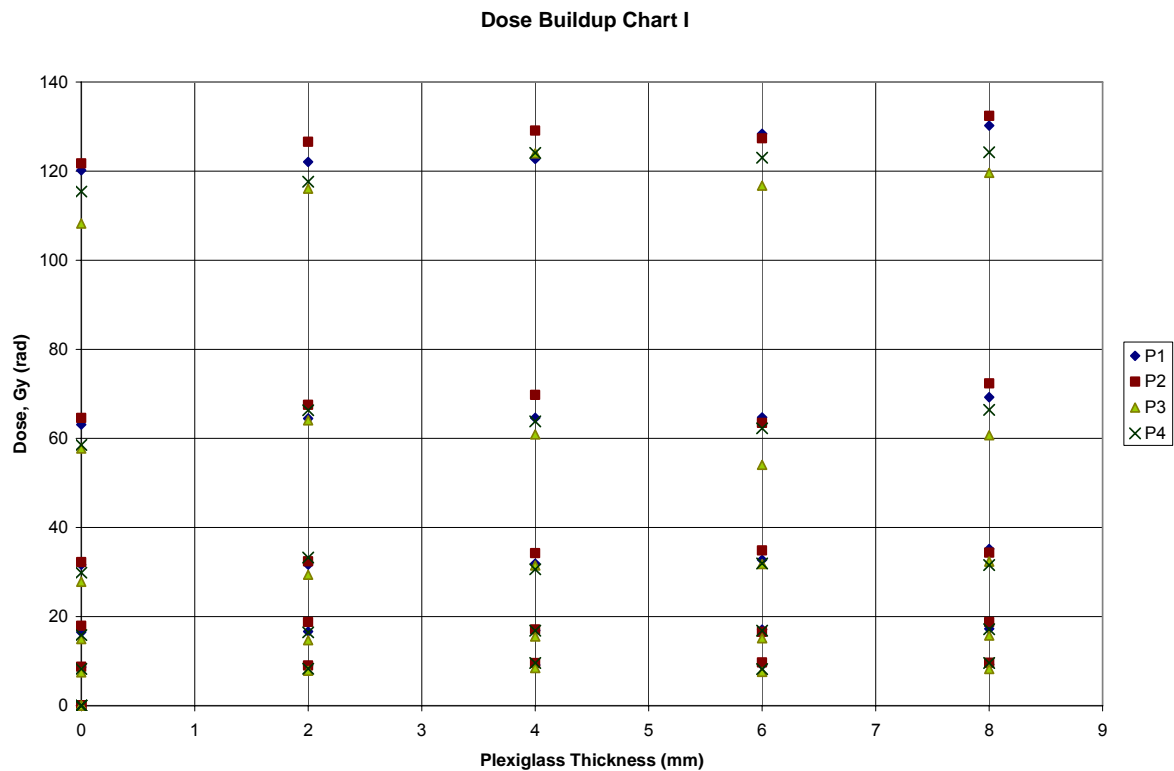


Figure C-3. Plot of NDC reported dose for all 4 chips, P1, P2, P3, and P4 versus the plexiglass thickness.

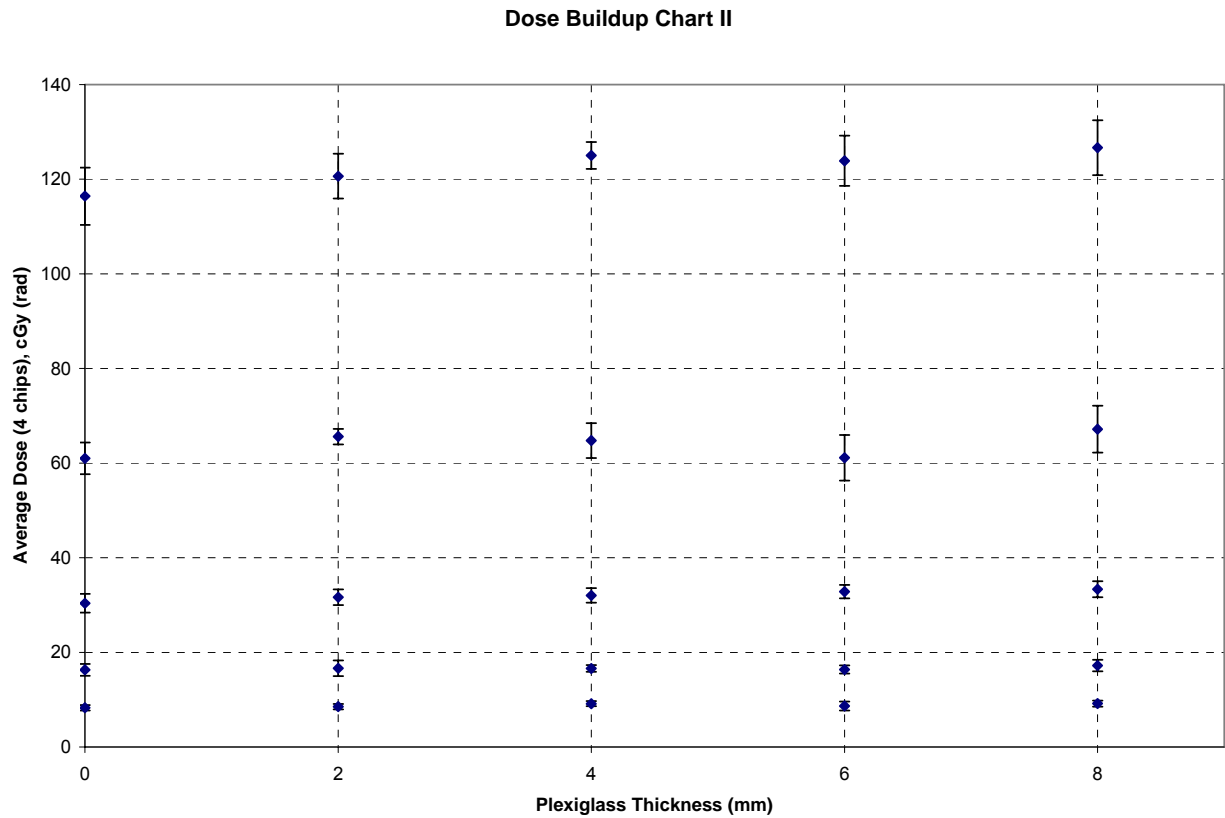


Figure C-4. Plot of NDC reported mean dose (averaged from all 4 chips, P1, P2, P3, and P4) versus the plexiglass thickness.

C-4. EXPERIMENT CONCLUSIONS

- 1) There is no apparent buildup with increasing thickness of plexiglass in the dose range used in this experiment. Therefore, we would not expect any buildup when using plexiglass containers in our experiments.
- 2) There is no need for buildup correction due to the experimental containers used during EPR experiments that require irradiation of samples using the Gammacell 40 Cesium 137 irradiator.

C-5. REFERENCES

1. Moscovitch, M., et al., *The application of LiF:Mg,Cu,P to large scale personnel dosimetry: current status and future directions*. Radiat. Prot. Dosim., 2006. **119**(1-4): p. 248-254.
2. Cassata, J.R., et al., *A New Paradigm in Personal Dosimetry Using LiF:Mg,Cu,P*. Radiat. Prot. Dosim., 2002. **101**(1-4): p. 27-42.
3. Moscovitch, M., *Personnel dosimetry using LiF:Mg,Cu,P*. Radiat. Prot. Dosim., 1999. **85**(1-4): p. 49–56.
4. AEC, *Instruction Manual for GAMMACELL 40 - Caesium 137 Irradiation Unit - 3rd Edition*, in 1977, Atomic Energy of Canada Limited: Ottawa, CA.

APPENDIX D

Study of the fading of the EPR signals after irradiation

D-1. EXPERIMENTAL GOALS

The goal of this experiment was to perform preliminary measurements in order to evaluate the fading of the RIS during storage. The RIS can be isolated from other signals, MIS1 and MIS2, by using treatment and the “algebraic manipulation of the microwave power” methods in order to eliminate their effect. However, due to the nature of the spongy tissue of fingernails, increases in EPR signals may occur from the contribution of the mechanical stress imparted on the alpha helix during plastic deformation as samples dry out when kept at normal ambient temperatures (MIS2 contribution). This occurs even after the MIS1 has faded away in about 20-24 hrs, complicating the measurement of the sole contribution of the RIS to the signal and hence its fading rate. In this experiment, we look at the changes in the signals using both stressed and unstressed samples at two temperature conditions, at freezing ($\approx -20^{\circ}\text{C}$) and at ambient ($20-24^{\circ}\text{C}$ in laboratory) temperatures.

D-2. MATERIALS AND METHODS

To study the fading of the RIS during storage and its variation with temperature we used 20 samples, 10 stressed and 10 unstressed, that had been irradiated to 15Gy and 20 Gy respectively. Since preliminary studies showed that samples kept at low temperatures

had persistent EPR signals, we kept samples in a freezer ($\approx -20^{\circ}\text{C}$) in between measurements. The two sets of samples were then split into two groups of 5 each. Five samples were stored at low temperature and the other 5 at ambient temperature and pressure (ATP). Measurements were done every few days after exposure and follow-up measurements continued for a period of a few months. Each sample was weighted prior to each measurement in order to normalize to weight.

A second experiment was performed to study the effect of storage on the fading of two high doses RIS using four stressed (untreated) samples from the same donor. Two of these were irradiated at 100 Gy and two at 200 Gy. As with previous experiment, we divided each sample set in half to observe the fading of the signal at a low temperature and at ATP.

A third experiment looked at the signals of nine “historical” samples, which had been irradiated a long time ago to 1, 3, 8, and 20 Gy, and kept in the freezer. Their EPR signal after irradiation was followed for months up to two years.

D-3. RESULTS

Figure D-1. shows the results for the stressed samples. Stressed samples 1–5, which were stored in the freezer, showed a significantly stable signal. Samples 6-10, kept at ATP, showed an initial decay/fading of the signal and then an increase with time. The average final value of the signal for stressed samples kept at low temperatures was 0.7547 (± 0.0455) and for samples kept at ATP was 50% higher, 1.5780 (± 0.0575). As the spongy tissue of the fingernails is drying out, the signal increases to an approximately saturation value of 1.6 a.u. for an irradiation of 15Gy in stressed samples.

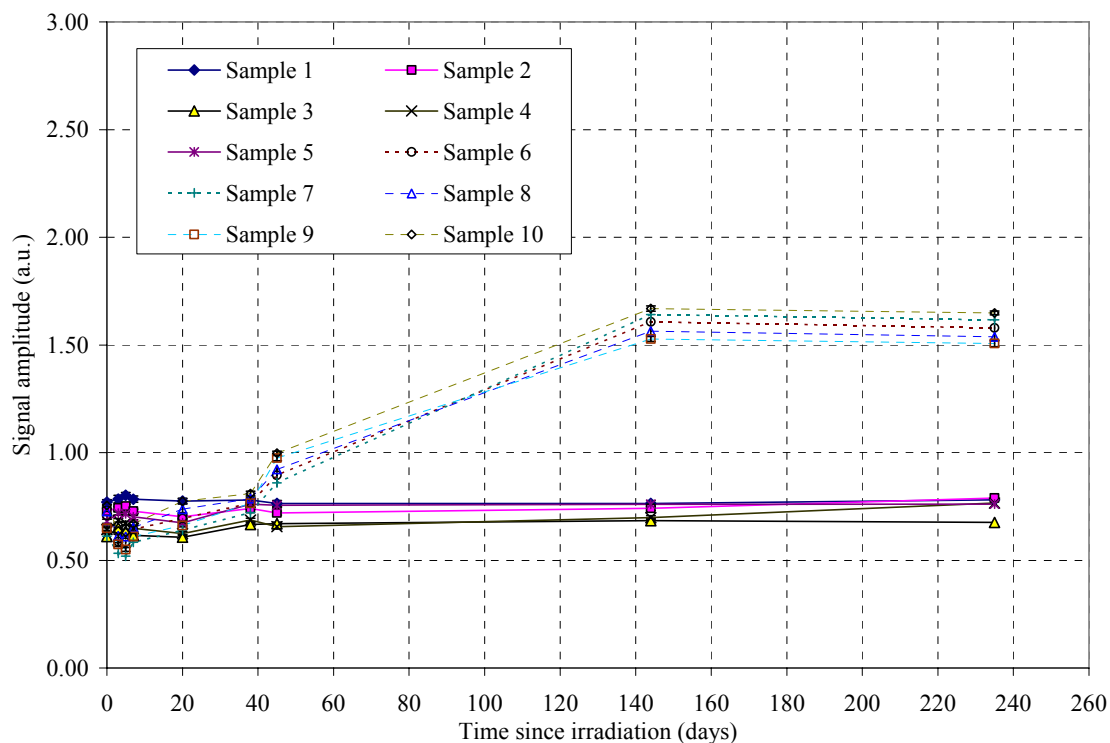


Figure D-1. EPR signal changes with time in stressed samples after 15 Gy irradiation. Samples 1-5 were kept in a freezer (-20°C) and samples 6-10 at ambient air temperature ($\approx 20-23^\circ\text{C}$).

Figure D-2 shows the results for the unstressed samples. Much like with the stressed samples, the unstressed samples 1–5, which were stored in the freezer, also showed a stable signal. The remaining samples 6-10, kept at ATP, showed an initial decay/fading of the signal and then an increase with time. The average final value of the signal for unstressed samples kept at low temperatures was $0.32211 (\pm 0.0614)$ and for samples kept at ATP was 80% higher, $1.5012 (\pm 0.05463)$.

When stored at ATP, unstressed samples reached a saturation EPR signal value of approximately 1.5 a.u. for a 20 Gy irradiation, which is coincidentally close to the value

obtained from stressed samples irradiated at 15Gy and also stored at ATP. Sometime after the 80th and the 124th day period at which measurements were taken, the signal reached this approximate saturation value at ATP. Afterwards, the signal fades slowly as shown in Figure D-3, which shows the average value for all stressed and unstressed samples kept at freezing temperatures and at ATP.

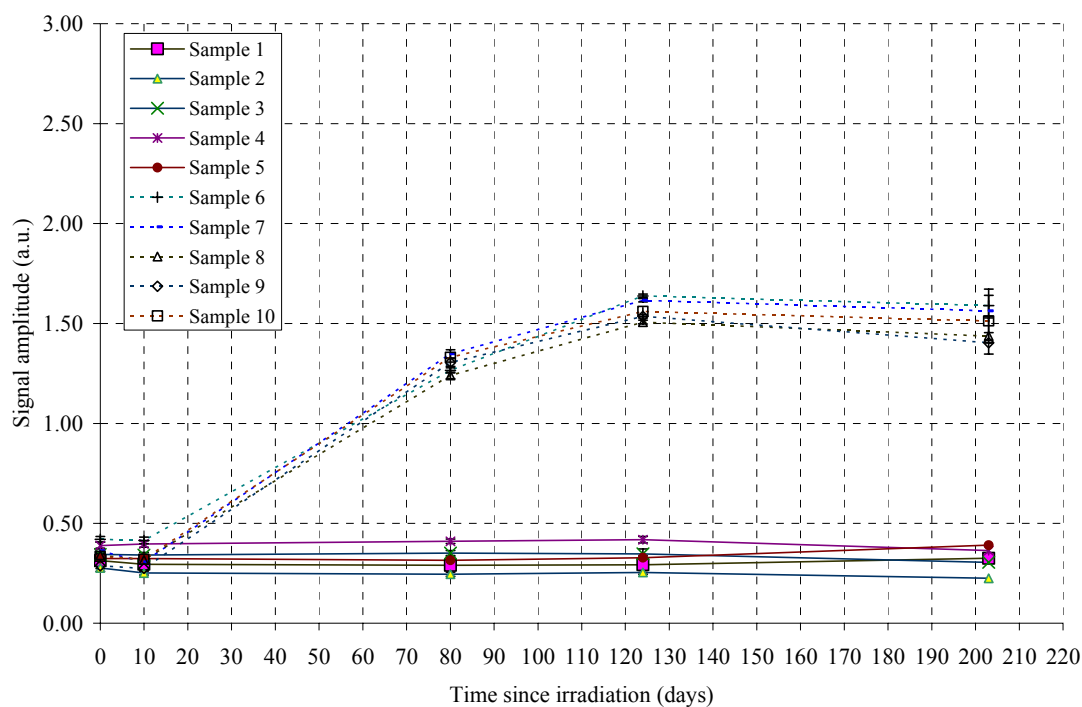


Figure D-2. EPR signal changes with time in unstressed samples after irradiation (20 Gy). Samples 1-5 were kept in a freezer (-20°C) and samples 6-10 at ambient air temperature ($\approx 20\text{-}23^\circ\text{C}$).

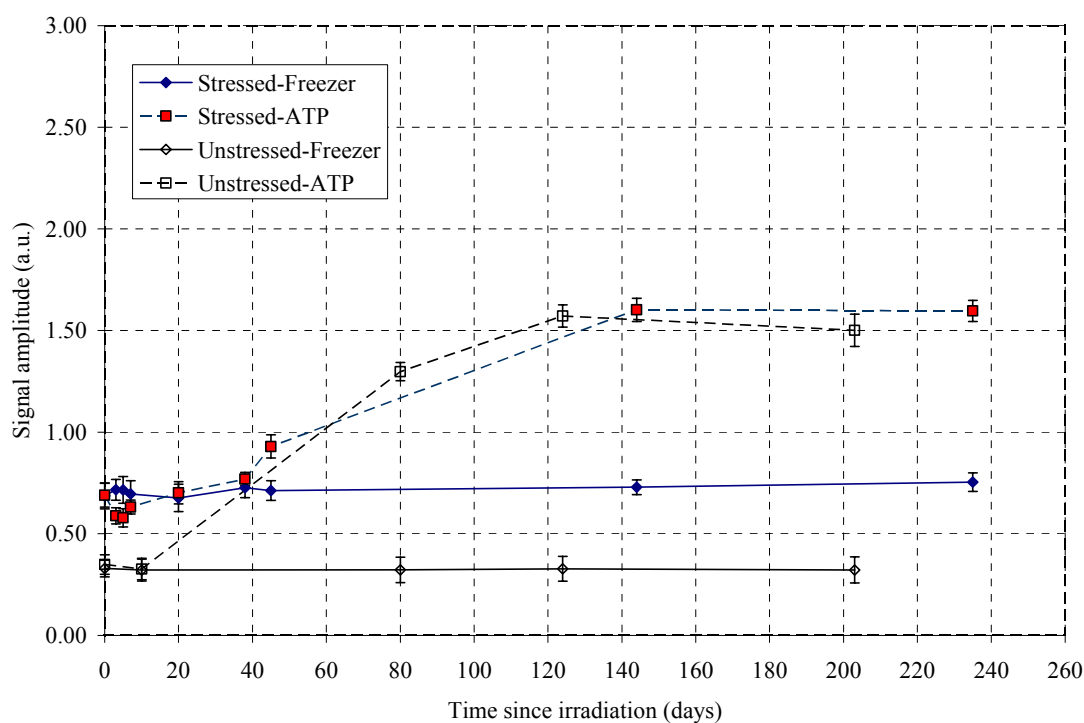


Figure D-3. EPR signal change with time in stressed (after 15 Gy irradiation) and unstressed (after 20 Gy irradiation) fingernail samples. Symbols represent the mean values of the amplitude peak-to-peak signal and the error bars the 1 standard deviation, $n=20$.

Figure D-4 shows the changes of the EPR signal after acute radiation doses of 100 and 200 Gy. At these high doses, samples kept at low temperatures showed a stable signal. Those kept at ATP showed a slight initial fading of the signal and then remained relatively stable (114 days evaluation time).

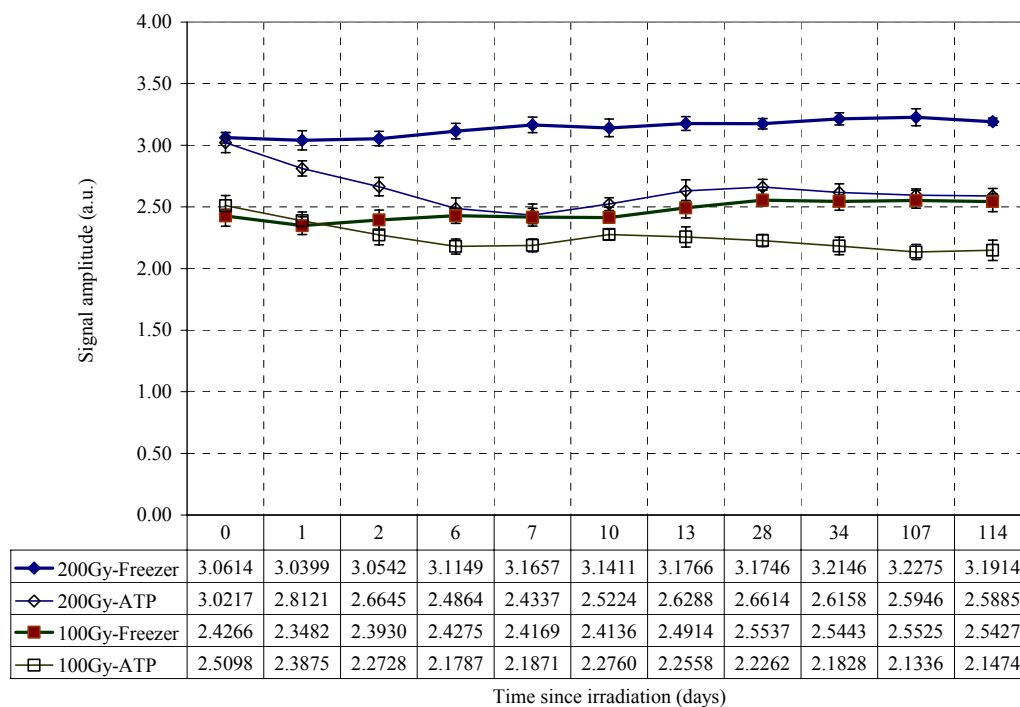


Figure D-4. EPR signal fading after high acute irradiations of 100 and 200 Gy for samples kept at freezing temperatures and ATP conditions. Error bars represent 1 standard deviation, 95% confidence interval.

Figure D-5 shows the magnitude of the EPR signal for nine samples that had been irradiated two years ago and kept in the freezer. A slight fading of the signal was observed for samples that were untreated (labeled U), which was not as noticeable in treated samples (labeled T). The magnitude of the signal of treated samples is much more stable even two years after exposure of the samples when they are kept at low temperatures ($\approx -20^{\circ}\text{C}$).

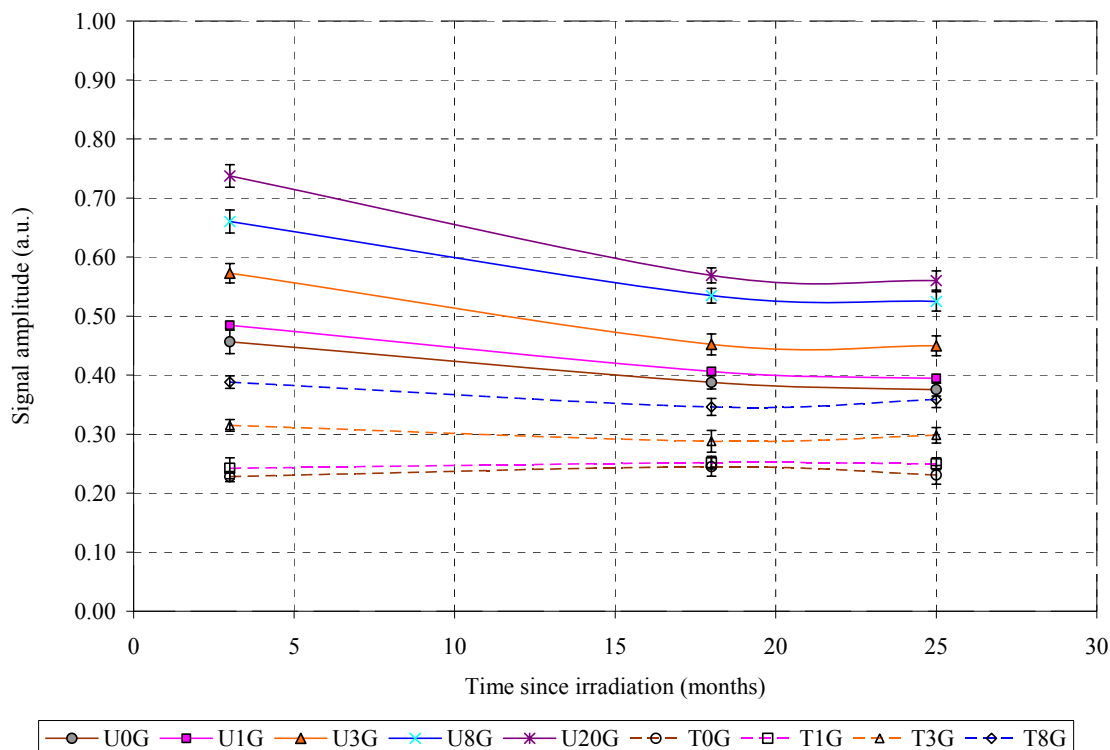


Figure D-5. EPR signal fading after irradiation of 8 samples that were followed for two years. Samples were labeled U for untreated and T for treated. The numerical values are the radiation doses given to the samples. Error bars represent 1 standard deviation, 95% confidence interval.

D-4. DISCUSSION AND CONCLUSIONS

Free radicals in stressed and unstressed samples kept at low temperatures induce a significantly stable EPR signal. Since there are not many mechanical changes in the structure of the fingernail tissue while they are kept at low temperatures, we do not see changes in the MIS2. The contribution of this MIS2 is the reason for an increase of the signal when samples are kept at ATP. The effect of storage of samples at ambient temperatures on EPR measurements is different for low and high radiation doses. At low

radiation doses, both stressed and unstressed samples displayed a slight fading of the signal and then an increase until a saturation value is reached. At this point, all samples are dried and stressed from the plastic deformation caused during its drying process. Therefore, the contribution of the MIS2 saturates at a value beyond which the sample is no longer drying. Any fading beyond this point may be attributed to the RIS. However, measurements of the RIS cannot be done in stressed samples because they are affected by the stress forces that *in vivo* samples would not have been subjected to. Since water treatment would only affect the mechanical signals and not the RIS, a more accurate method for measuring the changes in the RIS will require that samples at ATP be treated as they dry with time.

It is not practical to wait until fingernails are dried to observe any fading of the RIS. Moreover, dried fingernails are stressed and not a realistic representation of *in vivo* specimens. Treated fingernails offer a more credible representation to study the fading of the RIS. However, this study is complicated by the ongoing changes in the fingernail helical structure after samples are cut and while they are drying. The true measurement of the RIS fading would require periodic water treatments for restoring the tissue to its original shape in order to avoid the effect of any further mechanical stress on the samples that may cause a signal increase and therefore an overestimation in measurements.

BIBLIOGRAPHY

1. IAEA, *Use of electron paramagnetic resonance dosimetry with tooth enamel for retrospective dose assessment*. 2002, International Atomic Energy Agency: Vienna, Austria.
2. Turai, I., et al., *Response to radiological accidents: The role of the International Atomic Energy Agency*. . Radioprotection, 2001. **36**(1): p. 1-17.
3. ICRU, *Retrospective Assessment of Exposures to Ionising Radiation, Volume 2 No 2 in Journal of the ICRU*, N.T. Publishing, Editor. 2002, International Commission on Radiation and Measurements: Ashford, England.
4. Pass, B., *Collective radiation biodosimetry for dose reconstruction of acute accidental exposures: a review*. Environ Health Perspectives, 1997. **105 Suppl 6**: p. 1397-402.
5. Brady, J.M., N.O. Aarestad, and H.M. Swartz, *In vivo dosimetry by electron spin resonance spectroscopy*. Health Phys, 1968. **15**: p. 43-47.
6. Dalgarno, B.G. and J.D. McClymont, *Evaluation of ESR as a radiation accident dosimetry technique*. Appl Radiat Isot, 1989. **40**: p. 1013-1020.
7. Desrosiers, M., et al., *ESR dosimetry and applications. Proceedings of the 4th International Symposium. Munich, Germany, 15-19 May 1995*. Appl Radiat Isot, 1996. **47**(11-12): p. 1151-687.
8. Ikeya, M. and T. Miki. *ESR dating and dosimetry*. in *1st international symposium*. 1985. Ionics, Tokyo.

9. Regulla, D.F., *From Dating to Biophysics - 20 years of progress in applied ESR Spectroscopy*. Appl Radiat Isot, 2000. **52**: p. 1023-1030.
10. Regulla, D.F., A. Scharmann, and W.L. McLaughlin, *EPR dosimetry and applications. Proceedings of the 2nd international symposium, Munich 1988*. Appl Radiat Isot, 1989. **40**: p. 829-1246.
11. Romanyukha, A.A., et al., *Pilot study of the Urals population by tooth electron paramagnetic resonance dosimetry*. Radiat Environ Biophys, 1996. **35**(4): p. 305-10.
12. Shleien, B., A.J. Ruttenber, and M. Sage, *Epidemiologic studies of cancer in populations near nuclear facilities*. Health Phys, 1991. **61**(6): p. 699-713.
13. Skinner, A., et al., *ESR dosimetry and applications. Proceedings of the 6th international symposium, Campos de Jordao, SP, 2003*. Appl Radiat Isot, 2005. **62**: p. 115-381.
14. Skinner, A.R. and M. Desrosiers, *ESR dosimetry and applications. Proceedings of the 3rd international symposium, Gaithersburg, 1991*. Appl Radiat Isot, 1993. **44**: p. 1-472.
15. Ikeya, M., *Radiation Effects in organics and inorganics for ESR dosimetry*. Appl Radiat Isot, 1996(47): p. 1479-1481.
16. Gordy, W., W.B. Ard, and H. Shields, *Microwave Spectroscopy of Biological Substances. Ii. Paramagnetic Resonance in X-Irradiated Carboxylic and Hydroxy Acids*. Proc Natl Acad Sci U S A, 1955. **41**(11): p. 996-1004.
17. Gordy, W., W.B. Ard, and H. Shields, *Microwave Spectroscopy of Biological*

- Substances. I. Paramagnetic Resonance in X-Irradiated Amino Acids and Proteins.* Proc Natl Acad Sci U S A, 1955. **41**(11): p. 983-96.
18. Becker, R.O., *Electron paramagnetic resonance in non-irradiated bone.* Nature, 1963. **199**: p. 1304-1305.
 19. Desrosiers, M. and D.A. Schauer, *Electron Paramagnetic Resonance (EPR) Biodosimetry.* Nuclear Instruments and Methods in Physics Research Section B, 2001. **184**(1-2): p. 219-228.
 20. Ikeya, M., J. Miyajima, and S. Okajima, *ESR dosimetry for atomic bomb survivors using shell buttons and tooth enamel.* Jpn J Appl Phy, 1984. **23**: p. L697-L699.
 21. Pass, B. and J.E. Aldrich, *Dental enamel as an in vivo radiation dosimeter.* Medical Physics, 1985. **12**: p. 305-307.
 22. Aldrich, J.E., B. Pass, and C. Mailer, *Changes in the paramagnetic centres in irradiated and heated dental enamel studied using electron paramagnetic resonance.* Int J Radiat Biol, 1992. **61**(3): p. 433-7.
 23. Galtsev, V.E., et al., *Human tooth EPR dosimetry with enhanced sensitivity.* J Radioanal Nucl Chem Letters, 1994. **186**: p. 35-45.
 24. Ignatiev, E.A., et al., *Selective saturation method for EPR dosimetry with tooth enamel.* Appl Radiat Isot, 1996. **47**(3): p. 333-7.
 25. Romanyukha, A.A., M.F. Desrosiers, and D.F. Regulla, *Current issues on EPR dose reconstruction in tooth enamel.* Appl Radiat Isot, 2000. **52**(5): p. 1265-73.
 26. Zhong, Y.C. and J.R. Pilbrow, *Spectral diffusion in saturation-transfer EPR.* J Magn Res, 1992. **57**: p. 111-121.

27. Symons, M.C., H. Chandra, and J.L. Wyatt, *Electron paramagnetic resonance spectra of irradiated finger-nails: A possible measure of accidental exposure*. Radiat Prot Dosimetry, 1995. **58**(No. 1): p. 11-15.
28. Romanyukha, A., et al., *Mechanically-induced signal in fingernails as a confounding factor for EPR dosimetry*, in *2nd International Conference on Biodosimetry and 7th International Symposium on EPR Dosimetry and Applications*. 2006: USUHS, Bethesda, MD.
29. IAEA, *Planning the medical response to radiological accidents*, in *Safety Report Series*. 1998, IAEA and WHO: Vienna. p. 10.
30. Swartz, H.M., et al., *In vivo EPR dosimetry to quantify exposures to clinically significant doses of ionising radiation*. Radiat Prot Dosimetry, 2006. **120**(1-4): p. 163-70.
31. Swartz, H.M., et al., *Measurements of clinically significant doses of ionizing radiation using non-invasive in vivo EPR spectroscopy of teeth in situ*. Appl Radiat Isot, 2005. **62**(2): p. 293-9.
32. Alexander, G.A., et al., *BiodosEPR-2006 Meeting: Acute dosimetry consensus committee recommendations on biodosimetry applications in events involving uses of radiation by terrorists and radiation accidents*. Radiation Measurements, 2007. **42**(6-7): p. 972-996.
33. Trompier, F., et al., *Protocol for emergency EPR dosimetry in fingernails*. Radiation Measurements, 2007. **42**: p. 1085-1088.
34. Greenstock, C.L. and A. Trivedi, *Biological and biophysical techniques to assess radiation exposure: a perspective*. Prog Biophys Mol Biol, 1994. **61**(2): p. 81-

- 130.
35. Trompier, F., et al., *EPR dosimetry in a mixed neutron and gamma radiation field*. Radiat Prot Dosimetry, 2004. **110**(1-4): p. 437-442.
 36. Hayes, W., *Professor Brebis Bleaney*, in *Independent, The (London) Newspaper*. 2006: London, UK.
 37. Weil, J., J. Bolton, and J. Wertz, *ELECTRON PARAMAGNETIC RESONANCE Elementary Theory and Practical Applications*. 1994, New York: John Wiley & Sons, Inc.
 38. Al'tshuler, S.A. and B.M. Kozyrev, *Electron Paramagnetic Resonance*. 1964, New York, NY: Academic Press.
 39. Zovoiski, E., *Paramagnetic relaxation of liquid solutions for perpendicular fields*. J. Phys. USSR, 1945. **9**: p. 211-216.
 40. Carrington, S.A. and A. McLachlan, *Introduction to Magnetic Resonance*. 1967, London: Harper and Row.
 41. Kohler, J., et al., *Single Molecule Electron Paramagnetic Resonance Spectroscopy: Hyperfine Splitting Owing to a Single Nucleus*. Science, 1995. **268**(5216): p. 1457-1460.
 42. Wrachtrup, J., et al., *Optically detected spin coherence of single molecules*. Phys Rev Lett, 1993. **71**(21): p. 3565-3568.
 43. Odom, B., et al., *New measurement of the electron magnetic moment using a one-electron quantum cyclotron*. Phys Rev Lett, 2006. **97**(3): p. 030801.
 44. Swartz, H.M., B. JR, and B. DC, *Biological Applications of Electron Spin Resonance*. 1972, New York: Wiley.

45. McLaughlin, W.L., *ESR Dosimetry*. Radiat Prot Dosimetry, 1993. **47**: p. 255-262.
46. Jiang, J. and R.T. Weber, *Elexsys E 500 User's Manual Basic Operations*. 2001, Manual Version 2.0 - Bruker BioSpin Corporation: Billerica, MA.
47. Poole, S.P.J., *Electron Spin Resonance - A Comprehensive Treatise on Experimental Techniques*. 2nd Edition ed. 1983, New York, NY: Wiley Interscience.
48. Feher, G., *Observation of nuclear magnetic resonance via the electron spin resonance line*. Physics Review, 1956. **103**: p. 834-835.
49. Regulla, D. and U. Deffner, *Dosimetry by ESR spectroscopy of alanine*. Appl Radiat Isot, 1982. **33**: p. 1101-1114.
50. Yordanov, N.D. and E. Georgieva, *EPR and UV spectral study of gamma-irradiated white and burned sugar, fructose and glucose*. Spectrochim. Acta (Part A), 2004. **60**: p. 1307-1314.
51. Wieser, A., et al., *The second international intercomparison on EPR tooth dosimetry*. Radiation Measurements, 2000. **32**: p. 549-557.
52. Nagy, V., *Accuracy considerations in EPR dosimetry*. Appl. Radiat. Isot., 2000. **52**(5): p. 1039-1050.
53. Haskell, E.H., et al., *Preliminary report on the development of a virtually nondestructive additive dose technique for EPR dosimetry*. Appl Radiat Isot, 2000. **52**(5): p. 1065-70.
54. Hayes, R., et al., *Accurate EPR radiosensitivity calibration using small sample masses*. Nuclear Instruments and Methods in Physics Research, Section A, 2000. **441**: p. 535-550.

55. Wieser, A., et al., *The 3rd international intercomparison on EPR tooth dosimetry: Part 1, general analysis*. Appl Radiat Isot, 2005. **62**(2): p. 163-71.
56. Moens, P., et al., *Maximum-likelihood common-factor analysis as a powerful tool in decomposing multicomponent EPR powder spectra*. J. Magn. Reson., 1993. **101**: p. 1-15.
57. Pass, B. and A. Shames, *Signal processing for radiation dosimetry using EPR in dental enamel: comparison of three methods*. Radiation Measurements, 2000. **32**: p. 163-167.
58. Chumak, V., et al., *Lessons of the 3rd international intercomparison on EPR dosimetry with teeth: similarities and differences of two successful techniques*. Radiat Prot Dosimetry, 2006. **120**(1-4): p. 197-201.
59. Romanyukha, A.A. and D.F. Regulla, *Aspects of retrospective ESR dosimetry (invited paper)*. Appl Radiat Isot, 1996. **47**(11-12): p. 1293-7.
60. Swartz, H.M., et al., *Clinical applications of EPR: overview and perspectives*. NMR Biomed, 2004. **17**(5): p. 335-51.
61. Wieser, A., et al., *The Third International Intercomparison on EPR Tooth Dosimetry: part 2, final analysis*. Radiat Prot Dosimetry, 2006. **120**(1-4): p. 176-83.
62. Chumak, V., S. Sholom, and L. Pasalskaya, *Applications of high precision EPR dosimetry with teeth for reconstruction of doses to Chernobyl populations*. Radiat Prot Dosimetry, 1999. **84**: p. 515-520.
63. Cosset, J.M., et al., *Health consequences among the Lilo accident victims, medical monitoring in Georgia, France, and Germany*, in IAEA-TECDOC-1300.

- 2002, IAEA: Vienna. p. 49-55.
64. Gunalp, B., K. Ergen, and I. Turai, *Follow-up of delayed health consequences of the Istanbul radiological accident and lessons to be learned from its medical management*, IAEA-TECDOC-1300, Editor. 2002: Vienna. p. 67-75.
 65. Ivannikov, A., et al., *Results of EPR Dosimetry for Population in the Vicinity of the Most Contaminating Radioactive Fallout Trace After the First Nuclear Test in the Semipalatinsk Test Site*. J. Radiat. Res., 2006. **47**(Suppl. A): p. A39-A46.
 66. Nakamura, N., et al., *A close correlation between electron spin resonance (ESR) dosimetry from tooth enamel and cytogenetic dosimetry from lymphocytes of Hiroshima atomic-bomb survivors*. Int. J. Radiat. Biol., 1998. **73**: p. 619-627.
 67. Romanyukha, A.A., et al., *Correction factors in the EPR dose reconstruction for residents of the Middle and Lower Techa riverside*. Health Phys, 2001. **81**(5): p. 554-66.
 68. Stepanenko, V., et al., *International Intercomparison of Retrospective Luminescence Dosimetry Method: Sampling and distribution of the brick samples from Dolon' village, Kazakhstan*. J. Radiat. Res., 2006. **47**(Suppl. A): p. A15-A21.
 69. Swartz, H.M., et al., *In vivo EPR for dosimetry*. Radiation Measurements, 2007.
 70. Romanyukha, A., et al., *EPR dosimetry in chemically treated fingernails*. Radiation Measurements, 2007. **42**: p. 1110-1113.
 71. Romanyukha, A., F. Trompier, and H.M. Swartz, *EPR dosimetry with fingernails, in US Patent Provisional*. 2007: USA.
 72. Farren, L., S. Shayler, and A.R. Ennos, *The fracture properties and mechanical*

- design of human fingernails*. J Exp Biol, 2004. **207**(Pt 5): p. 735-41.
73. Fernandez-Rodriguez, A., et al., *Genetic analysis of fingernail debris: application to forensic casework*. International Congress Series, 2003. **1239**: p. 921-924.
 74. Piccinini, A., *A 5-year study on DNA recovered from fingernail clippings in homicide cases in Milan*. International Congress Series, 2003. **1239**: p. 929-932.
 75. Chaudhary, K., et al., *Trace element correlations with age and sex in human fingernails*. Journal of Radioanalytical and Nuclear Chemistry, 1995. **195**(1): p. 51-56.
 76. Fraser, I., W. Meier-Augenstein, and R.M. Kalin, *The role of stable isotopes in human identification: a longitudinal study into the variability of isotopic signals in human hair and nails*. Rapid Commun Mass Spectrom, 2006. **20**(7): p. 1109-16.
 77. Hayashi, M., et al., *Cadmium, lead, and zinc concentrations in human fingernails*. Bull Environ Contam Toxicol, 1993. **50**(4): p. 547-53.
 78. Mehra, R. and M. Juneja, *Fingernails as biological indices of metal exposure*. J Biosci, 2005. **30**(2): p. 253-7.
 79. Olabanji, S.O., et al., *Characterization of human fingernail elements using PIXE technique*. Nuclear Instruments and Methods in Physics Research Section B: Beam Interactions with Materials and Atoms, 2005. **240**(4): p. 895-907.
 80. Vance, D.E., W.D. Ehmann, and W.R. Markesbery, *Trace element content in fingernails and hair of a nonindustrialized US control population*. Biol Trace Elem Res, 1988. **17**: p. 109-21.
 81. Vellar, O.D., *Composition of Human Nail Substance*. The American Journal of

- Clinical Nutrition, 1970. **23**(10): p. 1272-1274.
82. Chandra, H. and M.C. Symons, *Sulphur radicals formed by cutting alpha-keratin*. Nature, 1987. **328**(6133): p. 833-4.
 83. Symons, M.C. and F.A. Taiwo, *Radiation Damage to Proteins: An EPR Study*. J. Chem. Soc. Perkin Trans. II, 1992. **1413**.
 84. Symons, M.C., F.A. Taiwo, and R.L. Peterson, *Electron Addition to Xanthine Oxidase. An ESR Study of the Effects of Ionizing Radiation*. J. Chem. Soc. Faraday Trans. I, 1989. **85**(4063).
 85. Reyes, R.A., et al., *Electron Paramagnetic Resonance in Human Fingernails: The Sponge Model Implication*. Radiation and Environmental Biophysics, 2008.
 86. USUHS, *Center for Biophysical Assessment and Risk Management Following Irradiation - EPR Dosimetry*, in *Protocol G18983*, C. Mitchell and A. Romanyukha, Editors. 2005, Uniformed Services University of the Health Sciences: Bethesda, MD.
 87. USUHS, *Development of Protocol for Dose Assessment of Victims of Radiological Accidents/Incidents Using Electron Paramagnetic Resonance (EPR) / Electron Spin Resonance (ESR) Dosimetry Technology*, in *T087M4*, R. Reyes and A. Romanyukha, Editors. 2007, Uniformed Services University of the Health Sciences: Bethesda, MD.
 88. Toyoda, S., et al., *Toward high sensitivity ESR dosimetry of mammal teeth: the effect of chemical treatment*. J Radiat Res (Tokyo), 2006. **47 Suppl A**: p. A71-4.
 89. Romanyukha, A.A., et al., *Parameters affecting EPR dose reconstruction in teeth*. Appl Radiat Isot, 2005. **62**(2): p. 147-54.

90. Dupont, W. and W. Plummer, *Power and sample size calculations for studies involving linear regression*. Controlled Clinical Trials, 1998. **19**: p. 589-601.